

DU

To: DDC

1

AD630293

AFCRL-63-631

INVESTIGATION OF REFRACTOMETER MEASUREMENTS IN THE ATMOSPHERE
AT HIGH RELATIVE HUMIDITIES AND TEMPERATURES

by

D. R. Hay, Ph.D., Professor of Physics

and

H. E. Turner, B.Sc., Research Assistant

The University of Western Ontario, London Canada

Department of Physics

Contract No. AF 19(623)-444

Project No. ES-2-GEN-509-6

Project 6682

Task 668202

AD NO. —
DDC FILE COPY

FINAL REPORT

July 1963

Prepared

for

DDC
APR 4 1966
JISIA E

CLEARINGHOUSE FOR FEDERAL SCIENTIFIC AND TECHNICAL INFORMATION		
Hardcopy	Microfiche	
\$ 5.00	\$ 1.00	160 pp as

ARCHIVE COPY
PROCESSING COPY

AIR FORCE CAMBRIDGE RESEARCH LABORATORIES

OFFICE OF AEROSPACE RESEARCH

UNITED STATES AIR FORCE

BEDFORD, MASSACHUSETTS

Code 1

AFCRL-63-631

INVESTIGATION OF REFRACTOMETER MEASUREMENTS IN THE ATMOSPHERE
AT HIGH RELATIVE HUMIDITIES AND TEMPERATURES

by

D. R. Hay, Ph.D., Professor of Physics

and

H. E. Turner, B.Sc., Research Assistant

The University of Western Ontario, London Canada

Department of Physics

Contract No. AF 19(628)-444

Project No. ES-2-GEN-509-6

Project 6682

Task 668202

FINAL REPORT

July 1963

Prepared

for

AIR FORCE CAMBRIDGE RESEARCH LABORATORIES

OFFICE OF AEROSPACE RESEARCH

UNITED STATES AIR FORCE

BEDFORD, MASSACHUSETTS

Notice

Requests for additional copies by Agencies of the Department of Defense, their contractors, and other government agencies should be directed to the:

DEFENSE DOCUMENTATION CENTER (DDC)

ARLINGTON HALL STATION

ARLINGTON 12, VIRGINIA

Department of Defense contractors must be established for DDC services or have their "need-to-know" certified by the cognizant military agency of their project or contract.

All other persons and organizations should apply to the:

U.S. DEPARTMENT OF COMMERCE

OFFICE OF TECHNICAL SERVICES

WASHINGTON 25, D.C.

When US Government drawings, specifications, or other data are used for any purpose other than a definitely related government procurement operation, the government thereby incurs no responsibility nor any obligation whatsoever; and the fact that the government may have formulated, furnished, or in any way supplied the said drawings, specifications, or other data is not to be regarded by implication or otherwise, as in any manner licensing the holder or any other person or corporation, or conveying any rights or permission to manufacture, use, or sell any patented invention that may in any way be related thereto.

FOREWORD

This report describes research which is part of the graduate studies program of the Department of Physics, University of Western Ontario. The period of study extended from May 1st 1962 to April 30th 1963. The authors are indebted to Dr. P. A. Forsyth, F.R.S.C., Head of the Department, for making available the facilities of the department for this research program.

Several members of the Tropospheric Physics Group, under the direction of the senior author, have contributed towards the study reported here. Mr. H. C. Martin, M.Sc., has provided information on the air-flow about the capacitor-type refractometer, and has worked out the programs for computation on the IBM 650 Computer. Mr. J. Kortschinski, a student in the third year of the Engineering Science course at this university, has designed the wind tunnel and supervised its construction while working with the Group during the summer of 1962. Messrs. H. Aitkenhead, K. McColl and D. Stewart, technicians in the Group, have assisted in many aspects of the research program.

H. E. Turner, the co-author, would like to acknowledge his indebtedness to the National Research Council of Canada for the Studentship awarded to him during the period of this study.

The authors would like to express their sincere appreciation to those outside of the Department of Physics who have contributed in various ways to the research program: They are grateful to the Chairman of the Defence Research Board and the Chief Superintendent of the Defence Research Telecommunications Establishment in Ottawa for the loan of some of the test instruments: to the Director of the Division of Applied Physics of the National Research Council in Ottawa for arranging for the calibration

of a precision resistor upon which the precise temperature measurements depend: and to Dr. J. F. Hart, Director of the U.W.O. Computing Center, for making available the facilities of the Center.

A paper on the research program described in this report was presented at the International Symposium on Humidity and Moisture, in Washington D.C., 20-23 May 1963.

Investigation of refractometer measurements in the atmosphere
at high relative humidities and temperatures

ABSTRACT

Two techniques for the precise measurement of changes in air refractivity within the troposphere are examined in the present study. These are the microwave refractometer which uses a ventilated metal cavity as the sensing element, and the Hay refractometer whose sensing element is an air capacitor. The effects of water vapour adsorption and condensation upon the sensing elements of these instruments at high relative humidities make the interpretation of such soundings uncertain, in view of the conflicting evidence of previous workers. This report describes a laboratory study of the interaction between the refractometer sensors and the air humidity.

Preliminary measurements upon the adsorption of water vapour on isolated quartz and invar plates have been carried out with the aid of an optical ellipsometer. With a ventilation speed of 800 feet per minute, the depth of the adsorbed layer on flat quartz plate increased as relative humidity increased beyond 20 percent; the increase became very rapid and erratic for relative humidities greater than 50 percent. However, no detectable adsorption was found on the flat invar plate, for relative humidities up to saturation.

An experimental wind tunnel of special design was constructed to provide a controlled environment for further adsorption studies. This tunnel contains a homogeneous jet of volume 8 cubic feet, in which wind speed is approximately 800 feet per minute, and in which temperature is variable between -20°C and $+50^{\circ}\text{C}$ for relative humidities variable up to saturation, at surface atmospheric pressure.

The refractive index of the air in the jet was ascertained from measurements of wet- and dry-bulb temperatures and air pressure. A hygrometer was developed for this purpose to indicate temperature with a precision of $\pm 0.01^{\circ}\text{C}$. Air refractivity was computed, with an accuracy of one part in 10^6 through the Wexler-Brombacher form of the psychrometric equation and the Smith-Weintraub form of the Debye equation. This information was compared with the refractometer indications, as relative humidity was varied for different fixed temperatures.

It has been found that adsorption occurs at high relative humidities in both the microwave refractometer cavity and in the Hay refractometer sensor, in amounts which cause apparent refractivity errors well in excess of one part per million. In the former, the apparent error increases approximately linearly with vapour pressure, beginning at a minimum relative humidity whose value depends upon the air temperature: in the latter, the apparent error increases non-linearly with vapour pressure, beginning at approximately 50 percent relative humidity for a wide range of air temperatures. The amount of refractivity error in the capacitor-type sensor decreases with decreasing amount of quartz in the capacitor: a further decrease in error results from the application of some types of hydrophobic materials to the sensor surface. A significant improvement in the capacitor sensor has been obtained by elimination of the quartz spacers and by coating the invar surface with beeswax. It is suggested that the process of water vapour adsorption on metals is governed by the electric field intensity at the surface, and that this may account for the difference in behaviour of the microwave cavity and the improved capacitor-sensor at high relative humidities.

TABLE OF CONTENTS

	page
Foreword	ii
Abstract	iv
Table of Contents	vi
List of illustrations	x
List of Tables	xii
1. Introduction	1
2. Statement of the problem	5
2.1 Principles of the Hay refractometer and microwave refractometer	5
2.2 Anomalies at high relative humidities	8
2.3 Experimental techniques for studying adsorption and condensation effects	12
(a) Optical ellipsometer	13
(b) The experimental wind tunnel	13
3. The experimental wind tunnel	15
3.1 Aerodynamic design	16
(a) The test section (jet)	16
(b) The contraction cone	18
(c) The settling chamber	19
(d) The return passage	19
(e) Power losses in the air stream	19
3.2 Tunnel construction	22
3.3 Jet speed	24
3.4 Thermodynamic design	24
(a) The cooling load	24
(b) The refrigeration unit	26

3.5	Control of temperature and humidity	29
3.6	Operation of the wind tunnel	31
4.	The test refractometers	38
4.1	The microwave refractometer	38
	(a) The refractometer circuit	38
	(b) Calibration	39
4.2	The capacitor-type (Hay) refractometer	45
	(a) The refractometer circuit	45
	(b) Calibration	47
5.	The measurement of temperature and pressure	52
5.1	Requirements upon the precision of measurement	52
5.2	The psychrometric formula	55
5.3	The measurement of temperature (dry-bulb)	58
5.4	The hygrometer	62
	(a) Calibration of the mercury-in-glass thermometer	63
	(b) Calibration of the barometer	63
	(c) Calibration of the hot-wire anemometer	64
	(d) The wet-bulb temperature probe	64
	(e) The calibration chamber for the wet- and dry-bulb temperature probes	70
	(f) Calibration procedure	73
5.5	Computation of refractive index	75
6.	The optical ellipsometer	79
7.	Experimental observations in the wind tunnel	82
7.1	Temperature coefficients of the refractometers	83
7.2	Refractivity change with humidity - The Microwave Refractometer	84

7.3	Refractivity change with humidity - The Capacitor-Type	
	Refractometer	87
(a)	Quartz-invar sensor with 6 quartz spacers, - uncoated ..	87
(b)	Quartz-invar sensor with 6 quartz spacers, - coated with siliclad	89
(c)	Quartz-invar sensor with 6 quartz spacers, - coated with cup-grease	89
(d)	Quartz-invar sensor with varied number of quartz spacers, - uncoated	91
(e)	Quartz-invar sensor and invar sensor, - coated with beeswax	91
8.	Interpretation and Remarks	94
8.1	Deductions from the present experiment	95
8.2	Comments upon practical applications	97
8.3	Comments upon the physical process of adsorption	98
Appendix I:	Circuits of the microwave refractometer	100
Appendix II:	Experimental procedure for calibration of the platinum-wire resistance hygrometer	106
Appendix III:	Sample analysis of observations taken in hygrometer calibration	108
Appendix IV:	Table of vapour pressure of liquid water (in millibars), for temperatures from 0°C to 50°C, corrected for atmospheric pressure of 1000 mb.	110
Appendix V:	Solution of Equation (57) on the IBM 650 computer	124
Appendix VI:	Computation of the refractive index of air in the jet, using the IBM 650 computer:	128

(a) SOAP - II	129
(b) Sample solution	132
Appendix VII: Bibliography on vapour adsorption	133
References	140

LIST OF ILLUSTRATIONS

Figure	page
1. Principle of the Hay refractometer	6
2. Capacitor-type refractometer soundings	10
3. Pattern of air flow around the refractometer	17
4. The experimental wind tunnel (diagram)	23
5. The trolley system for examination of the jet	25
6. Profiles of wind speed in the jet	26
7. Temperature and humidity controls for the wind tunnel	30
8. The experimental wind tunnel (photograph)	32
9. Details of the wind tunnel	34
10. Wet- and dry-bulb temperatures in the center of the jet, vacated	35
11. Wet- and dry-bulb temperatures in the center of the jet, with refractometer in position	37
12. The basic circuit of the microwave refractometer	40
13. The microwave sensing cavity	41
14. Calibration apparatus for the microwave refractometer	43
15. Calibration curve for the microwave refractometer	44
16. The capacitor-type refractometer and its recording receiver	46
17. The Hay refractometer and its sensing elements	48
18. Calibration curve for the capacitor-type refractometer	50
19. The temperature recording bridge	61
20. Anemometer probe and bridge circuit	65
21. Calibration curve of the hot-wire anemometer	66
22. The wet-bulb temperature probe and wetting system	68
23. The hygrometer probes	69

24. The hygrometer calibration chamber	72
25. Relationship between psychrometric constant and wet-bulb temperature	74
26. Sample chart listing information transcribed from recordings ...	78
27. The optical ellipsometer	80
28. Temperature coefficients of the refractometer sensors	85
29. Comparison between indicated and true refractivity, - The Microwave Refractometer	86
30. Comparison between indicated and true refractivity, - The Capacitor-Type Refractometer: Invar capacitor with 6 quartz spacers, - uncoated	88
31. Comparison ... (as in 30): Effects of hydrophobic coatings	90
32. Comparison ... (as in 30): Invar capacitor with variable number of quartz spacers, - uncoated	92

Figure

A-1 Block diagram of the microwave refractometer	101
A-2 Circuits of the cathode follower-integrator, and of blanking amplitude control	102
A-3 The pulse-sharpening circuits	103
A-4 The pulse and sawtooth waveform generators	104
A-5 The 1000 Mc/s crystal-controlled oscillator	105

LIST OF TABLES

	page
1. Summation of losses about the closed circuit (wind tunnel)	20
2. Conductance of the wall components (of the wind tunnel)	27
3. Minimum ventilation speed for constancy of psychrometer	
"constant"	56
4. Coefficients in psychrometric formula	57
5. Effect of error in psychrometric constant upon error in deduced	
vapour pressure	57
6. Properties of platinum resistance temperature probe	59
7. Standard solutions for hygrometer calibration	73
8. Ellipsometer observations upon samples of quartz plate and	
invar plate	81

1. Introduction

Irregularities in the refractive index of the troposphere are important to various aspects of radio wave transmission. It has been found, for example, that the frequency spectrum of a radio signal is broadened by the multi-path nature of the propagation through atmospheric turbulence (Chapman, Heikkila and Hogarth 1957; Bugnolo 1959). The same type of atmospheric inhomogeneity is capable of broadening the beam width of a high-gain radio antenna (Booker and de Bettencourt 1955; Waterman 1958); Muchmore and Wheelon (1955) have shown theoretically that the atmospheric inhomogeneities will introduce fluctuations in the phase of the radio signal at the radio antenna. The apparent position of a target, as observed by a precision radar, will fluctuate about a mean direction because of these changing inhomogeneities in the atmosphere (Hay, Storey, et. al. 1958; Wong 1958); Anderson, Beyers and Rainey (1960) have demonstrated that the precision of target location by a tracking radar is improved in direct proportion to the quality of the information on the refractive index of the atmosphere.

A source of annoyance to the operators of sensitive radars is the unpredictable reflection of radar waves from these atmospheric irregularities (Plank 1956, 1959). Yet another example is the limitation upon the accuracy with which distances may be measured by radio techniques (Smith 1960) as imposed by atmospheric irregularities: Thompson, Janes and Kirkpatrick (1960) have shown that the apparent length of a radio path fluctuates in association with measured changes of the refractive index. A study of the distribution of water vapour and heat within turbulent eddies near the ground also provides information that is important to the limitation on precision of microwave surveying techniques (Hay and Pemberton 1962).

It is only within recent years that information on atmospheric inhomogeneities has become available. Changes in the refractive index of the air that are of the order of one part in one million may occur over distances that range from several tens of meters to only a few centimeters (see, for example, Crain 1955). Although the physical form of these irregularities has not been established, studies of microwave radar angles have suggested that at least some of these inhomogeneities are essentially flat over horizontal distances of several meters, and are no more than a few centimeters in vertical depth (Hay and Reid 1962; Hay, Bell and Johnston 1962). Furthermore, these irregularities in refractive index may persist for periods as long as several tens of minutes or as little as a fraction of a second.

It is apparent that special techniques are required for the direct measurement of refractive index of these inhomogeneities. Bean and Dutton (1961) and Wagner (1961) have indicated that conventional radiosonde equipment is incapable of indicating the small-scale structure of the troposphere. However, several techniques of direct measurement are capable of indicating the small fluctuations in refractive index that are referred to above. One of these is the microwave refractometer which has provided most of the existing information on the refractivity fluctuations within the troposphere (Birnbaum 1950; Crain 1950). A second technique employs small bead thermistors to indicate the wet- and dry-bulb temperatures (Hirao and Akita 1957, Crozier 1958, and Theisen and Gossard 1961). A third method uses an air capacitor to indicate the refractive index of the air that passes between its plates (Hay, Martin and Turner 1961).

Numerous studies have been made upon these newly developed instruments to remove their undesired limitations. In the microwave refractometer,

Adey (1957), Thompson, Freethey and Waters (1959) and Thorn and Straiton (1959) have designed well-ventilated sensing cavities. Techniques for introducing temperature compensation into the sensing cavity have been examined by Thompson, Freethey and Waters (1958), and by Crain and Williams (1957). Reduction in the weight of the bulky apparatus that is associated with the microwave refractometer has been achieved by Thompson and Vetter (1958) and recently in a UHF refractometer by Deam (1962). Sargent (1959) and Vetter and Thompson (1962) have modified the refractometer circuit to improve upon its long-term stability.

Some limitations in these new techniques require further study. For example, the spatial resolution of the microwave refractometer is limited to approximately two feet (Cunningham, Plank and Campen 1956) although theoretical considerations suggest that the resolution should be somewhat better than this (Hartman 1960). The thermistor technique is limited by the thermal lag of the sensing elements, which lies between 0.1 and 3 seconds; the interpretation of the measurements at sub-freezing levels with the troposphere also requires further study. In the capacitor-type refractometer, the authors have measured fluctuations in refractive index over distances as small as a few centimeters; the time-constant of this refractometer is limited by the recording equipment to 0.01 second.

One aspect of these refractometer techniques which requires further study is their response to an environment of high relative humidity and temperature. It has been known for many years that the apparent capacitance of an air condenser differs from its theoretical capacitance in conditions of high relative humidity. Since an air capacitor is the sensing element in the Hay refractometer, it may be expected that this physical phenomenon will affect the interpretation of the refractivity measurements with this

instrument. A question exists also with regard to the measurement of refractive index of humid air by means of the microwave refractometer. Some consideration has been given to the latter problem, but a more careful study is desirable.

The purpose of the research described in this report is to study the measurement of refractive index of air at high relative humidities and temperatures, with the Hay refractometer and the microwave refractometer. The experimental study has been carried out between 1 May 1962 and 30 April 1963. A detailed statement of the problem is presented in the following section; subsequent sections present details on the environmental test chamber and its associated apparatus, on the calibration of the precision temperature probes, on the experimental studies with the refractometers, on the auxilliary experiments with an optical ellipsometer, and on the interpretation of these studies with regard to refractometer measurements at high relative humidities and temperatures.

2. Statement of the Problem

This section will review the principle of the capacitor-type (Hay) refractometer and the microwave refractometer. Information on the effects of high relative humidities upon air capacitors and upon microwave cavities, as was available at the beginning of this study, will be summarized; the requirements of the present experiment then will be indicated.

2.1 Principles of the Hay Refractometer and the Microwave Refractometer

The capacitor-type refractometer consists essentially of a resonant circuit as illustrated in Figure 1. When the switch is closed on the left, the air capacitor, C_a and the inductor L form the resonant circuit, whose resonant frequency, f , is given by Equation (1).

$$f = \frac{1}{2 \pi \sqrt{L C_a}} . \quad (1)$$

In operation, the switch periodically transfers its connection from the capacitor C_a to the reference (sealed) capacitor C_r . Comparison of the oscillator frequencies during the two parts of the cycle permits a comparison of the capacitance of the two condensers without consideration of the temperature characteristics of the remainder of the circuit (Hay, Martin and Turner 1961).

The capacitance of the air-sensing condenser, C_a , is related to its capacitance when in vacuum, C_0 , by Equation (2).

$$C_a = \epsilon \left(\epsilon_0 \frac{A}{d} = n^2 C_0 \right) \quad (2)$$

Here A is the plate area, d is the spacing between the plates of the condenser and ϵ_0 is the permittivity of a vacuum. ϵ is the dielectric constant of the air and n is the corresponding refractive index. This equation applies for a non-conducting, non-ferromagnetic gas between the

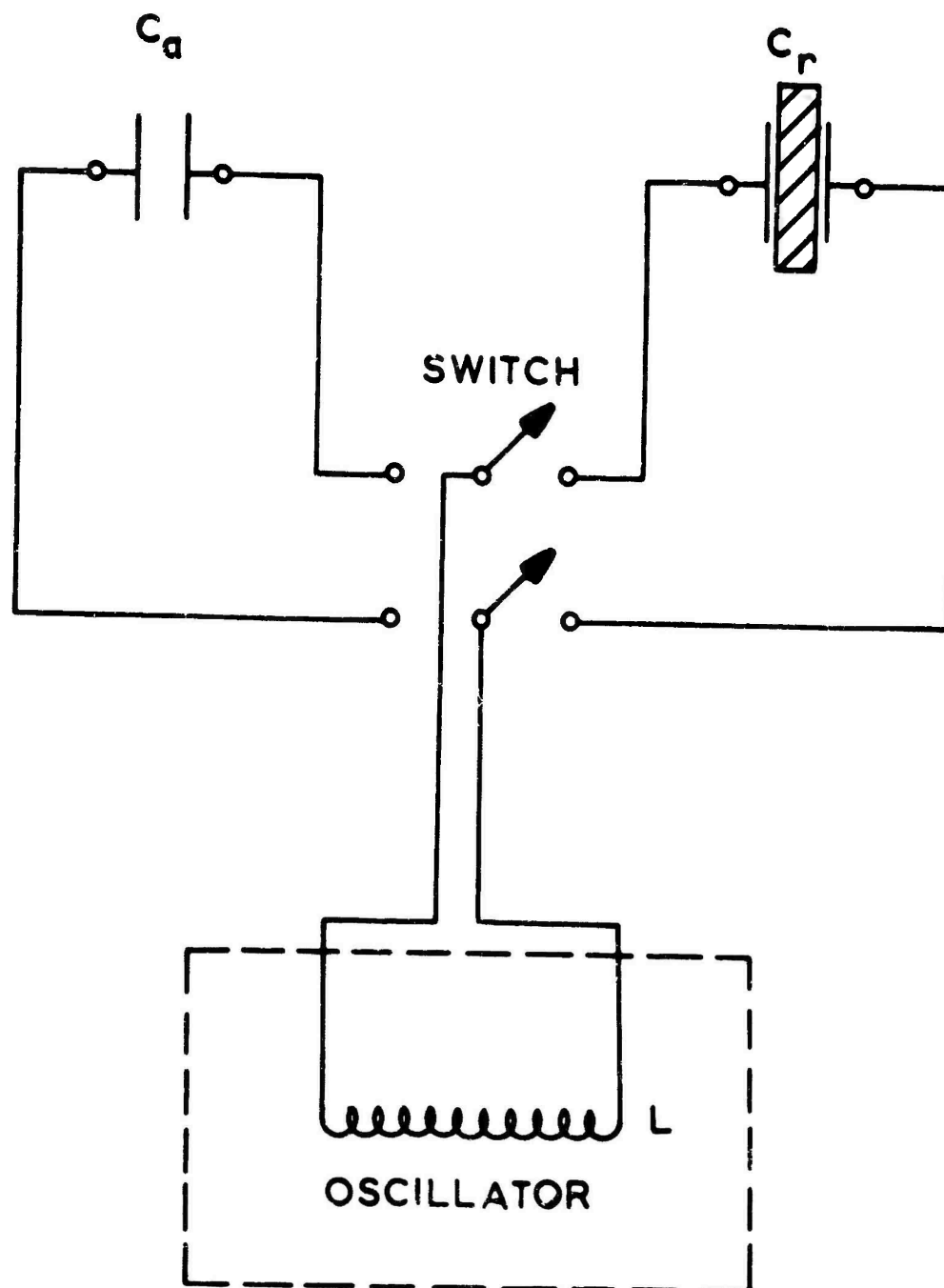


Figure 1: Principle of the Hay refractometer

plates of the air condenser and air in the troposphere may be represented as such a gas for radio frequencies below 25,000 Mc/s. (Stratton, 1941).

Equations (2) and (1) may be combined to indicate the relationship between the oscillator frequency and the refractive index of the air between the plates of the sensing capacitor:

$$f = \frac{f_0}{n} \quad (3)$$

where f_0 is the resonant frequency of the oscillator when the air is evacuated from the space between the capacitor plates. A change in the refractive index of the air from unity (Δn) is associated, then, with a change in oscillator frequency Δf , as indicated by Equation (4):

$$\Delta f = -\left(\frac{f_0}{n^2}\right) \Delta n \quad (4)$$

It will be noted that since the refractive index of the air in the troposphere is always very close to unity, the change in refractometer signal frequency is directly proportional to the change in refractive index of the air.

It is of interest here to note the relationship between the capacitance of the air-sensing capacitor and the uncondensed water vapour in the air. A change in this capacitance, ΔC_a , is related to a change in the refractive index of the air, Δn , by Equation (5):

$$\Delta C_a = (2n C_0) \Delta n \quad (5)$$

In turn, the refractive index is governed by the total air pressure, p , the air temperature, T , and the partial pressure of water vapour, e , of the air through Equation (6):

$$n = 1 + \left(\frac{A}{T}\right) p + \left(\frac{B}{T^2}\right) e \quad (6)$$

The values of the constant coefficients A and B are not universally accepted at the present time, but the following values are in common usage:

$$A = 7.76 \times 10^{-5}$$

$$B = 0.373$$

when pressures are expressed in millibars and temperature is in degrees Kelvin (Bean 1962). For normally encountered air temperatures and pressures in the troposphere, (i.e. when p is of the order of one thousand millibars and T is of the order of 300°K), Equation (6) shows that a change in refractive index of the air is approximately linearly related to a change in the partial vapour pressure of the air, even at conditions approaching saturation. The small non-linearity is caused by the dependence of p on e. Thus, Equations (5) and (6) indicate that the change in capacitance of the air condenser should follow approximately linearly the change of partial water vapour pressure of the air. Further reference will be made to this relationship in the next section.

A similar relationship exists in the microwave refractometer. The sensing device in this instrument is a ventilated microwave cavity, in which the resonant frequency is a measure of the refractive index of the air within the cavity (Birnbaum 1950, Crain 1950). Slater (1946) has shown that the resonant frequency of the microwave cavity, f, is related to its resonant frequency when evacuated, f_0 , by Equation (3). Then Equation (4) also holds for the microwave refractometer, and from Equations (4) and (6) it may be seen that the change in microwave refractometer signal frequency, Δf , is almost linearly related to a change in the partial vapour pressure of the air under standard conditions.

2.2 Anomalies at High Relative Humidities

Measurements with the capacitor-type refractometer have demonstrated its flexibility and its high degree of spatial resolution. When the

instrument is borne aloft by a standard meteorological balloon, and is tethered to a ground point, the vertical profiles of air refractivity in the lower troposphere may be obtained repetitively at intervals of only a few minutes. Further, as the sample profiles in Figure 2 indicate, the instrument is capable of resolving fluctuations in refractivity over height intervals as small as only a few inches.* The large change in refractivity at a height of about 33 feet was indicated when the refractometer ascended at its normal rate of one thousand feet per minute just above a condensation stratum. A question arises as to the interpretation of these indicated changes in refractivity, when the refractometer encounters air whose humidity approaches saturation.

The reason for the uncertainty under conditions of high relative humidity is indicated by the results of previous studies. In 1919, Jona reported that the capacitance of an air condenser did not follow the predictions of Equations (2) and (6) above. The apparent capacitance was greater than the theoretical capacitance by an amount which increased as the relative humidity increased. Zahn (1926) investigated this anomaly, and concluded that the departure was due to the adsorption of water vapour upon the condenser plates. The adsorbed layer increased in depth with increasing vapour pressure of the ambient air, to a maximum of about 200 molecule diameters.

*Note: These refractivity profiles have been obtained through a research program supported by the Defence Research Board of Canada, Grant Number 2801-12.

Capacitor-Type Refractometer Soundings
October 1, 1962

(University of Western Ontario)

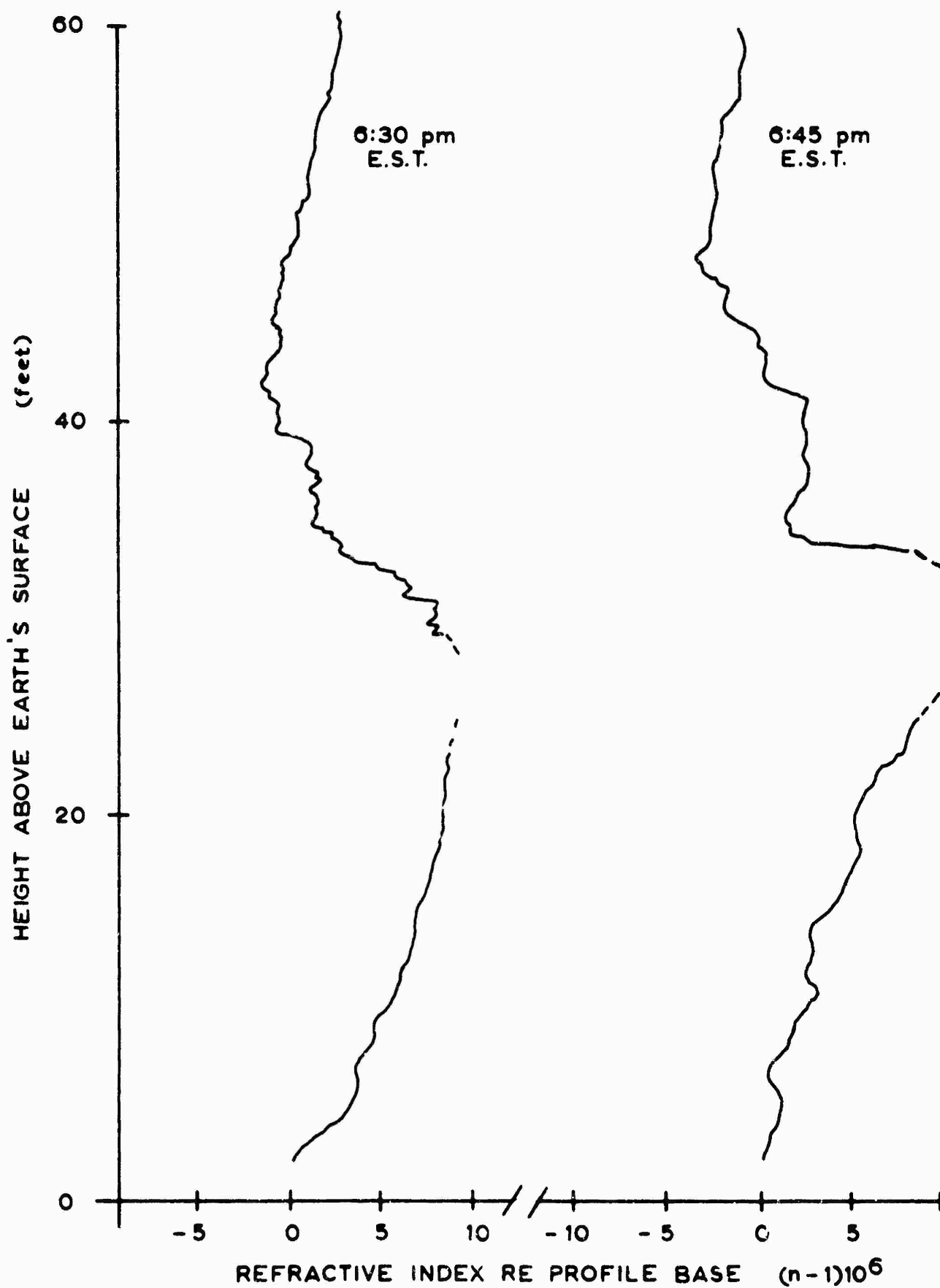


Figure 2

A detailed study of this anomaly in air capacitors was continued by Stranathan (1935). He considered three possible mechanisms for this increase in apparent capacitance: the association of water vapour molecules, increased polarization due to the adsorption of water vapour upon the capacitor plates, and a change in the conductivity of the surfaces of the capacitor insulator. Stranathan concluded that the anomaly is attributed to the added polarization that is contributed by water vapour adsorbed upon the surfaces of the insulators within the condenser. Ford (1948) used the results of measurements upon precision air condensers to support this suggestion. The capacitance anomaly increased with increasing relative humidity of the environment beyond 30 percent. The effect associated with adsorption upon the condenser plates decreased with increasing plate separation; while the effect that is associated with adsorption upon the insulators varies with the dimensions of the exposed surfaces. Veith (1960) has provided further information upon the penetration of moisture into various dielectrics within capacitors, as a function of the ambient humidity, temperature, elapsed time of exposure, and dielectric material.

The allied problem of water vapour adsorption in the sensing cavity of the microwave refractometer also has received some attention. Essen and Froome (1951), in commenting upon Stranathan's earlier work, indicated that there was disagreement among various workers in optical studies upon the depth of the adsorbed layer. They argued that the effects of water vapour adsorption in the microwave cavity of their refractometer were negligible because of the relatively large volume of the cavity with respect to the volume of an adsorbed layer. They noted that their suggestion is supported by the good agreement between their measurements upon the dielectric constant of moist air and the results of others as obtained by different methods.

In 1952, Birnbaum and Chatterjee reported that no anomalies in the dielectric constant of moist air were observed in measurements with their microwave refractometer, for relative humidities up to 90 percent. They suggested that although water vapour may be adsorbed upon the cavity walls, the effect would be negligible upon the cavity resonant frequency because the electric field vanishes at the cavity walls. Three years later, Birnbaum and Bussey (1955) noted that a microwave cavity removes a negligible amount of water vapour from still air through adsorption of the water vapour upon its surfaces. However, they suggested that condensation and evaporation of water upon the cavity surfaces when the ambient air is saturated may have a significant effect upon the indication of the dielectric constant of the air.

The need for a careful study of refractometer measurements under conditions of high relative humidity is apparent. The sensitivity of the capacitor-type refractometer provides a means of examining the adsorption of water vapour within the sensing capacitor, with a high degree of precision. Since the previously reported studies have applied to stationary ambient air at the capacitor, it is important that the present study be extended to include air motion through the sensing elements at the rate normally encountered during a sounding. Further, the instrumentation for this study also will provide a means of examining further the effects of water vapour adsorption and condensation upon the walls of the microwave refractometer cavity.

2.3 Experimental Techniques for Studying Adsorption and Condensation Effects

Two approaches have been followed in studying adsorption and condensation effects in the refractometers. Attention here is concentrated upon the sensing elements of these instruments, and upon their interaction with water vapour in the air at temperatures above freezing.

(a) Optical Ellipsometer

This technique uses polarized monochromatic light to determine the depth of an adsorbed layer upon the surface of a solid material. An incident polarized beam of light is reflected first from the uncontaminated surface, and the polarization of the reflected light is determined by an analyzer. Then the surface of the material is exposed to water vapour in the air, under appropriate conditions, and the resultant change in polarization of the reflected light is observed. The depth of the adsorbed layer upon the material is determined from these measurements and a calibration. The effects of ventilation, changes in relative humidity and temperature are studied, for the metals and dielectrics that are used in the refractometer sensors. This technique and the experimental study will be described in more complete detail in Section 6.

(b) The Experimental Wind Tunnel

This technique provides an environment for the refractometers which is similar in many respects to those found during a normal sounding. In the test volume of the wind tunnel, the air speed is approximately one thousand feet per minute, as found during normal ascents of a radiosonde instrument (Middleton and Spilhaus 1953, Chapter VII). The temperature and relative humidity of the air within the test volume are uniform; the temperature is variable between -20°C and 50°C , while the relative humidity may be changed from 10 to 100 percent. Practical design limitations have required that the air pressure be maintained at surface atmospheric.

The refractive index of the air within the test volume is determined by special instruments. Precise thermometers of the platinum wire type have been constructed and calibrated to measure wet- and dry-bulb temperatures. From these, and the observed air pressure, the refractive index of the air

within the test volume is calculated with a precision of one part in one million; this information then may be compared with the refractivity of the air in this chamber as indicated by the capacitor-type refractometer and the microwave refractometer.

This technique provides a more precise method of studying adsorption effects than the optical ellipsometer. After the thermal coefficients of expansion of the sensors in the capacitor type and the microwave refractometers have been determined, the true and indicated refractivities are observed for various modifications of the refractometer sensing elements and for a wide range of air temperatures and relative humidities.

The results of both of the above procedures are applied to the interpretation of water vapour adsorption effects on the sensing elements. The implications of this study upon the design of the refractometer sensing element will be considered.

3. The Experimental Wind Tunnel

An experimental wind tunnel has been designed and constructed to provide a controlled environment for the refractometers. Since the Hay refractometer ascends at a rate of approximately one thousand feet per minute during a normal sounding, this ventilation speed has been adopted in the wind tunnel. The volume of the test chamber must be adequate to receive the refractometer and other test probes. It is desirable that the wind speed, air temperature and relative humidity within the test volume be maintained as uniform as possible. No attempt has been made to change the air pressure within the test volume from surface atmospheric, since changes in air pressure are of only minor importance to changes in air refractivity.

The range of control of conditions within the test volume exceeds that as specified in the requirements for this study. Air temperature is variable between -20°C and 50°C , while relative humidity may be varied from 10 to 100 percent. The flow of air is essentially uniform throughout the test volume.

A Prandtl-type wind tunnel with single return channel has been chosen as the most practical form for this experiment. The tunnel has a square cross section, and air is circulated by a constant-speed fan. The air temperature is varied by an electric heater and by a refrigeration coil. Steam injection and a dehumidifier refrigeration coil are used to vary the air humidity. Although not required for the present experiment, provision has been made for a rapid change in the air temperature of the test volume, through the use of a by-pass system at the settling chamber.

3.1 Aerodynamic Design

(a) The Test Section (Jet)

A study of the air flow around a model of the Hay refractometer has been carried out by Martin (1961). These observations are summarized in the photographs of Figure 3. In Figure 3(a), it will be seen that the air, which is flowing at a speed of one thousand feet per minute, flows readily through the plates of the sensing capacitor. The laminar flow of air along the baffle adjacent to the sensing capacitor is indicated in Figure 3(b). Figure 3(c) illustrates the flow of air around the refractometer in a plane which is perpendicular to that of the two previous photographs. Here, it will be seen that the air entering the region between the baffle plates is deflected away from the instrument.

It is apparent from this study of wind flow, that an open jet at the test chamber is desirable. This will provide a minimum of interference with the natural air flow about the refractometer. The open jet will have a cross section of two feet by two feet and an axial length of two feet; this test chamber will be located without physical boundaries within a four foot square channel of the wind tunnel.

The design of the jet and other sections of the wind tunnel is based upon the following considerations. For the air moving through the jet,

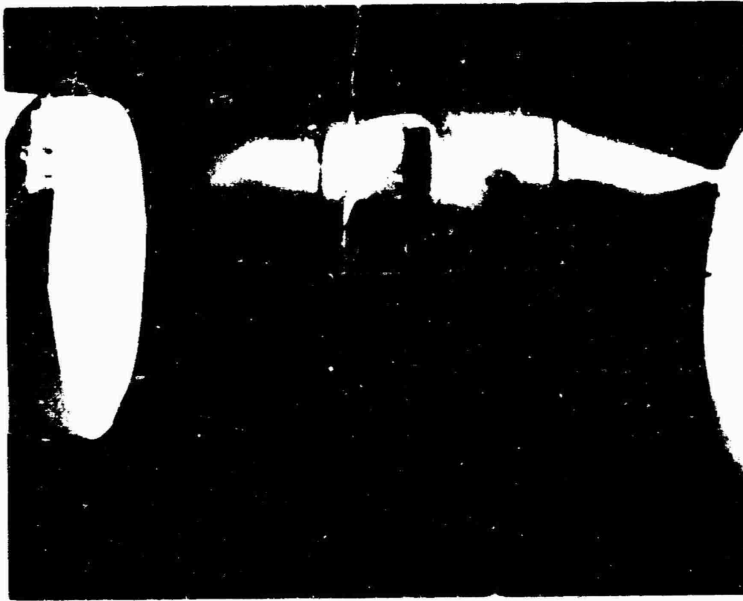
$$\text{Volume of air moved} = \bar{V}_J W_J^2 = 4000 \text{ cu. ft. per minute} \quad (7)$$

where \bar{V}_J = mean air speed at the jet.

W_J = jet cross-section at the test chamber.

An indication of the stability of the air within the jet is the Reynolds' number (R.N._J):

$$\text{R.N.}_J = \frac{\text{forces of inertia}}{\text{forces of viscosity}} = \frac{\bar{V}_J W_J}{\nu} \approx 2 \times 10^5. \quad (8)$$



(a) Through the
sensing capacitor



(b) Along the
baffle plate



(c) Between the
baffle plates

Figure 3: Patterns of air
flow around the
refractometer

where ν = kinematic viscosity of air $\simeq 1.6 \times 10^{-4}$ ft²/sec. at room temperature and surface pressure. (Prandtl 1952, Ch. III).

The largest cross-section of the wind tunnel is four-feet square (W_{\max}), from practical considerations. Here, the air speed is 250 feet per minute (\bar{V}_{\min}) and Reynolds' number is given by Equation (9).

$$R.N. = \frac{\bar{V}_{\min} W_{\max}}{\nu} = 10^5 \quad (9)$$

It will be noted that the Reynolds' numbers for these two critical sections of the wind tunnel are less than 3×10^5 , indicating that turbulent conditions must predominate (Pope 1958, page 108). Consequently, it is desirable that turbulence within the jet (test chamber) be minimized through the appropriate design of the settling chamber and the contraction cone.

(b) The Contraction Cone (Entrance Cone)

A contraction cone provides a gradual transition from the large cross-section of the settling chamber to the small cross-section of the jet. This cone reduces the longitudinal fluctuations in the air speed of the jet, according to Equation (10) (Pope 1958, Ch. II):

$$\frac{\Delta v_J}{\bar{V}_J} = \frac{1}{r^2} \frac{\Delta v_e}{\bar{V}_e} \quad (10)$$

where Δv_J = longitudinal variations of air speed in the jet.

Δv_e = longitudinal variations of air speed ahead of the entrance cone.

\bar{V}_e = mean wind speed ahead of the entrance cone.

$r = \frac{\text{input cross-sectional area}}{\text{output cross-sectional area}}$ of the contraction cone.

For the contraction from the four-foot cross-section of the settling chamber to the two-foot cross-section of the jet, $r = 4$ and \bar{V}_e is 250 feet per minute. Hence,

$$\Delta v_J = 0.25 \Delta v_e \quad (11)$$

The length of the entrance cone is approximately equal to its cross section.

(c) The Settling Chamber

This section of the wind tunnel is located at the input to the entrance cone. Its axial length is long compared with the width of the jet, to reduce the magnitude of the air turbulence. Screens may be inserted in the settling chamber to reduce turbulent fluctuations in the air, if desirable. However, these have not been included in the present design.

(d) The Return Passage

The power that is associated with the flow of air in the wind tunnel is lost at a rate which is proportional to the cube of the air speed. Consequently, it is desirable to make the air speed small as rapidly as possible beyond the jet. Yet the expansion beyond the jet should not be so great that air becomes separated from the walls of the tunnel. An expansion angle of between eight and twelve degrees has been found satisfactory through experience (Pope 1958, Ch. II). In the present tunnel, the expansion angle is 8° . The use of corner turning vanes permits right-angle turns in the direction of the return passage, with little loss of power (Pope 1958, Ch. II).

(e) Power Losses in the Air Stream

Frictional losses within the wind tunnel result in a decrease in static pressure along the axis of flow (Δp). From Bernoulli's equation, it is found that

$$\Delta p = K q \quad (12)$$

where K = loss coefficient for the section.

q = dynamic pressure at the section.

Equation (12) may be applied to each section of the wind tunnel.

The total drop in static pressure around the closed circuit of the wind tunnel may be calculated by the Wattendorf method (Pope 1958, Ch. II). This computation relates losses in all parts of the tunnel to the dynamic pressure of the jet (q_J):

$$Kq/q_J = \frac{\Delta p}{q} \cdot \frac{q}{q_J} = K_o \quad (13)$$

When Equation (13) is applied to each section of the tunnel separately, the total drop in static pressure around the closed circuit is given by Equation (14).

$$\Delta p_{\text{Total}} = q_J \sum K_o \quad (14)$$

The various values of K_J for the different sections of the wind tunnel are listed in Table 1:

TABLE 1
Summation of Losses About Closed Circuit

<u>Section</u>	<u>Formula (Pope 1958, Ch. II)</u>	<u>K_o</u>
Open jet	$K_o = \lambda \left(\frac{L_J}{D_J} \right)$ and $\frac{1}{\sqrt{\lambda}} = 2 \log_{10}(R.N. \lambda) - 0.8$	0.080
Straight Section	$K_o = \lambda \left(\frac{L}{D} \right) \left(\frac{D_J^4}{D^4} \right)$	0.020
Divergent Section	$K_o = \left[\frac{\lambda}{8 \tan(\frac{\alpha}{2})} + 0.6 \tan(\frac{\alpha}{2}) \right] \left(1 - \frac{D_1^4}{D_2^4} \right) \left(\frac{D_J^4}{D_2^4} \right)$	0.025
Corners	$K_o = \left[0.10 + \frac{4.55}{(\log_{10} R.N.)^{2.58}} \right] \left(\frac{D_J^4}{D_4^4} \right)$	$\begin{cases} 2 \times 0.083 \\ 2 \times 0.035 \end{cases}$
Contraction Cone	$K_o = 0.32 \lambda \left(\frac{L}{D_J} \right)$	0.006
Settling Chamber	(same as for straight section)	0.008
Total		<u>0.375</u>

(Subscript J refers to jet section)

where D = tunnel diameter

L = tunnel length

λ = skin friction

R.N. = Reynolds' number

α = divergence angle (wall-to-wall)

Note: Above apply to circular cross-sections, and are taken as representative of conditions in tunnel with square cross-section. (Guide, 1959).

Then the total pressure drop in all tunnel sections is given by Equation (15):

$$\begin{aligned} P_{\text{Total}} &= q_J \sum K_o = \left(\frac{1}{2} \rho V_J^2\right) \sum K_o \\ &= (0.5 \times 0.00237 \times 17^2) \times 0.375 \\ &= 0.128 \text{ pounds/ft}^2 \end{aligned} \quad (15)$$

where ρ = air density

To this must be added the estimated drop in pressure across the refrigeration coil; if this pressure drop is taken as 0.11 pounds per square foot, (a representative value for commercial elements) the total pressure drop around the closed circuit is 0.24 pounds per square foot. This value may be increased to 0.3 pounds per square foot to account for other losses within the tunnel and the square rather than circular cross section.

The energy ratio for the air within the closed circuit is defined through Equation (16):

$$\text{Energy ratio} = \text{E.R.} = \frac{\frac{1}{2} \rho V_J^2}{\Delta P_{\text{Total}}} = 1.14 \quad (16)$$

Hence the net power required to circulate the air is

$$\text{Net power required} = \frac{q_J A_J V_J}{550 \times \text{E.R.}} = \frac{0.34 \times 4 \times 17}{550 \times 1.14} = 0.036 \text{ h.p.} \quad (17)$$

If the efficiency of the electric motor which drives the fan is 0.5, and

the fan blade efficiency is taken as 0.5, the required power of the fan motor is

$$\text{Fan motor power} = \frac{\text{Net horsepower}}{\text{total efficiency}} = \frac{0.036}{0.5 \times 0.5} = 0.144 \text{ H.P.} \quad (18)$$

Thus, it is seen that a 0.25 horsepower fan motor should be adequate for wind propulsion within the tunnel. The rate of rotation of the motor shaft should be such as to provide a wind speed of approximately 1000 feet per minute with a fan blade whose diameter is two feet. A curved, sheet-metal blade is to be used as the propeller.

3.2 Tunnel Construction

The construction of the low-speed wind tunnel has followed the design as indicated above. A wooden framework has been used throughout, with plywood walls 5/8" in thickness. Figure 4 illustrates the details of construction and the physical dimensions. It will be noted that the air channel is square in cross section. The air is moved by a sheet-metal fan which is coupled directly to a 1/3 horsepower motor. The jet or test chamber is a cubic volume, two feet to the side; access to this test chamber is provided by an insulated door containing a window of triple thickness Thermopane glass. A similar window is located on the remote side of the test chamber wall, to permit additional illumination of the jet. All inner surfaces of the wind tunnel are coated with a layer of plastic varnish to provide a moisture seal and a smooth boundary.

The location of other components for the control of air temperature and humidity also is shown in Figure 4. These components will be described in more detail in Section 3.5.

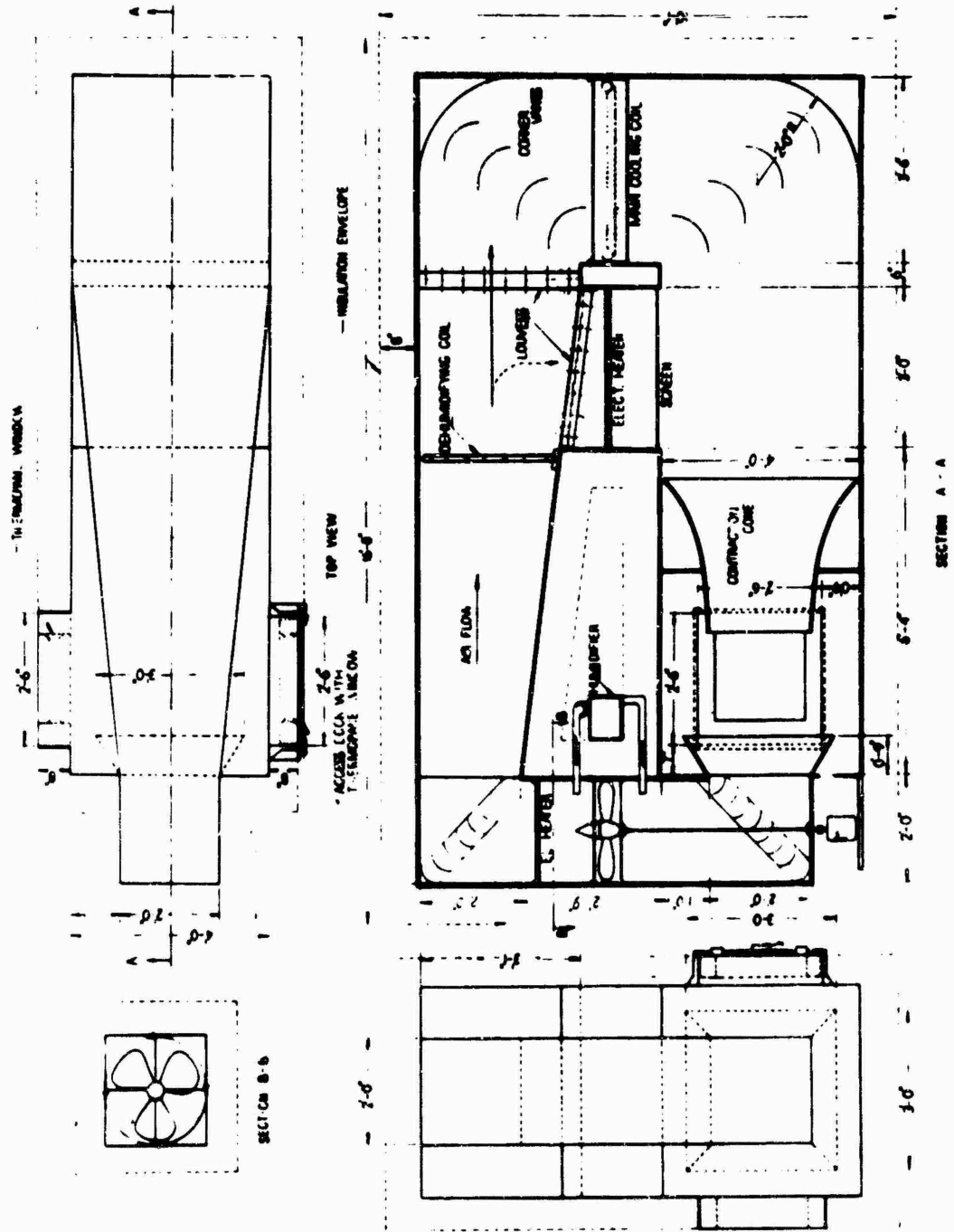


Figure 4: The experimental wind tunnel

3.3 Jet Speed

The degree of uniformity in wind speed within the jet has been examined with a hot-wire anemometer. For this purpose, a trolley system has been constructed around the jet volume, as illustrated in Figure 5. A nylon cord that supports the anemometer probe may be moved in three dimensions by a pulley system that is controlled by electric motors and a crank. All measurements upon the jet are made with the access door closed.

Information on the wind speed within the jet has been obtained with an Alnor Thermo-anemometer, type 8500, serial number 330* accurate to ± 5 feet per minute. Profiles of the wind speed have been obtained for planes which are perpendicular to the jet axis, and separated by axial distances of two inches. Figure 6 illustrates the wind speed profiles in three of these planes. It will be noted that the mean wind speed is 808 feet per minute, and that the variation in wind speed about this mean is within 3 percent over most of the cross-section of the jet.

3.4 Thermodynamic Design

(a) The Cooling Load

Cooling of the air within the wind tunnel is obtained through a commercial refrigeration unit. The principal contributors to the heating of the air within the tunnel, at a given air temperature, are the heat flow through the walls of the wind tunnel and the heat generated by the circulating fan. The contributions from these two sources are calculated as follows:

* Alnor Instrument Company, Division of Illinois Testing Laboratories
Incorporated, 420 North LaSalle Street, Chicago 10, Illinois.

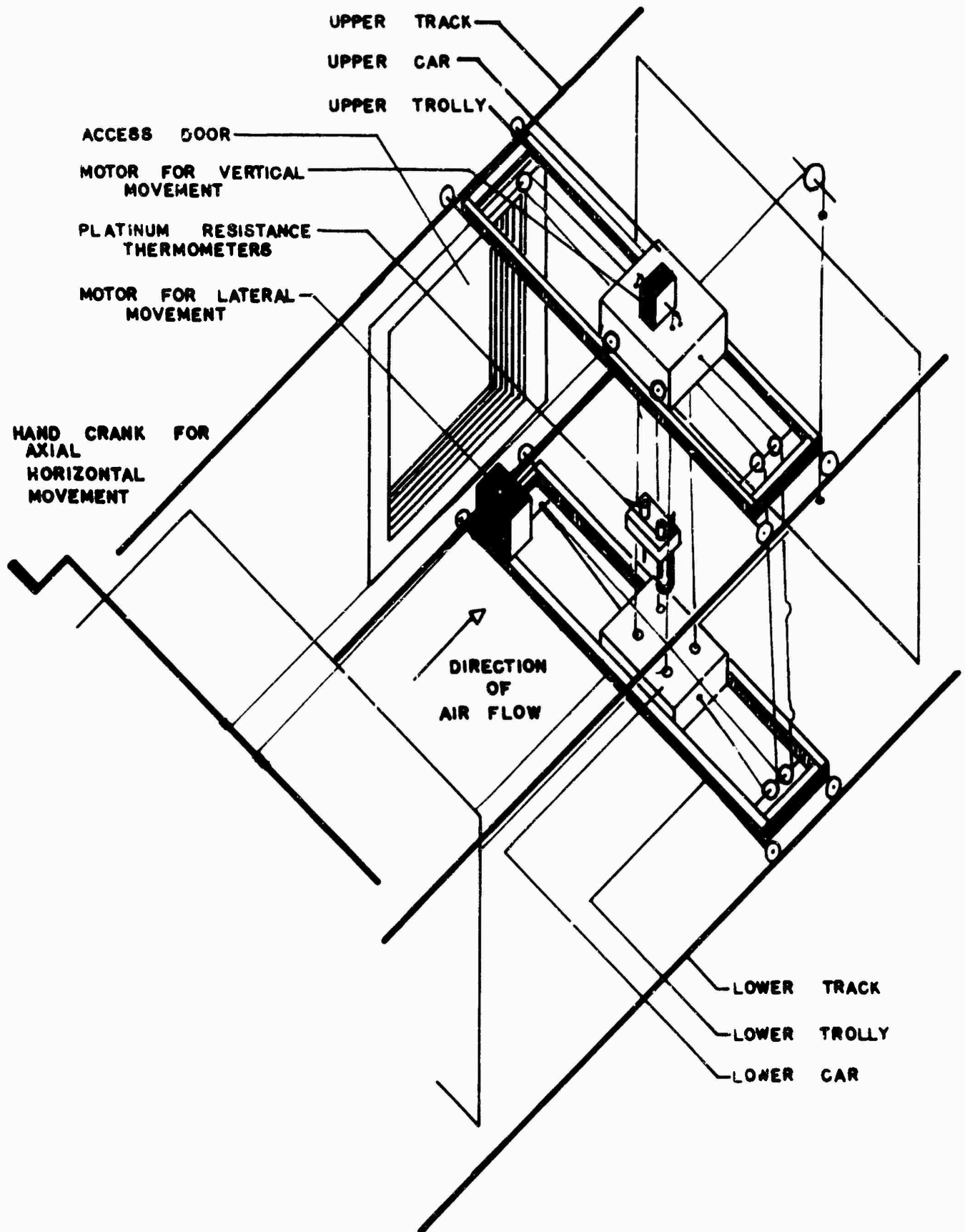


Figure 5: The trolley system for examination of the jet

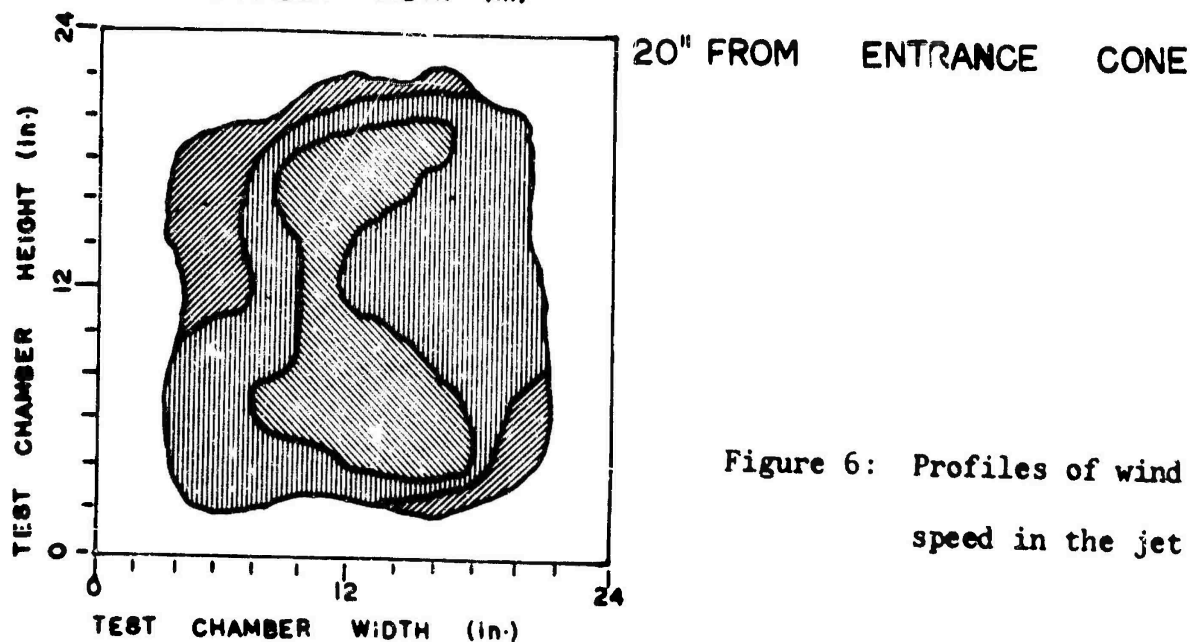
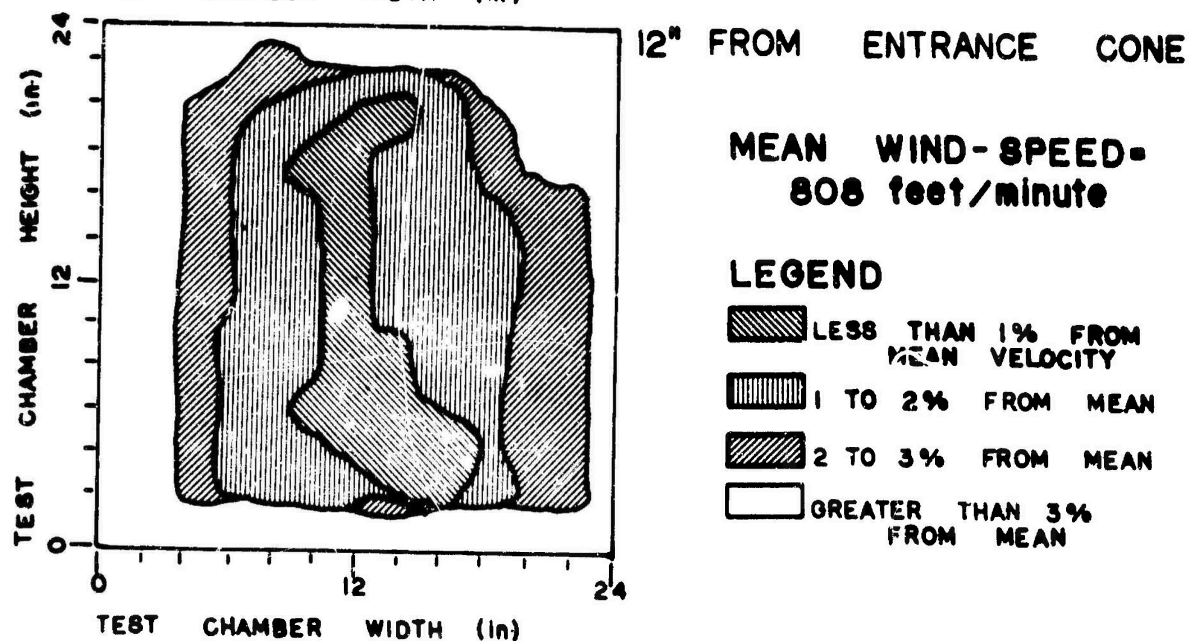
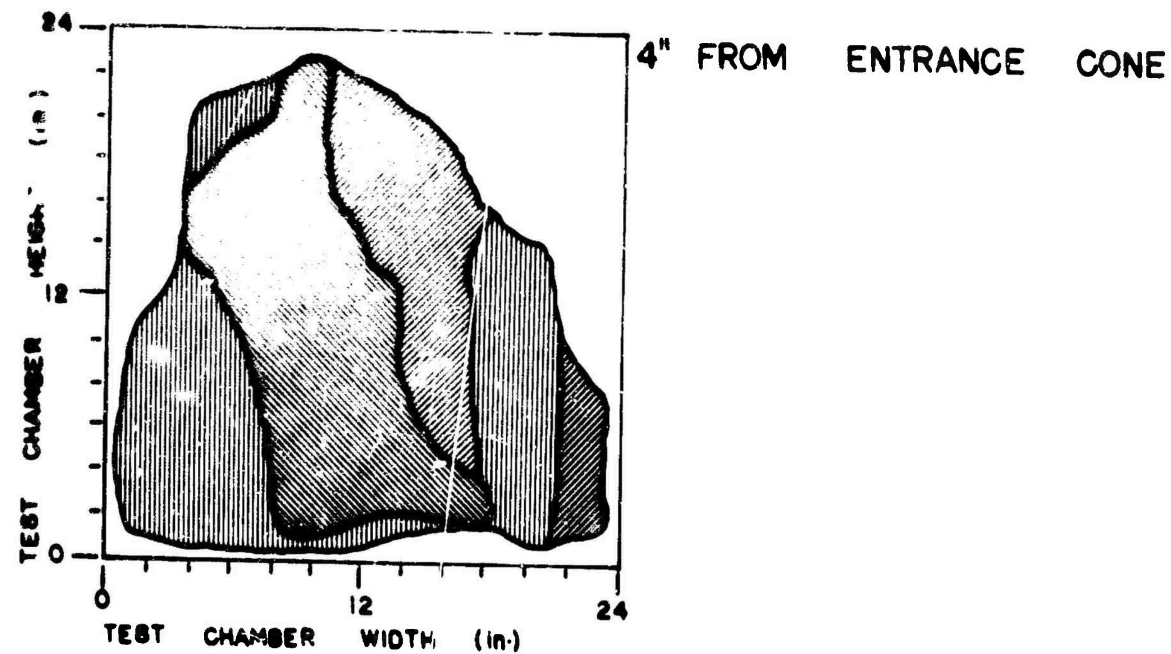


Figure 6: Profiles of wind speed in the jet

Practical considerations have limited the thickness of the insulated wall to approximately 9 inches. This wall consists of an inner surface layer of plastic varnish, applied to 5/8" plywood, which is adjacent to a layer of glass wool insulation 8 inches in depth, held in place by an outer surface layer of greenboard. The heat conductances of these surfaces are listed in Table 2 (Guide 1959, and Eshbach 1961).

TABLE 2
Conductance of the Wall Components

	<u>Conductance</u>
Inner surface layer (air boundary layer)	4.0 BTU/hr. ft. ² °F
Plywood (5/8 in. thick)	1.0 BTU/hr. in. ft. ² °F
Glass wool insulation (8 in. thick)	0.27 BTU/hr. in. ft. ² °F
Outer surface layer (air boundary layer)	1.7 BTU/hr. ft. ² °F

The total conductance (G_{Total}) of the tunnel walls is found through Equation (19):

$$\frac{1}{G_{\text{Total}}} = \sum \frac{1}{G_{\text{component}}} = \frac{1}{4.0} + \frac{5/8}{1.0} + \frac{8}{0.27} + \frac{1}{1.7} = 31 \quad (19)$$

and $G_{\text{Total}} = 0.032 \text{ B.T.U./hr. ft.}^2 \text{ °F.}$

The total outside surface area of the wind tunnel is

$$A = 440 \text{ ft.}^2 \quad (20)$$

If the tunnel is to operate in an environment at 70° Fahrenheit, and if the minimum air temperature within the tunnel is to be -58° Fahrenheit (-50°C), then the maximum temperature difference between the inside and outside of the wall is

$$\Delta T_{\text{max}} = 70^\circ - 58^\circ = 120^\circ \text{F} \quad (21)$$

The total heat transfer (Q) at maximum temperature difference then becomes

$$Q = C_{\text{Total}} \times A \times \Delta T_{\text{max}} = 0.032 \times 440 \times 128 \quad (22)$$

$$= 1800 \text{ BTU/hr.}$$

This value may be increased to 2000 BTU/hr. to account for heat transfer through the thermopane glass windows and through air leakage.

The heat generated by the circulating fan may be calculated by assuming a fan efficiency of 0.5 and recalling the power requirement of Equation (17). Hence the total power converted into heat by the fan is

$$P_{\text{Total}} = \frac{0.036}{0.5} = 0.072 \text{ h.p.} = 180 \text{ BTU/hr.} \quad (23)$$

Thus, the total heat to be removed by the refrigeration unit at maximum temperature difference is

$$Q_{\text{Total}} = Q_{\text{Transfer}} + Q_{\text{Fan}} = 2180 \text{ BTU/hr.} \quad (24)$$

(b) The Refrigeration Unit

The minimum design temperature of the wind tunnel will be considerably lower than that required for the experiments described in this report, for the sake of expediency. As indicated in the previous section, this minimum design temperature is -58°F ; Freon 22 will be used as refrigerant to provide this low temperature. The approximate size of the refrigeration unit is determined from the following considerations:

The pressure-enthalpy chart for Freon 22 refrigerant is drawn for maximum temperature 80°F and minimum temperature -60°F (Eshbach 1961; Jordan and Priester 1956). Between these temperature limits,

$$\text{Cooling effect } Q' = 64 \text{ BTU/lb.} \quad (25)$$

$$\text{Mechanical work } W = 33 \text{ BTU/lb.}$$

Hence the hourly refrigerant weight (ω) is, from Equation (24),

$$\omega = \frac{Q_{\text{Total}}}{Q'} = 34 \text{ lb/hr.} \quad (26)$$

and the mechanical work required per hour is

$$W_{\text{Net}} = (33 \text{ BTU/lb}) \times (34 \text{ lb/hr.}) = 1100 \text{ BTU/hr.} = 0.43 \text{ h.p.} \quad (27)$$

The mechanical efficiency coefficient for a commercial refrigeration unit is taken to be 0.6. Then the total power of the refrigeration unit is

$$W_{\text{Unit}} = \frac{0.43}{0.6} = 0.72 \text{ h.p.} \quad (28)$$

A $\frac{3}{4}$ horsepower refrigeration unit should provide adequate cooling for this wind tunnel.

3.5 Control of Temperature and Humidity

Provision for varying the temperature and humidity of the air within the wind tunnel is made through four controls. In addition to the refrigeration unit described above, there is included also an electric air heater, a steam injector, and a dehumidifying coil. Details of the controlling system are given in Figure 7.

The main evaporator of the refrigeration system is located across the air stream of the wind tunnel to maintain intimate contact with the moving air. The temperature of this evaporating coil may be reduced to -58°F through adjustment of the regulating valves. The area of the evaporating coil fins and the dimensions of the coil are adequate to maintain a maximum temperature difference of about 2°F between the coil temperature and the temperature of the circulating air. This maximum temperature difference (ΔT_{max}) must occur at the lowest coil temperature; as the coil temperature increases, the difference between the coil temperature and the temperature of the circulating air will decrease because of the lessened work load upon the refrigerating coil.

The main evaporator coil provides little control over the relative humidity of the air within the wind tunnel. If the temperature difference between the evaporator coil and the circulating air is the dew point

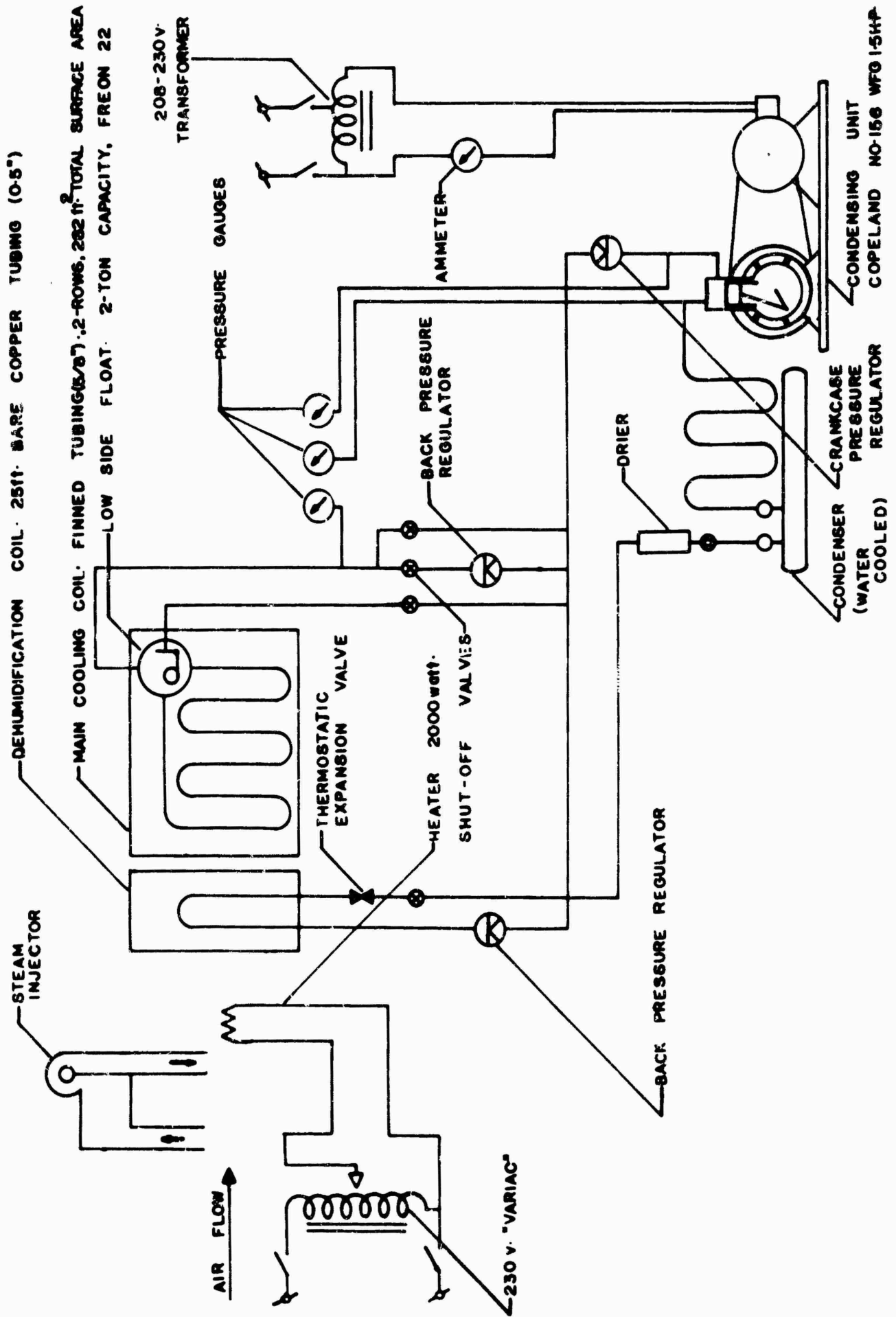


Figure 7: Temperature and humidity controls for the wind tunnel

depression, the relative humidity of the air at -50°F is approximately 88 percent. When the air temperature within the tunnel increases to 32°F , the heat that must be removed from the air by the refrigeration unit is

$$Q_{32} = (Q_{\max} \times \frac{\Delta T_{32}}{\Delta T_{\max}}) + Q_{\text{Fan}} \quad (29)$$

(where ΔT_{32} = difference between ambient temperature and tunnel air temperature)

$$\begin{aligned} &= 2000 \times \frac{70-32}{70-58} + 180 \\ &= 750 \text{ BTU/hr.} \end{aligned}$$

The difference in temperature between the evaporator coil and the circulating air at this new temperature is

$$T_{32} = 2 \times \frac{750}{2180} = 0.7^{\circ}\text{F} \quad (30)$$

and the corresponding relative humidity is greater than 90 percent.

It is apparent that an auxilliary means of controlling air humidity is desirable. For this purpose, a small dehumidifying coil is inserted in the air stream of the tunnel. This coil will have little effect upon the air temperature; temperature compensation may be introduced through use of the electric heater element. By operating the dehumidifying coil at a temperature well below that of the circulating air, the relative humidity of the air may be reduced to the desired value. A steam injector is provided, to increase the relative humidity of the air at a given temperature, when required.

3.6 Operation of the Wind Tunnel

The completed wind tunnel has provided very satisfactory operation during the course of the study reported here. A general view of the tunnel with its associated apparatus is shown in Figure 8. The jet is located behind the door in the center foreground; the air circulation is clockwise in this photograph. The circulating fan and the electric heating coil are

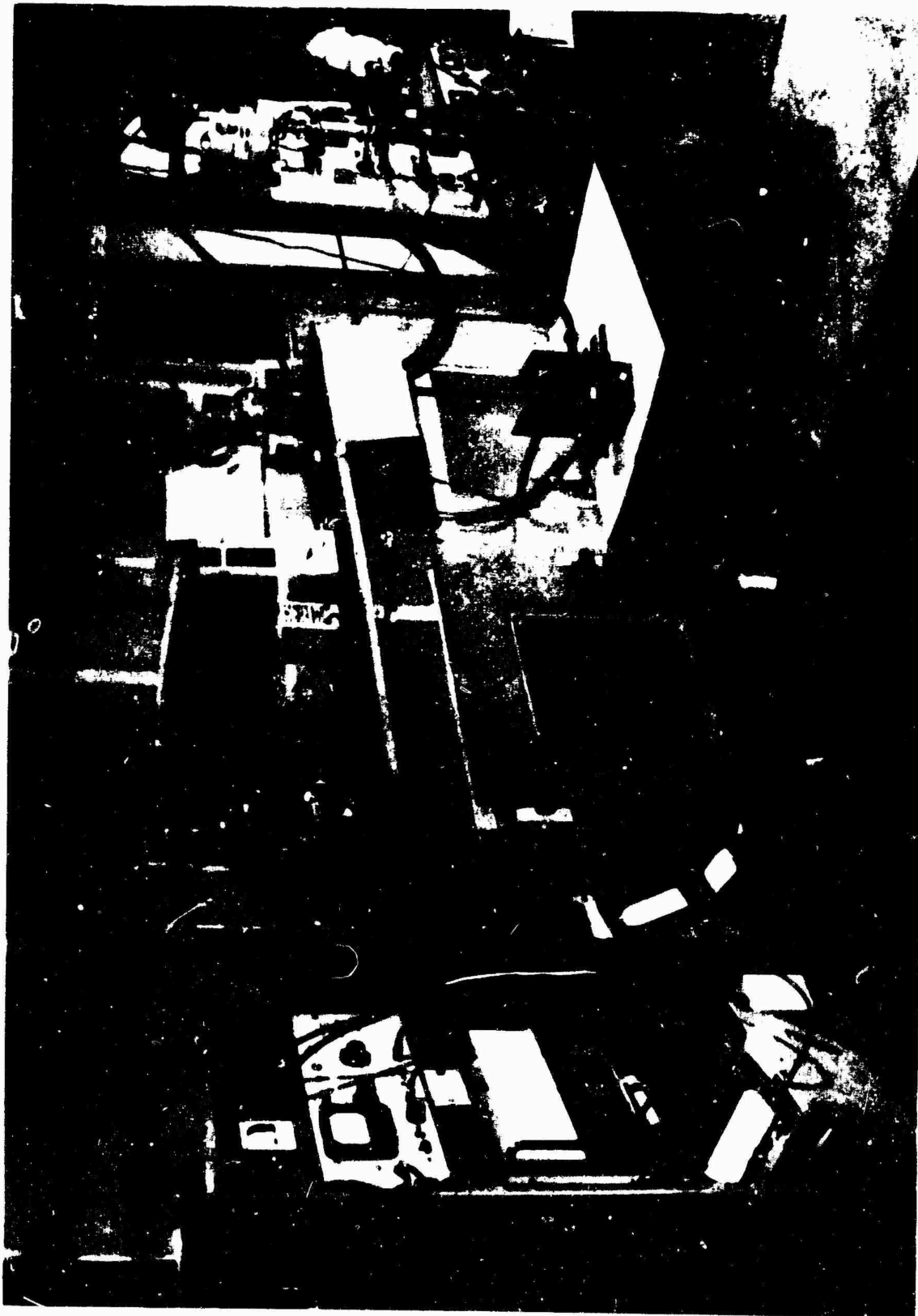
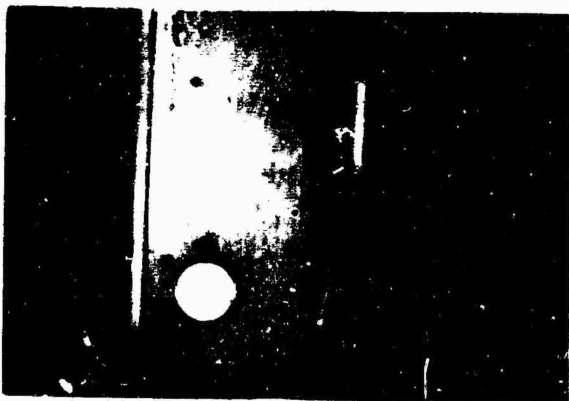


Figure 8: The experimental wind tunnel

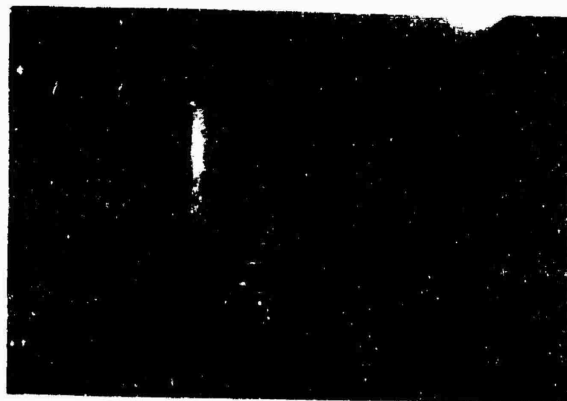
located in the vertical arm at the left, and a steam injector introduces water vapour into the tunnel at this same point. A dehumidifier coil is located in the center of the top arm of the tunnel, while the refrigeration coil is found in the center of the vertical arm at the right. The control panel for the refrigerator and the refrigeration unit are located on the extreme right of the photograph. Photographs of construction details of the wind tunnel are found in Figure 9.

Experience has shown that a high degree of control in air temperature and humidity is available in the jet. The electric heater will increase the air temperature at approximately 5°C per hour, while the refrigeration unit will decrease the air temperature at a rate of approximately 6°C per hour. During most of the experimental observations reported here, the air temperature within the jet has been maintained at some stationary value between 10 and 50°C ; at each temperature, the relative humidity of the air has been varied from about 20 percent to saturation. Careful adjustment of the heater and refrigerator controls will maintain the air temperature within 0.1°C for the complete range of relative humidities.

The uniformity of temperature and humidity within the jet has been ascertained through measurements with precision thermometers. These thermometers have been calibrated to read temperatures with an accuracy of $\pm 0.01^{\circ}\text{C}$; they will be described in greater detail in Sections 5.3, 5.4. Figure 10 shows the measured distribution of wet- and dry-bulb temperatures within the empty jet. Over the volume which would be occupied by the Hay refractometer, the variation in dry-bulb temperature is within 0.03°C , while the change in wet-bulb temperature is within 0.05°C . These measurements were made at a mean air temperature of 40°C and a relative humidity of approximately 75%; the temperatures are even more uniform for lower humidities and mean temperatures of 30, 20 and 10°C .



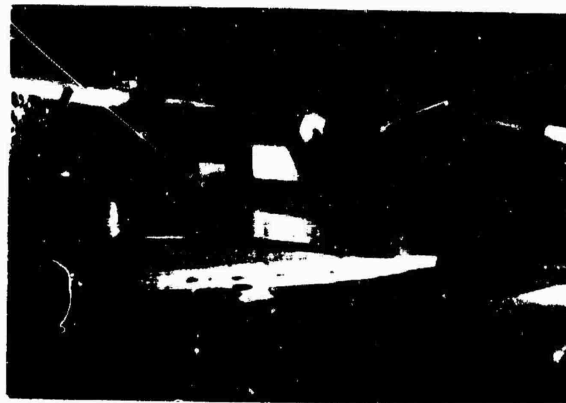
(a) The jet, showing hygrometer and barometer at exit cone, and refractometer on glass stand



(b) The entrance cone, looking through the jet to the exit cone



(c) The propeller (lower), humidity injector (center), and electric heater (upper)



(d) The steam generator (humidifier)

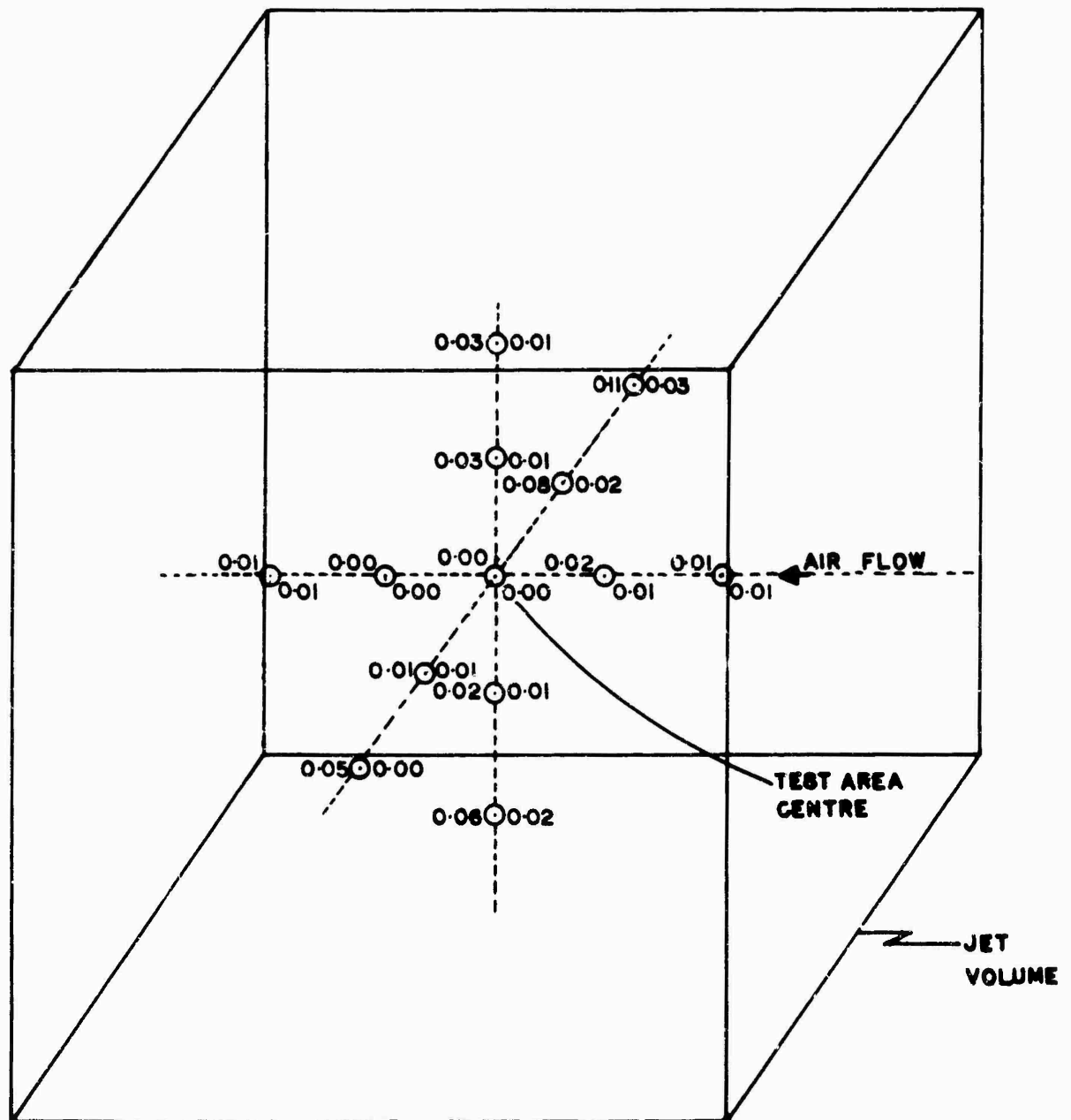


(e) Turning vanes below the refrigeration coil, at input to the settling chamber



(f) The refrigeration system

Figure 9: Details of the wind tunnel

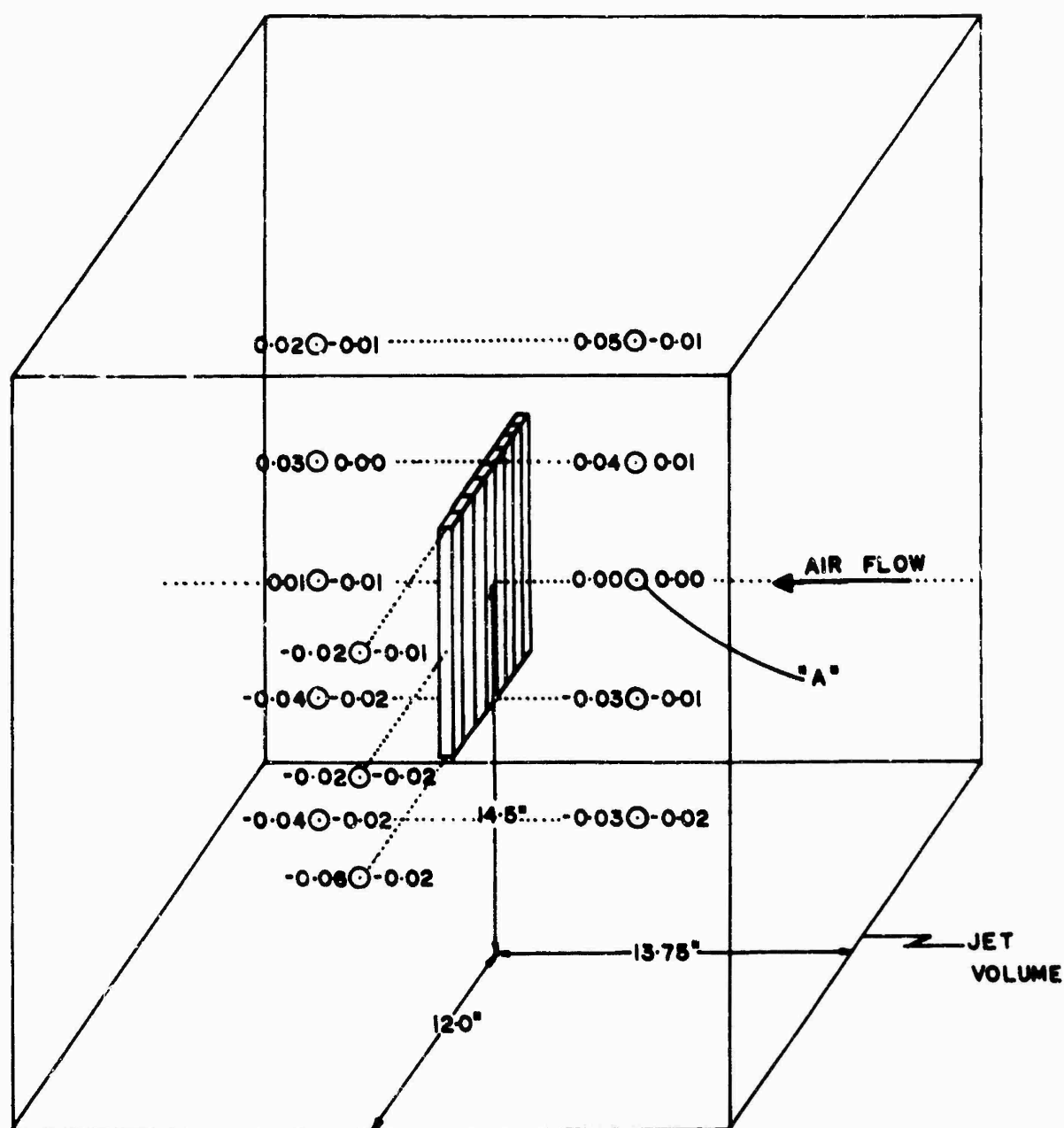


CENTRE TEMPERATURE: 40.64°C
 CENTRE HUMIDITY: 76%
 MEASUREMENT POINTS SEPARATED BY 4"
 AND TAKEN RE TEST AREA CENTRE

NOTE:
 DRY BULB TEMP. ◯ WET BULB TEMP.
 (ON LEFT) (ON RIGHT)

Figure 10: Wet- and dry-bulb temperatures in the center of the jet, -
 Vacated

The insertion of the Hay refractometer in the jet has been found to modify the previous distributions of temperatures by a negligible amount. Figure 11 represents the measured temperatures about the refractometer when inserted in the jet. Again, the mean temperature for this series of measurements is 40°C, and the mean relative humidity is 71%.



CENTRE TEMPERATURE: 39.52°C

CENTRE HUMIDITY: 71%

READINGS TAKEN 4" FROM CAPACITOR PLATES
AND TAKEN RE POINT "A"

NOTE:

DRY BULB TEMP ⊙ WET BULB TEMP
(ON LEFT) (ON RIGHT)

Figure 11: Wet- and dry-bulb temperatures in the center of the jet, -
With refractometer in position

4. The Test Refractometers

Two refractometers of different design have been used in the experimental study that is reported here. One is the microwave refractometer, that has been in wide-spread use for more than ten years. The other is the capacitor-type (Hay) refractometer, which has been undergoing development recently.

In principle, both types of refractometers make use of a resonant circuit to indicate changes in the refractive index of the sampled air. The governing equations for these instruments have been presented in Section 2.1. However, there is a significant difference in the physical construction of the sensing elements of these two refractometers; the microwave refractometer has an all-metal sensing element in the form of a ventilated resonant cavity, whereas the sensing element in the Hay refractometer is an air capacitor with metal plates and dielectric insulators. More complete details are given in the references published elsewhere.

The principal interest in the study reported here is in the interaction between the sensing elements of these refractometers and the humidity of the sampled air. Attention will be confined chiefly to these aspects of the instruments in the following sections.

4.1 The Microwave Refractometer

(a) The Refractometer Circuit

The circuit of the microwave refractometer used in the current experimental study is essentially that described by Birnbaum (1950). The instrument operates at a frequency of approximately 9100 Mc/s. During a measurement upon air refractivity, the sampled air is passed through a ventilated microwave cavity and the resonant frequency of this cavity is

compared with the resonant frequency of a sealed reference cavity. A change in the frequency of the ventilated cavity is an indication of a change in the refractive index of the sampled air, according to Equation (4).

The components of the microwave refractometer are indicated in Figure 12.* Some modifications of the Birnbaum refractometer, as suggested by Thompson and Vetter (1958), are included in this circuit; other changes have been made at this laboratory to improve upon the circuit stability. Further details on the microwave components and the electronic circuits are found in Appendix I.

The microwave sensing cavity is similar to those in current use elsewhere. This cavity has been described by Adey (1957); 67 percent of the end-plate area has been removed for good ventilation. The barrel of the cavity is of invar, and the end plates are of brass. The TE_{011} mode is employed, and the loaded Q is approximately 16,000. A photograph of the microwave cavity is shown in Figure 13.

(b) Calibration

A test of the refractometer stability has been made before the calibration was carried out. This test was made after a complete servicing of the electronic equipment and the incorporation of minor changes in the circuit. It was found necessary to shield the electronic circuit from drafts within the laboratory, to mount the reflex klystron in an oil bath that is water cooled, and to insulate the reference cavity, in order to achieve acceptable stability in the refractometer operation. After the

* The electronic circuits, microwave cavities and other components of the microwave refractometer have been obtained on loan from the Defence Research Board of Canada, Ottawa.

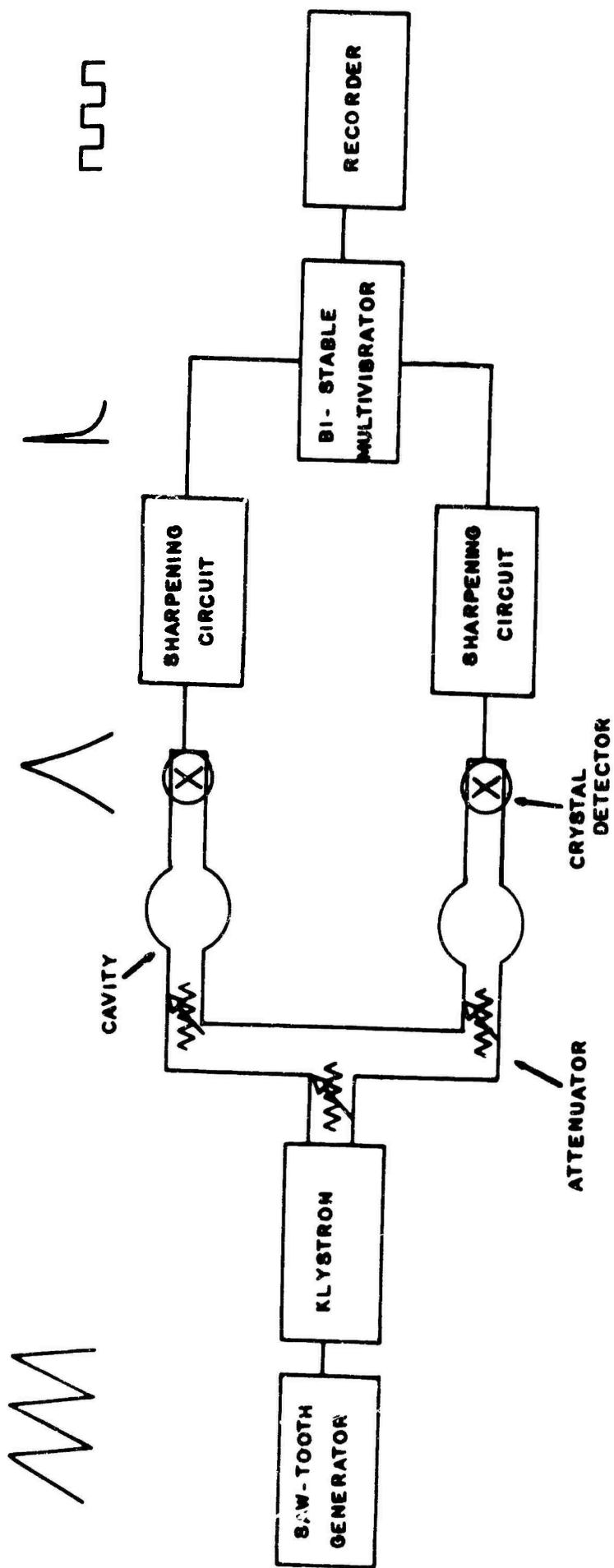


Figure 12: The basic circuit of the Microwave Refractometer



Figure 13: The microwave sensing cavity

equipment has been operating for several hours, the refractometer is sufficiently stable over a period of one hour to indicate a change in refractive index of the sampled air as small as one part in one million.

The calibration of the microwave refractometer is based upon the following considerations. It is well known that dry nitrogen gas at normal temperatures and pressures obeys the ideal gas law. Then the dielectric constant of dry nitrogen gas is related to the gas pressure and temperature through Equation (31) (Lyons, Birnbaum and Kryder 1948; Essen and Froome 1951):

$$\epsilon = 1 + 2.11 \times 10^{-4} \frac{p}{T} = n^2 \quad (31)$$

where p = gas pressure in mm. of Hg.

T = absolute gas temperature.

ϵ = dielectric constant.

n = index of refraction.

at radio frequencies remote from resonances.

For a gas temperature of 21°C, the change in gas pressure (Δp millimeters of Hg.) is related to a change in the refractive index (Δn) by Equation (32) (for $n \approx 1.0003$)

$$\Delta n \Big|_{(T = 21^\circ\text{C})} = 3.57 \times 10^{-7} \Delta p \quad (32)$$

The microwave refractometer is calibrated by inserting the sensing cavity in a sealed and evacuated cavity, and by varying the pressure of dry nitrogen gas that is introduced into this chamber. The temperature of the gas is maintained at 21°C, as indicated by a precision thermometer (see Figure 14).

The experimental calibration of the microwave refractometer is indicated in Figure 15. The experimental procedure was repeated three times.

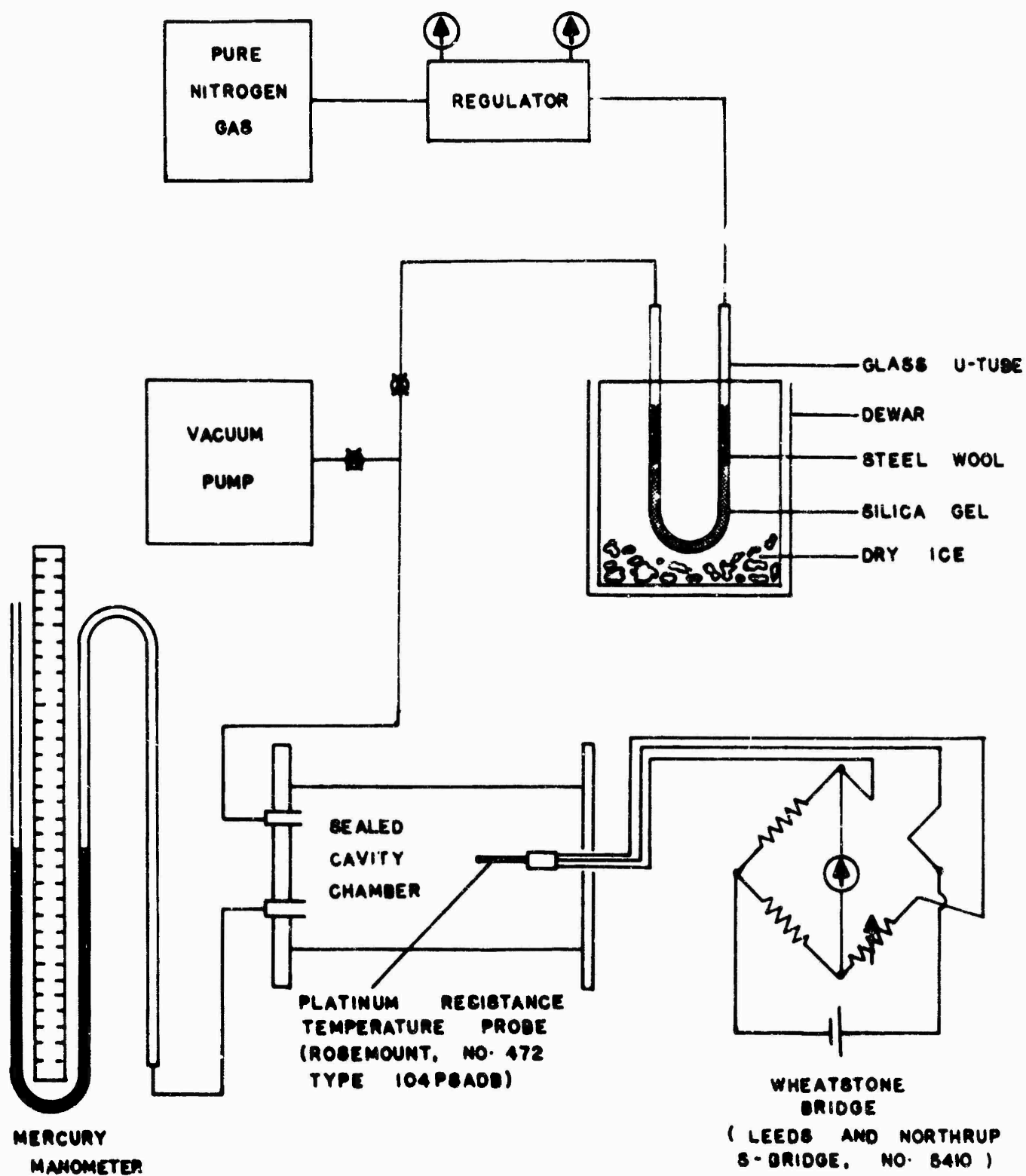


Figure 14: Calibration apparatus for the Microwave Refractometer

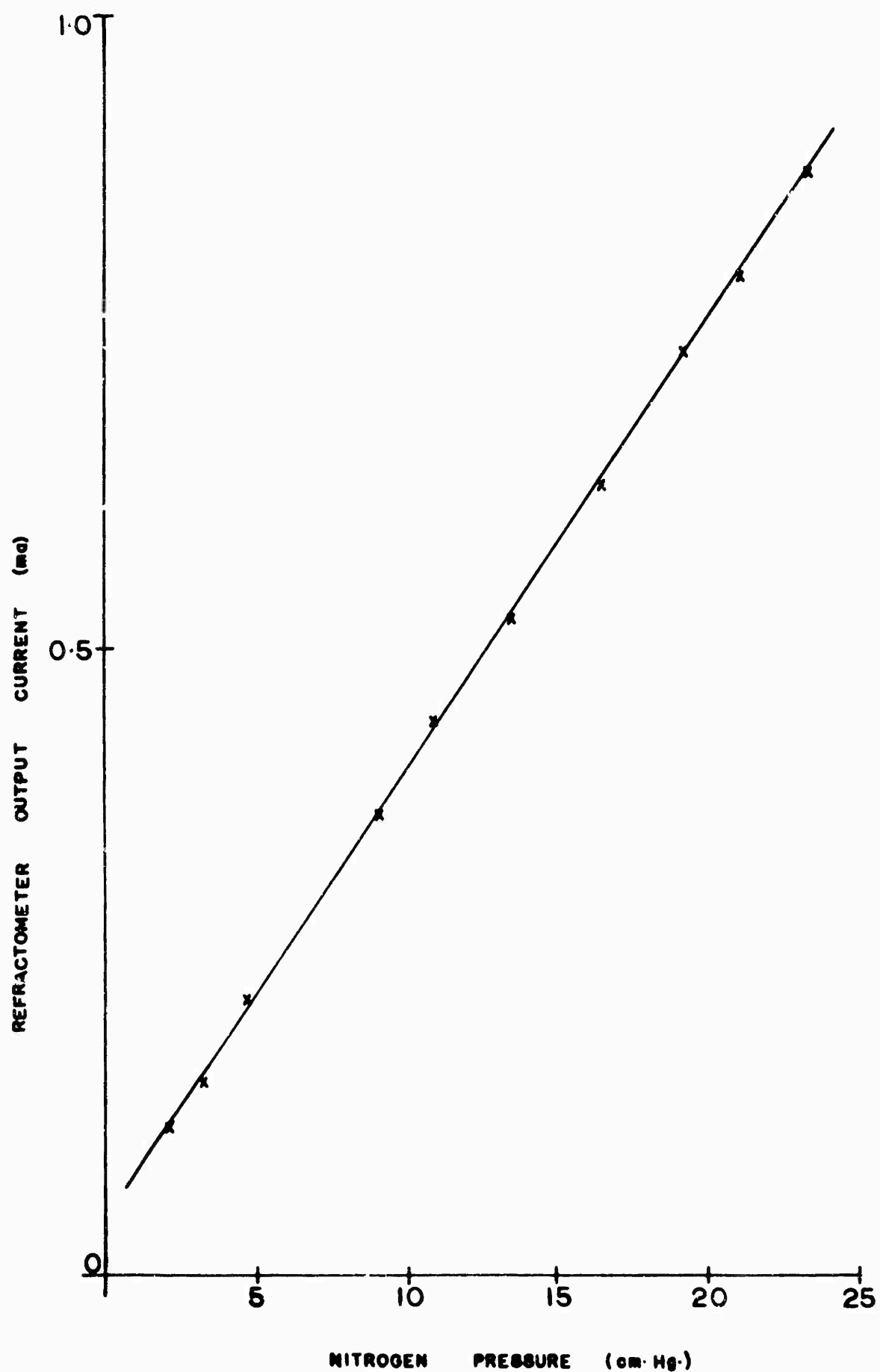


Figure 15: Calibration curve for the Microwave Refractometer

and the slope of the current vs. gas pressure curve was ascertained. From this information, and Equation (32), it was found that the recorder output varied linearly with the change in refractive index of the test gas; a change in recorder current of 0.010 milliamperes represents a change in refractive index of the test gas of one part per million.

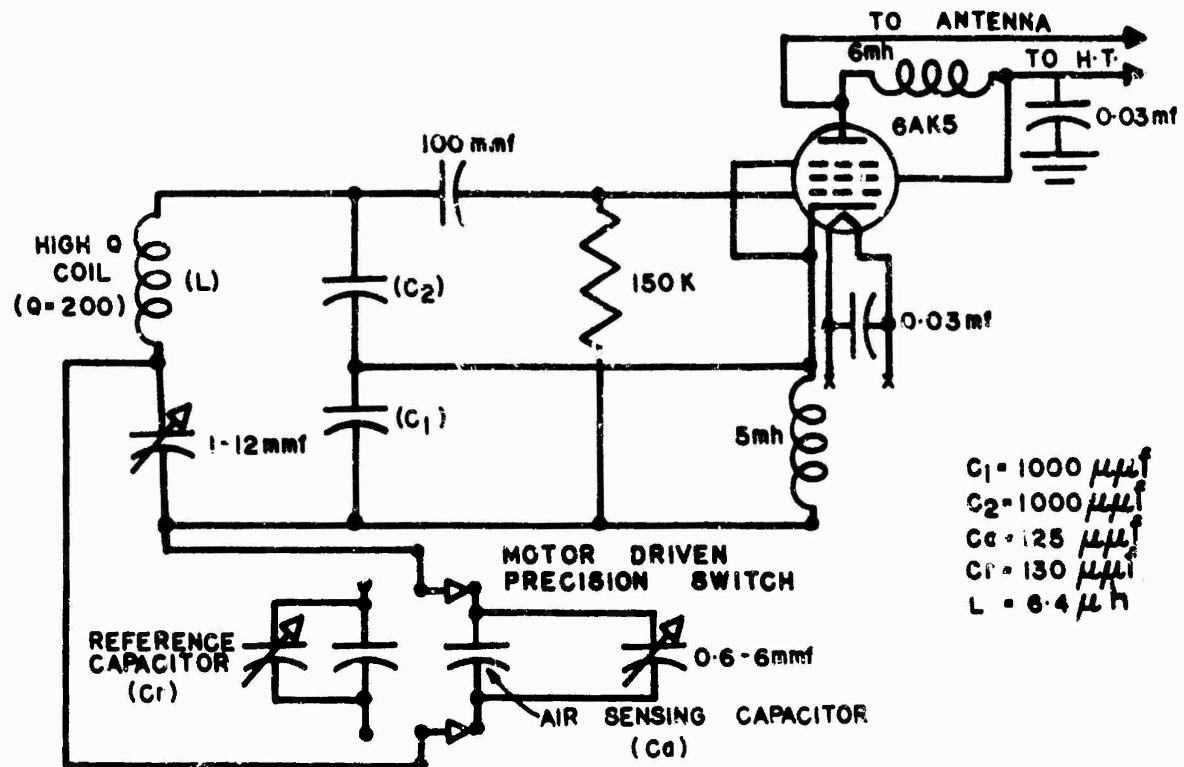
4.2 The Capacitor-Type (Hay) Refractometer

(a) The Refractometer Circuit

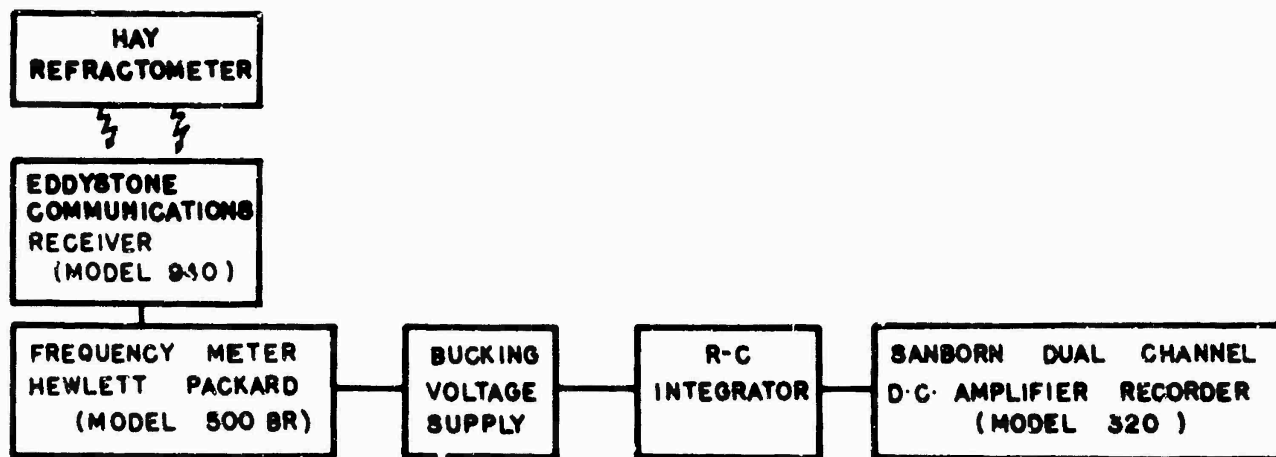
The second of the test refractometers used in the current study is the capacitor-type refractometer. The sensing element is an air capacitor that forms part of the resonant circuit of an oscillator (Hay, Martin and Turner 1961). The change in resonant frequency of the oscillator is proportional to the change in refractive index of the air between the plates of the capacitor, according to Equation (4). The purpose of the reference capacitor in this refractometer is to eliminate the need for further consideration of the electronic circuit. In this study, the reference capacitor is housed in a water-tight capsule, to prevent interaction between this capacitor and the humidity of the air. Further attention then is directed only to the air-sensing capacitor.

The refractometer instrument used in these studies operates at a frequency of approximately 6 Mc/s. The oscillator section of the circuit is illustrated in Figure 16a. The capacitance of the air-sensing condenser (C_a) is 125 micromicrofarads; the reference capacitor is a quartz-invar cylindrical condenser located near the sensing capacitor.

Figure 16b is a block diagram of the recording receiver for this refractometer. It will be noted that this system consists almost entirely of commercially available components. A high-speed recorder permits careful examination of the refractometer signal.



(a) REFRACTOMETER CIRCUIT (OSCILLATOR SECTION ONLY)



(b) BLOCK DIAGRAM OF RECORDING RECEIVER

Figure 16: The Capacitor-Type Refractometer and its recording receiver

A photograph of the refractometer is shown in Figure 17a. The case is made of smooth bakelite, with baffle projections in the direction of wind flow to permit laminar flow into the sensing capacitor. The latter is supported on bakelite pedestals, out of the turbulent boundary layer of the bakelite box. The reference capacitor is located near the sensing capacitor, in the same wind stream.

The air-sensing capacitor has been modified in numerous ways throughout the study reported here. These various modifications have been made to permit an examination of the interaction between water vapour in the air and the materials of the capacitor. The two basic forms of the sensing capacitor are illustrated in Figure 17b. In one, the capacitor is constructed of invar plates with quartz spacers; the body of the condenser in the second form is entirely of invar plates, with the metal supports for these plates meeting the bakelite of the refractometer box well away from the body of the condenser. Other modifications of these capacitors will be described in Section 7.3.

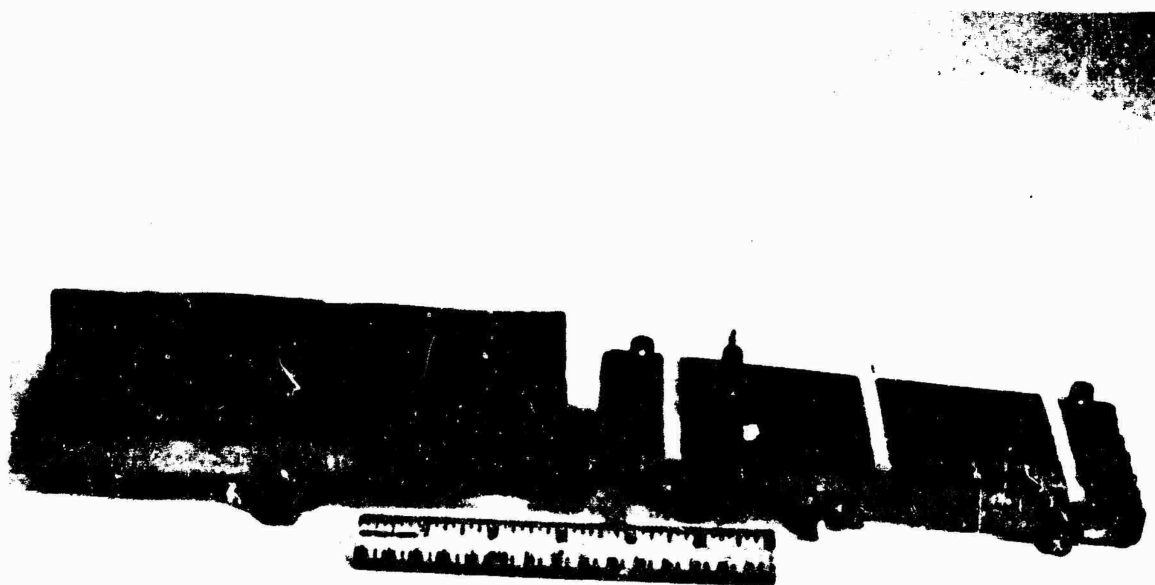
(b) Calibration

A theoretical calibration of the capacitor-type refractometer may be obtained from the analysis of the oscillator circuit. In Figure 16a, it will be noted that the Clapp oscillator frequency is governed by the resonant circuit containing condensers C_1 , C_2 , L and C_3 (i.e. C_a in parallel with its trimmers). The interelectrode impedances of the 6AK5 pentode have negligible effect upon the resonant frequency of this circuit. Then, the resonant frequency (f_0) is given to a good approximation by Equation (33)

$$f_0^2 = \frac{1}{(2\pi)^2 L} \left[\frac{1}{C_1} + \frac{1}{C_2} + \frac{1}{C_3} \right] \quad (33)$$



(a) The refractometer



(b) The dismounted sensing elements: invar capacitor (left)
quartz-invar capacitor (right)

Figure 17: The Hay refractometer and its sensing elements

If the component values of Figure 16a are inserted in Equation (33), with $C_3 = 125 + 10$ micromicrofarads, the resonant frequency of the circuit is

$$f_0 = 6.08 \text{ Mc/s} \quad (34)$$

Small changes in the resonant frequency of the refractometer may be associated with small changes in the refractive index of the sampled air by differentiating Equation (33). Here, it is assumed that other components remain invariant. Equation (35) is obtained directly from Equation (33).

$$\Delta f_0 = - \frac{1}{8 \pi^2 f_0} \cdot \frac{1}{L} \cdot \frac{1}{C_3^2} \cdot \Delta C_3 \quad (35)$$

Since a change in C_3 is identical with a change in C_a (the air-sensing capacitor) then Equation (35) takes the form of Equation (36) for the indicated component values:

$$\Delta f_0 = -1.79 \times 10^{16} \Delta C_a \quad (36)$$

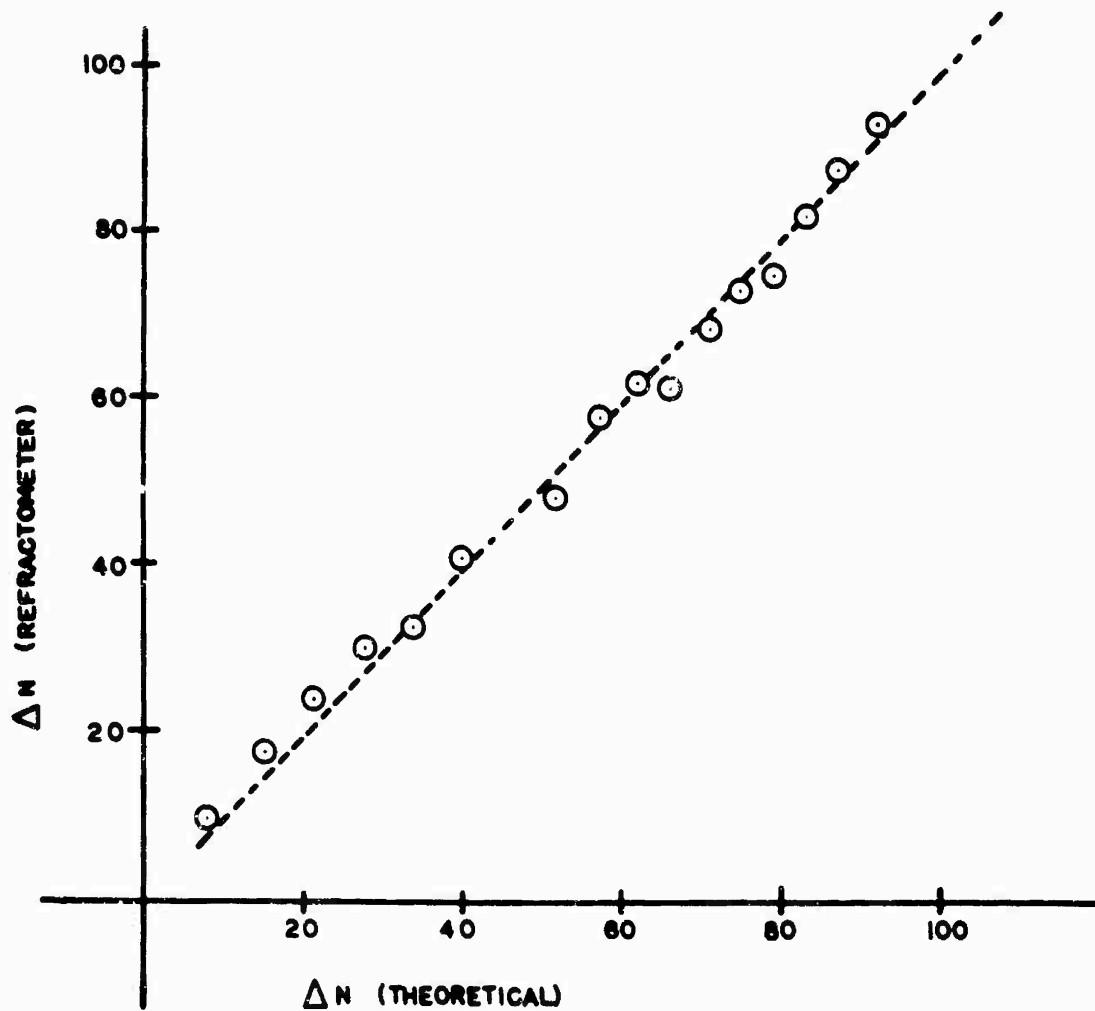
The refractive index of the air in the troposphere is approximately 1.0003, and Equation (5) takes the form of Equation (37).

$$\Delta C_a = 2 C_a \Delta n = 2.70 \times 10^{-10} \Delta n \quad (37)$$

The theoretical calibration of the refractometer is obtained by combining the two previous equations to give Equation (38).

$$\Delta f_0 \text{ (c/s)} = -4.82 \times 10^6 \Delta n \quad (38)$$

Experimental confirmation of this calibration has been obtained by inserting the refractometer in the jet of the wind tunnel. The air temperature in the jet has been maintained at 40°C and the relative humidity at less than 50 percent, to avoid the complication of adsorption effects upon the sensing capacitor. The results of this measurement are indicated in Figure 18. It will be noted that the agreement between the



NOTE: THE ORDINATE SCALE DENOTES THE CAPACITOR-TYPE
REFRACTOMETER OUTPUT FOR A WATER VAPOUR
PRESSURE CHANGE FROM 19 TO 47 mbs. AT 46.5°C

Figure 18: Calibration curve for the Capacitor-Type Refractometer

theoretical and the experimental calibrations is good; the spread in the points about the straight line results from the fact that only one determination of the experimental calibration is shown.

$$(n - 1) 10^6 = N = \frac{77.6}{T} (p + 4810 \frac{e}{T}) \quad (40)$$

where T = absolute temperature

p, e are measured in millibars

The precision that is required in the measurement of the parameters of Equation (40) may be determined as follows. Let Δp be the error in the measurement of total air pressure, ΔT be the error in the measurement of air temperature, and Δe be the error in the measurement of partial vapour pressure of water. It is assumed that these errors are distributed normally about the mean values. Then the rms error in refractivity (ΔN) is obtained by differentiation of Equation (4) to give the following:

$$\Delta N = \frac{77.6}{T} \left[(\Delta p)^2 + \left(\frac{p}{T} + \frac{9620 e}{T^2} \right)^2 (\Delta T)^2 + \left(\frac{4810}{T} \right)^2 (\Delta e)^2 \right]^{\frac{1}{2}} \quad (41)$$

If it is assumed that the errors are distributed equally among the given parameters, and that refractivity is to be ascertained within one part per million, then the required precisions in pressure, temperature and vapour pressure are as given by Equation (42):

$$\Delta p = 7.44 \times 10^{-3} T \quad (42)$$

$$\Delta T = 7.44 \times 10^{-3} T \left/ \left(\frac{p}{T} + \frac{9620 e}{T^2} \right) \right.$$

$$\Delta e = 1.55 \times 10^{-6} T^2$$

It will be assumed in this study that the air pressure is approximately one thousand millibars, and that the air temperature lies between 0°C and 40°C. Then the partial pressure of water vapour in the air lies between 0 and 75 millibars. Equation (43), then, gives the highest required precisions of measurement of each of these parameters throughout this range of variables:

$$\Delta p = \pm 2.3 \text{ millibars (at lowest temperature)} \quad (43)$$

$$\Delta T = \pm 0.23^\circ\text{K (at highest temperature and vapour pressure)}$$

$$\Delta e = \pm 0.15 \text{ millibar (at lowest temperature)}$$

$$(n - 1) 10^6 = N = \frac{77.6}{T} (p + 4 \times 10 \frac{e}{T}) \quad (40)$$

where T = absolute temperature

p, e are measured in millibars

The precision that is required in the measurement of the parameters of Equation (40) may be determined as follows. Let Δp be the error in the measurement of total air pressure, ΔT be the error in the measurement of air temperature, and Δe be the error in the measurement of partial vapour pressure of water. It is assumed that these errors are distributed normally about the mean values. Then the rms error in refractivity (ΔN) is obtained by differentiation of Equation (4) to give the following:

$$\Delta N = \frac{77.6}{T} \left[(\Delta p)^2 + \left(\frac{p}{T} + \frac{9620 e}{T^2} \right)^2 (\Delta T)^2 + \left(\frac{4 \times 10}{T} \right)^2 (\Delta e)^2 \right]^{\frac{1}{2}} \quad (41)$$

If it is assumed that the errors are distributed equally among the given parameters, and that refractivity is to be ascertained within one part per million, then the required precisions in pressure, temperature and vapour pressure are as given by Equation (42):

$$\begin{aligned} \Delta p &= 7.44 \times 10^{-3} T \\ \Delta T &= 7.44 \times 10^{-3} T \left/ \left(\frac{p}{T} + \frac{9620 e}{T^2} \right) \right. \\ \Delta e &= 1.55 \times 10^{-6} T^2 \end{aligned} \quad (42)$$

It will be assumed in this study that the air pressure is approximately one thousand millibars, and that the air temperature lies between 0°C and 40°C. Then the partial pressure of water vapour in the air lies between 0 and 75 millibars. Equation (43), then, gives the highest required precisions of measurement of each of these parameters throughout this range of variables:

$$\begin{aligned} \Delta p &= \pm 2.3 \text{ millibars (at lowest temperature)} \\ \Delta T &= \pm 0.23^\circ\text{K (at highest temperature and vapour pressure)} \\ \Delta e &= \pm 0.15 \text{ millibar (at lowest temperature)} \end{aligned} \quad (43)$$

A further step must be taken in the analysis of the measurement of partial water vapour pressure. The psychrometric formula, as given by Equation (44) provides a practical relationship between the partial vapour pressure of water and the temperatures of the air.

$$e = e_w - a (1 + bT_D)p (T - T_D) \quad (44)$$

where T_D = wet-bulb temperature

e_w = saturation vapour pressure at T_D (in millibars)

$a \simeq 6.6 \times 10^{-4}$ (for T, T_D in $^{\circ}\text{C}$)

$b \simeq 11.5 \times 10^{-4}$ (for T, T_D in $^{\circ}\text{C}$)

This equation is based upon experimental observations; the coefficients "a" and "b" vary among different authors, as will be indicated later.

The results of the above analysis now may be extended to the psychrometric equation. Equation (44) may be differentiated; and if it is assumed that the errors are distributed equally among the variables, an rms error of 0.15 millibars in e will place the following requirements upon the parameters of Equation (44):

$$\begin{aligned} \Delta p &= \pm \frac{0.15}{2} \left[aT (1 + bT_D - \frac{T_D}{T} - b \frac{T_D^2}{T}) \right]^{-1} \\ \Delta T &= \pm \frac{0.15}{2} \left[ap (1 + bT_D) \right]^{-1} \\ \Delta T_D &= \pm \frac{0.15}{2} \left[ap (1 - bT + 2bT_D) \right]^{-1} \end{aligned} \quad (45)$$

Examination of Equation (45) shows that the most stringent requirements upon the precision of measurement of the variables to ascertain partial water vapour pressure are those given by Equation (46):

$$\begin{aligned} \Delta e_w &= \pm 0.075 \text{ mb.} \\ \Delta p &= \pm 3.7 \text{ mb. (at highest } T \text{ and lowest } T_D, \text{ with } e = 0) \\ \Delta T &= \pm 0.09^{\circ}\text{K (at highest } T_D) \\ \Delta T_D &= \pm 0.09^{\circ}\text{K (at highest } T, \text{ lowest } T_D) \end{aligned} \quad (46)$$

Yet another step must be made to determine the ultimate precision of measurement. Examination of tables of the saturation vapour pressure (e_w) shows that the greatest precision in ascertaining T_D for the range of measurement and for the specified accuracy in e_w , is represented by Equation (47):

$$\Delta T_D = \pm 0.019^\circ\text{K} \quad (\text{at highest } T_D) \quad (47)$$

The final requirements upon the precision of measurement are taken from all of the above considerations. If the refractive index of the air within the jet of the wind tunnel is to be measured with an accuracy of one part in one million, then the error limitations on the measured quantities are those given by Equation (48).

$$(\Delta T)_{\min.} = \pm 0.09^\circ\text{K} \quad (48)$$

$$(\Delta p)_{\min.} = \pm 2.3 \text{ mb.}$$

$$(\Delta T_D)_{\min.} = \pm 0.019^\circ\text{K}$$

Further consideration will be given to the coefficients in the psychrometric formula, in the following section.

5.2 The Psychrometric Formula

The basis for the psychrometric formula has been given in numerous texts [see for example Bird, Stewart and Lightfoot (1960), Kerr (1951)]. For sufficient ventilation of the hygrometer probes, an alternative form of the psychrometric formula is given by Equation (49).

$$e = e_w - A p (T - T_D) \quad (49)$$

where e_w = saturation vapour pressure at the wet-bulb temperature

p = total air pressure

T = dry-bulb temperature

T_D = wet-bulb temperature

A = psychrometric "constant"

$$= 0.660 \times 10^{-3} (1 + 11.5 \times 10^{-4} T_D)$$

Various authors have reported upon the minimum ventilation requirements; the wide variation in these requirements is illustrated by Table 3.

Table 3

Minimum Ventilation Speed for Constancy of Psychrometer "Constant"

<u>References</u>	<u>Min. Speed (feet per minute)</u>	<u>Remarks</u>
Noakes (1953)	485	mercury-in-glass thermometers
Long (1957)	200	nickel-wire elements
Ewell (1941)	600	
Berry, Bollay and Beers (1945)	900	mercury-in-glass thermometers
Middleton and Spilhaus (1953)	585	" " " "
Wexler and Brombacher (1951)	900	for sea level; increases with altitude.
Carrier et al (1937)	800-900	

The saturation vapour pressure (e_w) is not related in a simple way to the wet-bulb temperature (T_D). However, the relationship has been determined by numerous experiments (see for example Washburn 1928). The available tablets have been interpolated to give e_w (in millibars) for temperature increments of 0.01°C over the range 0 to 50°C , in Appendix IV.

Even the values of the psychrometric coefficients, "a" and "b" in Equation (44), show considerable variance among different authors. Table 4 gives some of the commonly-used values of these coefficients.

Table 4

Coefficients in Psychrometric Formula

$$e = e_w - a (1 + b T_D) p (T - T_D)$$

where p , e , e_w are in millibars

T , T_D are in degrees Kelvin.

<u>Reference</u>	<u>a</u>	<u>b</u>
Wexler and Brombacher (1951)	6.60×10^{-4}	1.15×10^{-3}
Kerr (1951)	6.46×10^{-4}	0.94×10^{-3}
McGavin (1962)	8.84×10^{-2}	0
Monteith (1954)	6.24×10^{-4}	0

Partial differentiation of Equation (44) with respect to "a" will show the contribution of error in this variable (Δa) to the error in partial vapour pressure (Δe):

$$\Delta e = - (1 + b T_D) p (T - T_D) \Delta a \quad (50)$$

It will be noted that for temperatures within the range 0 to 50°C, and for surface atmospheric pressure, a fixed error in "a" makes the error in e approximately proportional to the wet-bulb depression ($T - T_D$). It is only at high relative humidities, then, that the variation in "a" may become tolerable in the present experiment (see Table 5).

Table 5

Effect of Error in Psychrometric Constant (a) Upon Error in
Deduced Water Vapour Pressure

<u>Temperature (T°C)</u>	<u>Relative Humidity (per cent)</u>	<u>Δa</u>	<u>Δe (mb)</u>
22	15	0.1×10^{-3}	-1.3
22	50	0.1×10^{-3}	-0.7
22	90	0.1×10^{-3}	-0.12
30	90	0.1×10^{-3}	-0.14

The variation in "b" still remains. It is apparent that a careful study of the psychrometric coefficients is required, for the present purpose. The form of Equation (49) will be used for this purpose.

5.3 The Measurement of Temperature (Dry-Bulb)

The requirements upon the temperature probe for the wind tunnel are manifold. As indicated above, temperature must be measured within 0.01°C . However, in addition, it is desirable to have the temperature probe small in size (approximately 1 inch long) to examine changes in the temperature distribution over dimensions of the order of the sensing capacitor of the refractometer. The temperature should be indicated remotely from the probe with electrical recording, since the jet of the wind tunnel is enclosed during operation. The operation of the probe should be reliable and its calibration should remain stable over prolonged periods; it is desirable also that the response of the temperature probe be moderately rapid (of the order of one second). The temperature probe must be sufficiently rugged to withstand a moving air stream of one thousand feet per minute.

Numerous techniques for recording electrical thermometers have been described in the literature. These include nickel or platinum resistance wire probes, thermocouples and thermistors. Of these, thermistors suffer from instability of calibration over prolonged periods; thermocouples do not permit the desired accuracy of temperature measurement. The platinum resistance wire probe is an international standard with a stable calibration over prolonged periods; it also permits determination of temperature with the desired accuracy. For this reason, the latter technique has been chosen for the present experiment.

The chosen temperature probe is of commercial design. Details on this probe are given in Table 6.

Table 6

Properties of Platinum-Resistance Temperature Probe

Manufacturer: Rosemont Engineering Co., Minneapolis, Minnesota.

Model: 104P 8 ADB. (Serial No. 893)

Sensing element: platinum wire, mounted strain-free and sealed within ceramic rod.

element hermetically sealed within cylindrical sheath of tightly fitting, thin-walled stainless steel.

Nominal resistance: $R_0 = 100$ ohms (at $T = 0^\circ\text{C}$)

Element well length: 1 inch

Immersion length (element well + stem): 2 inches

Diameter of element well: 0.084 inch

Time constant: 1 second

Resistance at temperature $T = R_T = \{1 + a [T - d(0.01 T - 1)(0.01 T) - b(0.01 T - 1)(0.01 T)^3] \} R_0$ (Callendar-Van Dusen equation)

Calibration of R_T vs. T supplied for temperature range -50°C to 500°C .

From the calibration supplied by the manufacturer, the dry-bulb temperature is related to the probe resistance (R_T) by Equation (51).

$$T_{\text{(for dry-bulb probe)}} = \frac{6.65776 \times 10^3 - [44.3258 \times 10^6 - 0.666775 \times 10^5 (R_T - 100.322)]^{\frac{1}{2}}}{2} \quad (51)$$

Consideration must be given to the self-heating of the platinum wire temperature sensor. In the present application, the voltage applied to the sensor by the bridge network dissipates approximately 0.097 milliwatts of power within the sensor. This results in a rise of temperature of 0.0005°C , - an amount which is negligible for the present purpose.

The recording system for the temperature probe also is of commercial design. It is capable of indicating temperature changes as small as 0.01°C readily. Figure 19 gives the details of this system. It will be noted that two channels are provided; the second is for the measurement of wet-bulb temperature as described later.

The temperature-recording circuit must be able to indicate temperatures that are off the balance-point of the bridge circuit. Equation (52) shows the governing conditions for this bridge circuit.

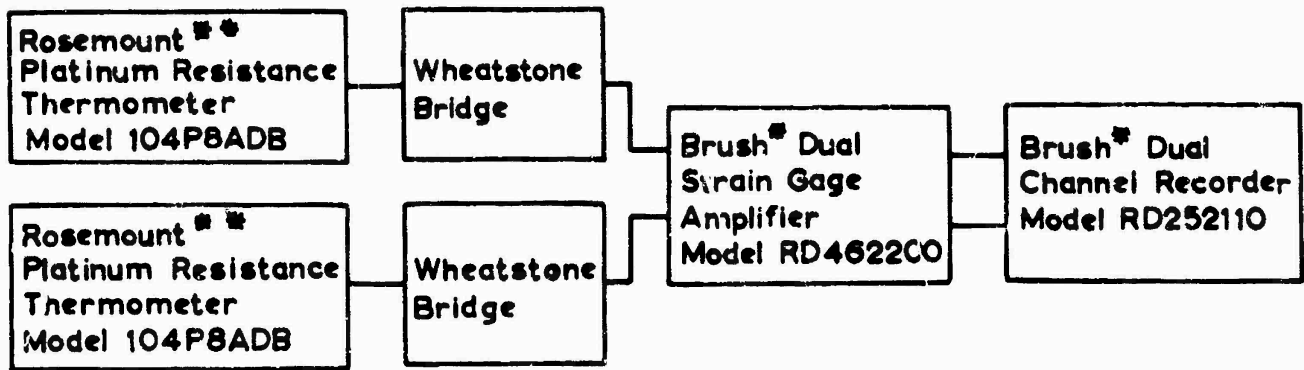
$$\frac{E_o}{E} = \frac{R_T}{R_T + R} - \frac{R_b}{R_b + R} \quad \text{where } R = \frac{R_1 + R_2}{2} \quad (52)$$

It will be seen that non-linearity of the bridge for off-null operation is reduced by making R much greater than R_T , and by balancing the bridge at the center of the desired temperature range. The incremental calibration for the recorder pen deflection away from the null setting position is obtained for various settings of the amplifier gain control and the sensitivity settings, through the use of a GR decade resistance box type 602-N in place of the platinum probe, at the end of the probe cables within the wind tunnel.

It will be noted that the above procedure permits only the measurement of relative temperatures, with a precision of 0.01°C. The recorder sensitivity is ascertained before and after each set of observations by the above procedure (q ohms per millimeter deflection). If R_0 is the resistance for zero pen deflection of the recorder, and dx is the pen deflection, then the indicated probe resistance is given by Equation (53).

$$R_x = R_0 + q \, dx \quad (53)$$

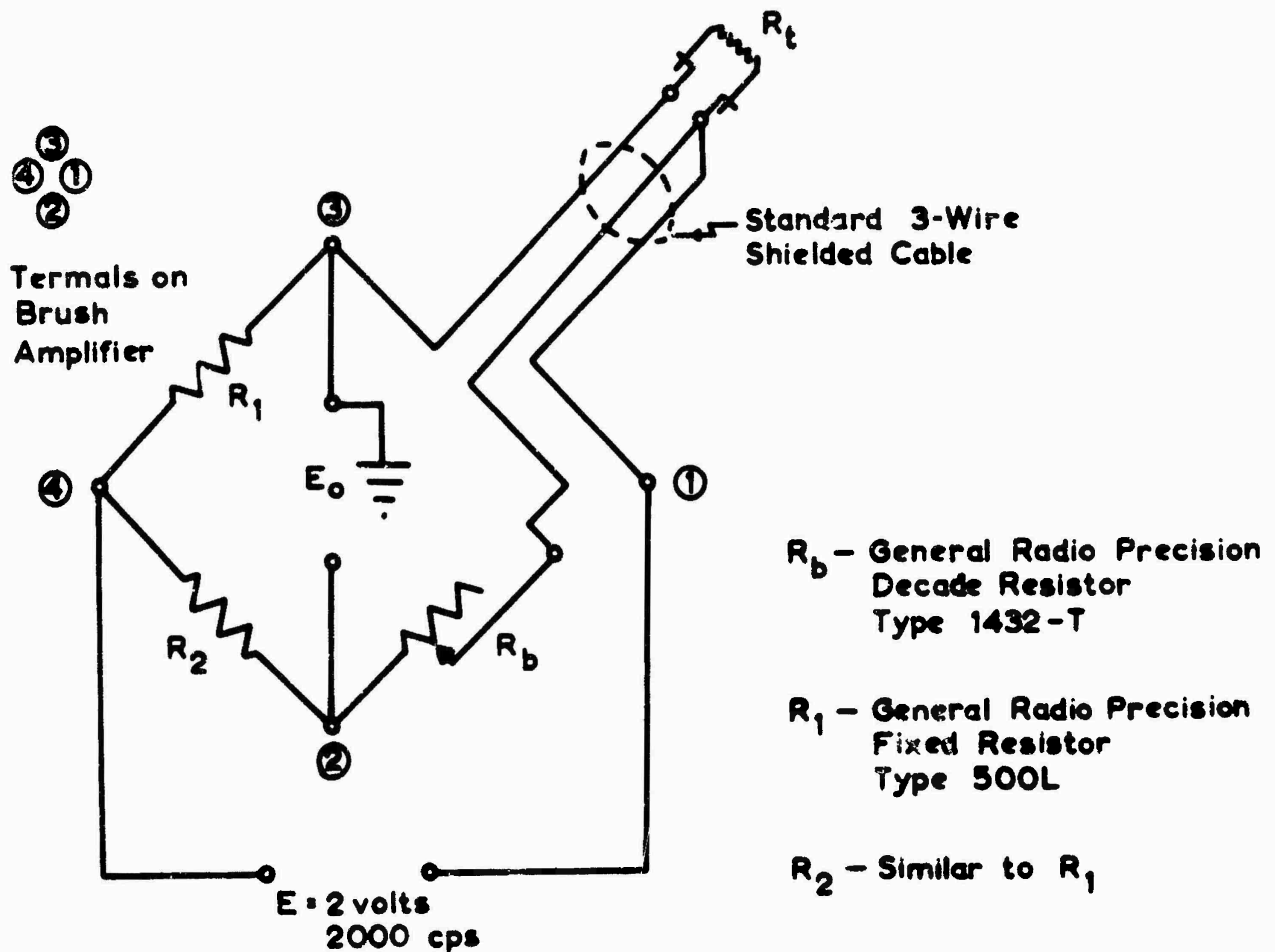
The correction for resistance of the shielded leads between the bridge network and the probe is obtained by using a calibrated precision



• • Rosemount Engineering Co.,
Minneapolis, Minn.

• Brush Instruments,
Cleveland, Ohio.

(a) BLOCK DIAGRAM OF RECORDING SYSTEM



(b) THE WHEATSTONE BRIDGE

Figure 19: Temperature recording bridge

resistor in place of the platinum-wire temperature probe.* This provides a correction factor (Z) such that

$$Z R_x = R_T = \text{corrected platinum probe resistance.} \quad (54)$$

The above procedure has given the following correction factor for the dry-bulb temperature probe:

$$Z (\text{for dry-bulb probe}) = 1.01034 \quad (55)$$

The precise temperature of the air in the jet is ascertained, then, through the use of Equations (51), (53) and (54). These calculations are carried out on an IBM 650 Computer, with a program which is described in Section 5.5.

5.4 The Hygrometer

The requirements upon the precision of measurement of the wet-bulb temperature have been outlined in Section 5.1. It was noted that wet-bulb temperature must be ascertained within $\pm 0.01^\circ\text{C}$. Since this precision is available in the dry-bulb temperature probe described above, a similar probe will be used as a basis for the wet-bulb temperature instrument. A hygrometer is formed by mounting the wet- and dry-bulb temperature probes close to each other, so that they may observe the same volume of air. A survey has shown that no hygrometer with this precision was readily available. Consequently, it was necessary to develop the hygrometer, in making use of the best available techniques, as indicated in the following sections.

* Calibration of the GR precision resistor type 500D (100 ohms ± 0.05 percent), serial number 194827 over the range of temperatures from 21°C to 30°C was provided with an accuracy of ± 0.001 ohm by the Division of Applied Physics of the National Research Council of Canada, Ottawa, - Report No. APE-57 (23 April 1963).

The procedure in developing and calibrating the hygrometer probes has followed several steps. These have included: construction of the wet-bulb temperature probe; the comparison of the calibrations of a mercury-in-glass thermometer (which is used to indicate the temperature of the calibrating solution) and the platinum-wire temperature probe; the calibration of a barometer; the calibration of a hot-wire anemometer to ascertain the ventilation rate of the probes in the calibration chamber; the construction of a calibration chamber for the hygrometer, which makes use of salt solutions; and the ascertaining of the coefficients in the psychrometric formula.

(a) Calibration of the Mercury-in-Glass Thermometer

The calibration of a mercury-in-glass thermometer has been compared with that of the platinum-resistance probe by mounting these probes adjacent to each other in the jet of the wind tunnel. The wind tunnel was operated at a low relative humidity, and the air temperature was varied slowly from 20°C to 25°C. The platinum resistance probe has provided the reference temperature, and the correction to the mercury-in-glass thermometer indication was consistently +0.1°C over this range.

(b) Calibration of the Barometer

The air pressure within the laboratory has been indicated by a System Paulin Aneroid Barometer, type VBTB1. The readings of this instrument have been compared with the indication of a barometer that is operated by the Department of Transport at the London Airport. When a small correction is applied for the difference in elevation between the London Airport and the University laboratory, the correction to the Aneroid barometer reading is given as in Equation (56).

$$\text{True air pressure} = P_{\text{aneroid}} - 13.2 \text{ millibars} \quad (56)$$

(c) Calibration of the Hot-Wire Anemometer

A need existed for a reliable anemometer, of small probe size, to measure the ventilation wind speed within the calibrating chamber and also to provide a comparison with other anemometers that are used in the wind-tunnel study. For this purpose, an anemometer probe has been constructed, as based upon the design described by Anderson (1959). Details on the probe construction and on the associated bridge circuit are given in Figure 20.

The calibration of this anemometer has followed standard laboratory procedure. The probe was mounted on the end of a rotating arm that describes a circle of known radius within the still air of the laboratory. A variable speed motor was used to rotate the arm, and the rate of rotation was determined by a calibrated GR Strobotac, Model 631-B86 (Serial number 8184-348). The calibration of this hot-wire anemometer is shown as a function of the meter current in Figure 21.

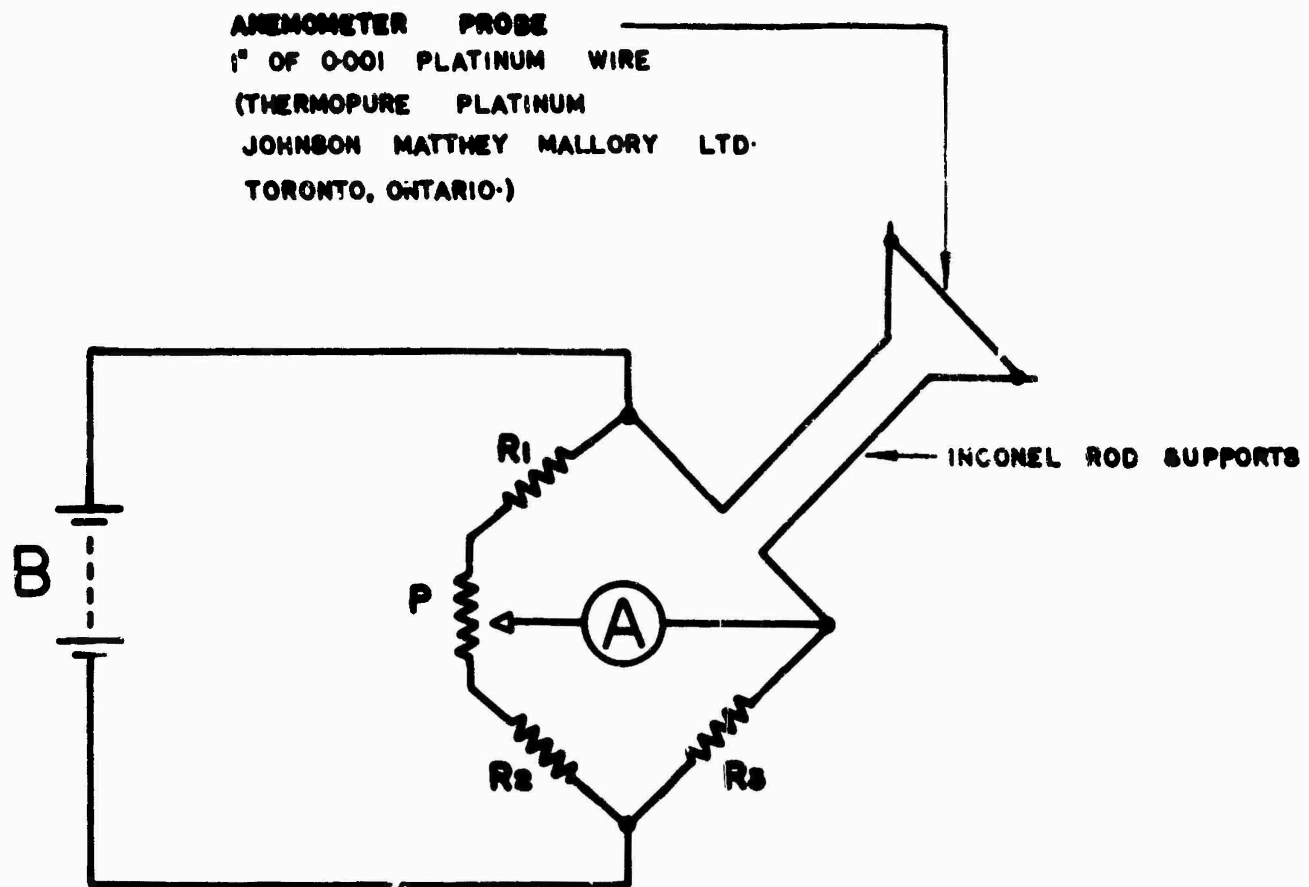
(d) The Wet-Bulb Temperature Probe

The basic element of the wet-bulb temperature probe is similar to that used for the dry-bulb temperature. From the calibration provided by the manufacturer, the wet-bulb temperature (T_D) is related to the platinum wire resistance (R_{TD}) through Equation (57)

$$T_D(\text{for wet-bulb probe}) = \frac{6.80079 \times 10^3 - [46.2507 \times 10^6 - 0.683183 \times 10^5}{2} \times (R_{TD} - 100.109)]^{\frac{1}{2}} \quad (57)$$

and the correction factor for the leads between the bridge and the wet-bulb probe is

$$Z(\text{for the wet-bulb probe}) = 1.01095 \quad (58)$$



LEGEND

A: TRIPLETT DC AMMETER
 MODEL 675

B: FIVE 1.55 BURGESS MERCURY CELLS
 TYPE HG-42R

P: 20 OHM POTENTIOMETER

R1: 47 OHM RESISTOR

R2: 47 OHM RESISTOR

R3: 14 OHM RESISTOR

Figure 20: Anemometer probe and bridge circuit

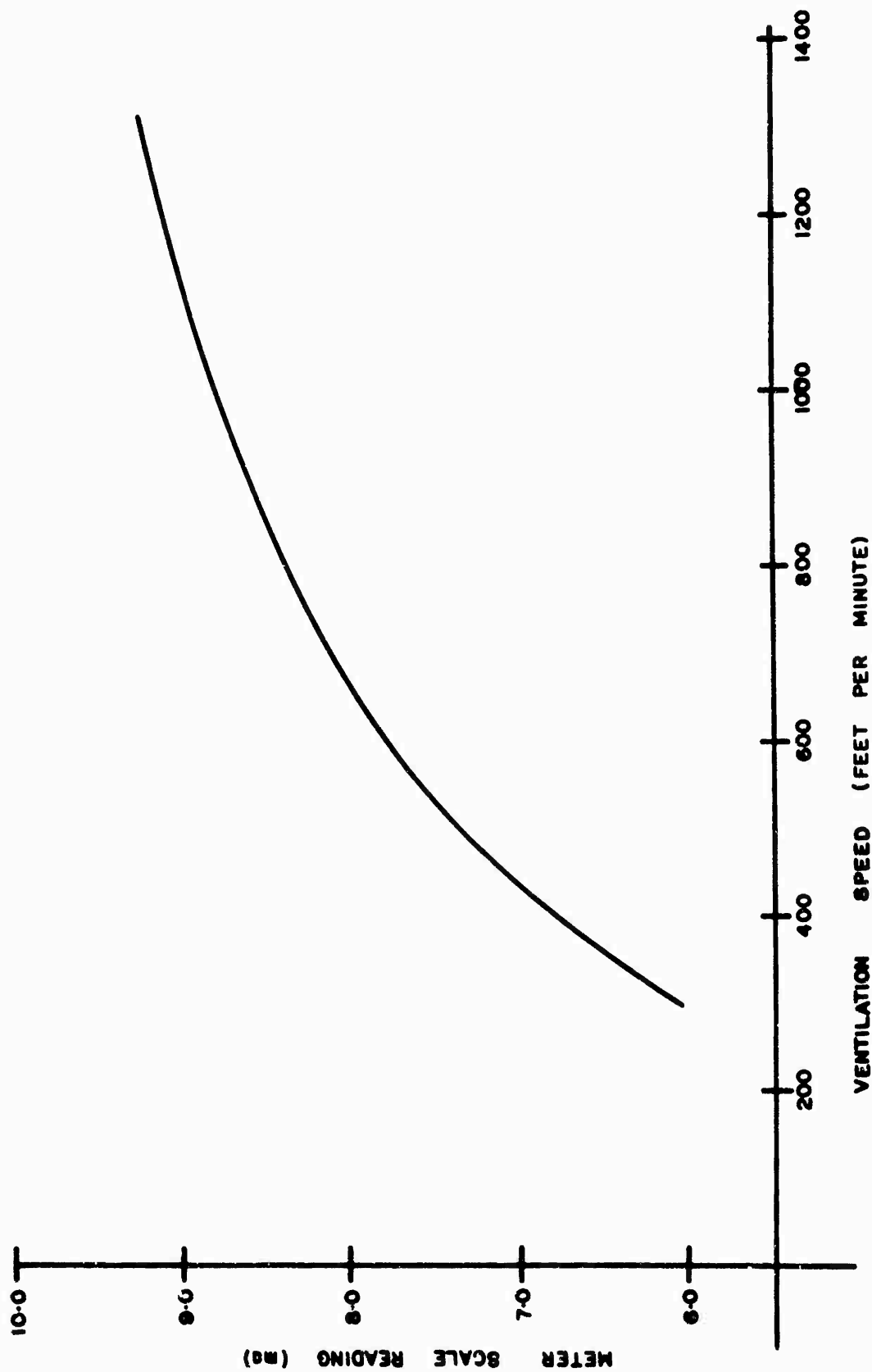


Figure 21: Calibration curve of the hot-wire anemometer

The method of wetting the platinum wire probe has required careful study. Various types of wicks and of wetting systems have been examined both within the jet of the wind tunnel and in the hygrometer calibration chamber that is described below. A study of the effects of varying ventilation speed upon the wet-bulb indication showed that the latter was independent of ventilation speed for speeds between 300 and 1200 feet per minute. The wet-bulb indication changed only when the wick began to dry or when a drop of water formed upon the wick.

The configuration of the wet-bulb temperature probe, shown in Figure 22, has been found to be reliable and to give repeatable indications. It will be seen that the water is applied to the wet-bulb platinum resistance probe through a cylindrical wick which is in tight contact; the water is supplied through a plastic tube from an elevated reservoir. The only part of the wick that is exposed to the surrounding air is that at the probe. The probe is mounted in a vertical position, and water is introduced to the wick from below. The height of the water reservoir is adjusted to make the wick remain wet without an excess of water, at the required ventilation speed.

The hygrometer is formed by mounting the wet-bulb temperature probe adjacent to the dry-bulb probe that has been described in Section 5.3. This arrangement is shown in Figure 22 and the photograph of Figure 23. The two probes are separated by a distance of 0.75 inch in the direction perpendicular to air flow, and a thin metallized shield is mounted between them, parallel to the direction of air flow. The latter acts not only as a radiation shield between these probes, but prevents the transfer of water vapour from the wet-bulb to the dry-bulb thermometer. A shield surrounds the twin-leads between each probe and the thermometer bridge.

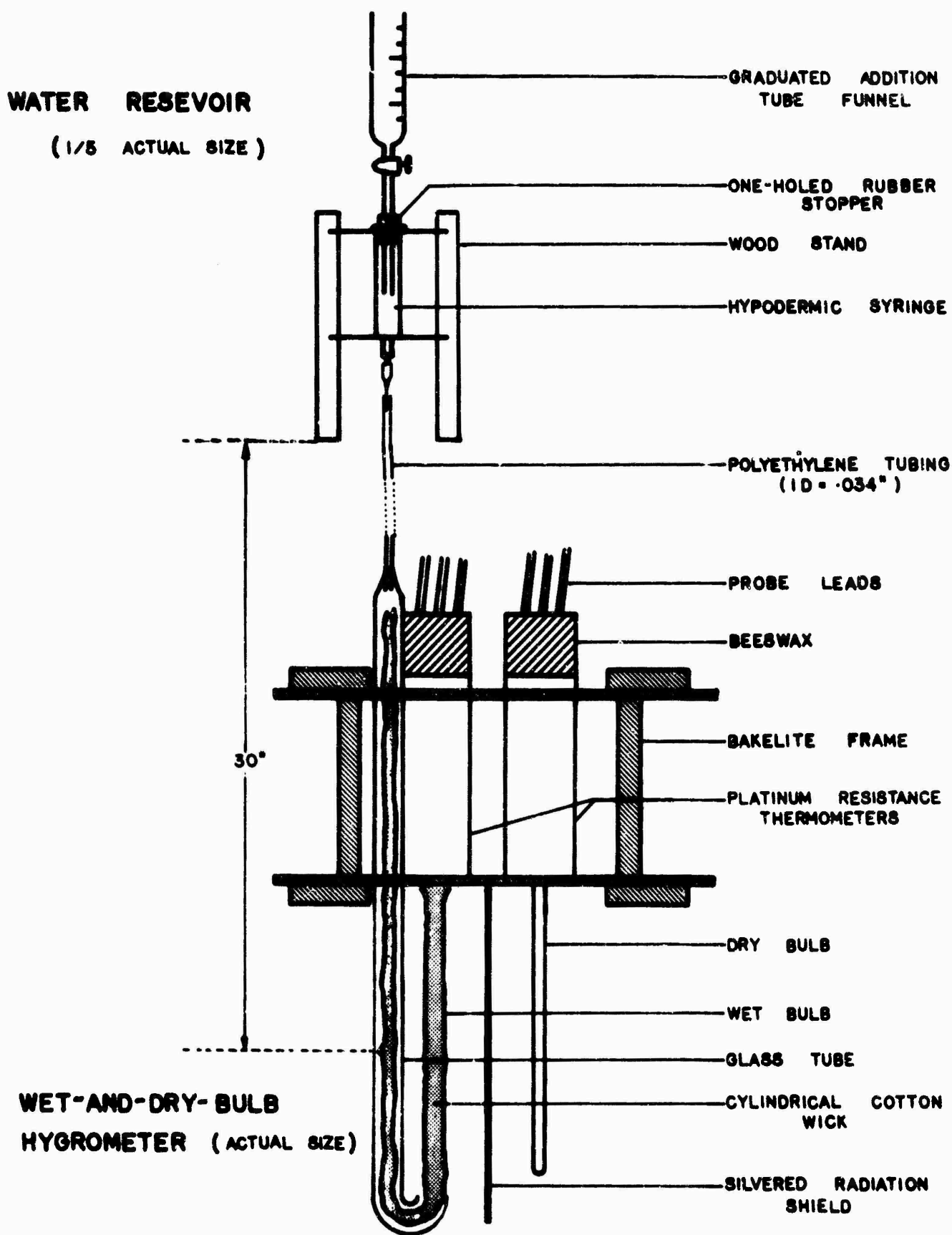
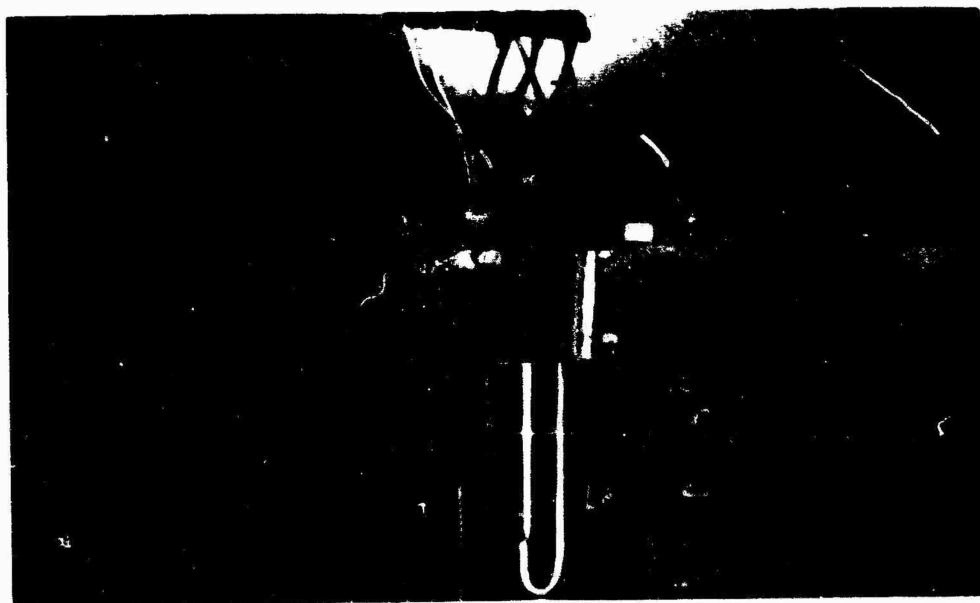
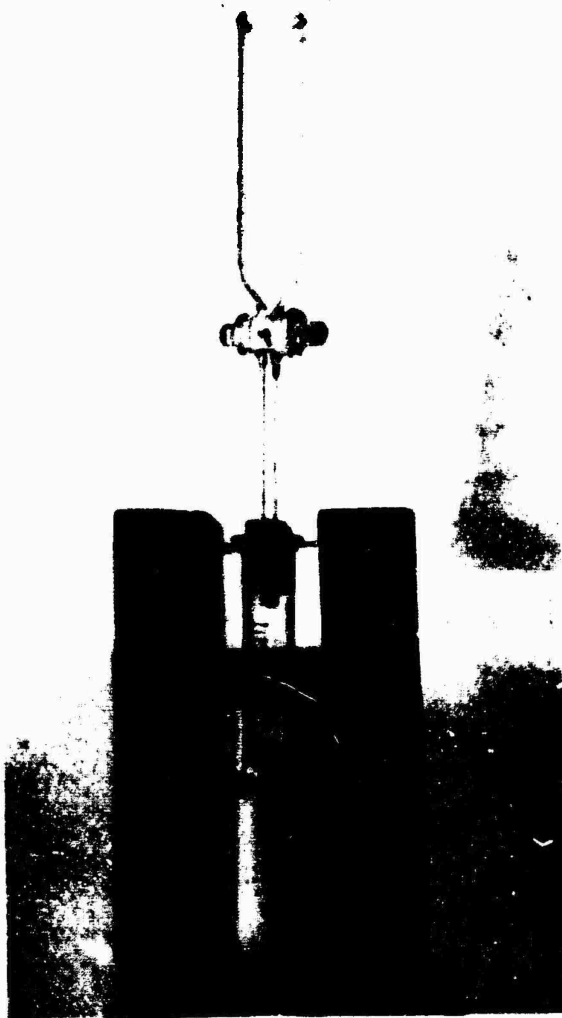


Figure 22: The wet-bulb temperature probe and wetting system

The water
reservoir



The platinum-wire sensors

Figure 23: The hygrometer probes and wetting system

(e) The Calibration Chamber for the Wet- and Dry-Bulb Temperature Probes

Methods of calibrating wet- and dry-bulb temperature probes have been reviewed extensively by Wexler and Brombacher (1951), Middleton and Spilhaus (1953), and by McGavin (1962). In each of these, the probes are exposed to a series of environments, each having the desired temperature and vapour pressure. Then the wet-bulb temperature may be deduced from information on the vapour pressure as found in physical tables.

There are three primary methods of obtaining the desired vapour pressure (Middleton and Spilhaus 1953 page 116). In one of these, dry air and saturated air are mixed in known proportions; in another, a volume of air is saturated at a specified temperature, and then the temperature is raised to a new value without changing the vapour content; in the third, air is saturated with vapour at a high specified pressure, and then the air pressure is reduced to a new value without a change in vapour content.

A less precise alternative makes use of a secondary method of calibration. One such method employs saturated solutions of salts, which have specified vapour pressures. Wexler and Hasegawa (1954) have studied this method extensively. Further information on the vapour pressures of saturated salt solutions is given also by Spencer (1926), by Middleton and Spilhaus (1953, page 117), by O'Brien (1948) and by Martin (1962). An attempt has been made in the present experiment to use this secondary method of calibration, not only to examine the stability and repeatability of the new hygrometer probe measurements, but also to derive the appropriate form of the psychrometric formula.

The experimental arrangement for the calibration of the hygrometer has been developed from techniques described by Wexler and Hasegawa (1954) and by Monteith and Owen (1958). In addition, a number of modifications

have been made upon numerous factors that affect the calibration of thermometers. These include a study of the difference in temperature between the calibrating solution and the air above it, - as a function of time, ventilation rate, and location of air stream within the chamber; the location of the calibration chamber within the laboratory room; the effect of insulation and radiation protection in the calibration chamber; the suspension of the temperature probes; the intercomparison of thermometers; the heating of the air by the circulating fan and motor within the calibration chamber; the method of ventilating the temperature probes; the effects of various materials for supports within the chamber; and the ability to obtain saturation vapour pressures within the chamber. Figure 24 shows the details of the calibration chamber.

Several features of the hygrometer calibration chamber may be noted. An insulating, light-tight enclosure surrounds the glass bell-jar to reduce the effects of direct external radiation. Access is obtained through a small door in one side of the enclosure. A mercury manometer indicates the pressure differential between the inside and outside of the chamber. A precision mercury-in-glass thermometer indicates the temperature of the calibrating salt solution. The wet- and dry-bulb probes are mounted in a glass tube of diameter $1\frac{1}{2}$ inch, through which the re-circulating air (from a centrifugal fan) is moved at various controlled speeds. The ventilation speed is determined by the calibrated hot-wire anemometer, which has been described in Section 5.4(c).

The calibrating solutions are contained in a flat pyrex plate. The salts are of reagent grade, and the saturated solutions are of slushy consistency. Table 7 indicates the solutions that are used in this calibration, for the desired range of relative humidities.

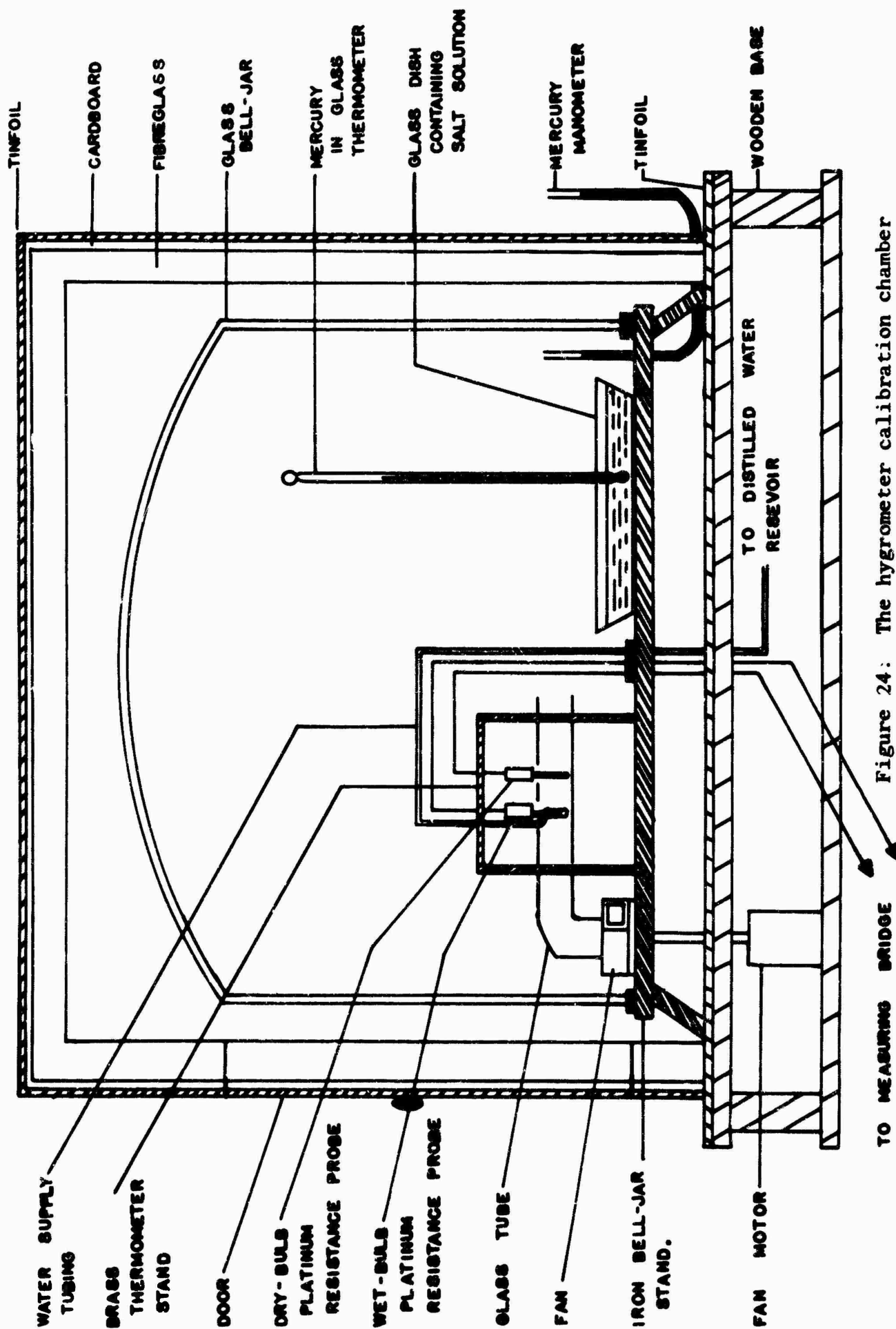


Figure 24: The hygrometer calibration chamber

Table 7

Standard Solutions for Hygrometer Calibration

<u>Saturated Aqueous Solution</u>	<u>Relative Humidity at T = 20°C (approx.)</u>
K ₂ SO ₄	97 percent
KNO ₃	93 "
(NH ₄) ₂ SO ₄	80 "
Na Cl	75 "
Mg (NO ₃) ₂ · 6H ₂ O	54 "
Na ₂ Cr ₂ O ₇ · 2H ₂ O	55 "
Mg Cl ₂ · 6H ₂ O	33 "
Li Cl · H ₂ O	12 "

The change in relative humidity with solution temperature, for each of these salts, has been indicated by Wexler and Hasegawa (1954).

(f) Calibration Procedure

A procedure for calibration of the hygrometer probes has been developed from an extensive series of trials. Details on this procedure are given in Appendix II. This experimental procedure has been repeated several times with each calibrating solution.

The experimental calibration of the hygrometers has been analyzed to ascertain the coefficients of the psychrometric equation (Equation 49). It may be noted that all errors in the hygrometer calibration with the exception of errors in the temperature probes themselves, are in the direction which raises the wet-bulb temperature; thus, these errors tend to increase the apparent relative humidity above the true value. The desired wet-bulb temperature in the calibration is the minimum one. A sample analysis of the calibration observations is given in Appendix III. The results of all such observations, as analyzed for the psychrometric constant, are presented in Figure 25.

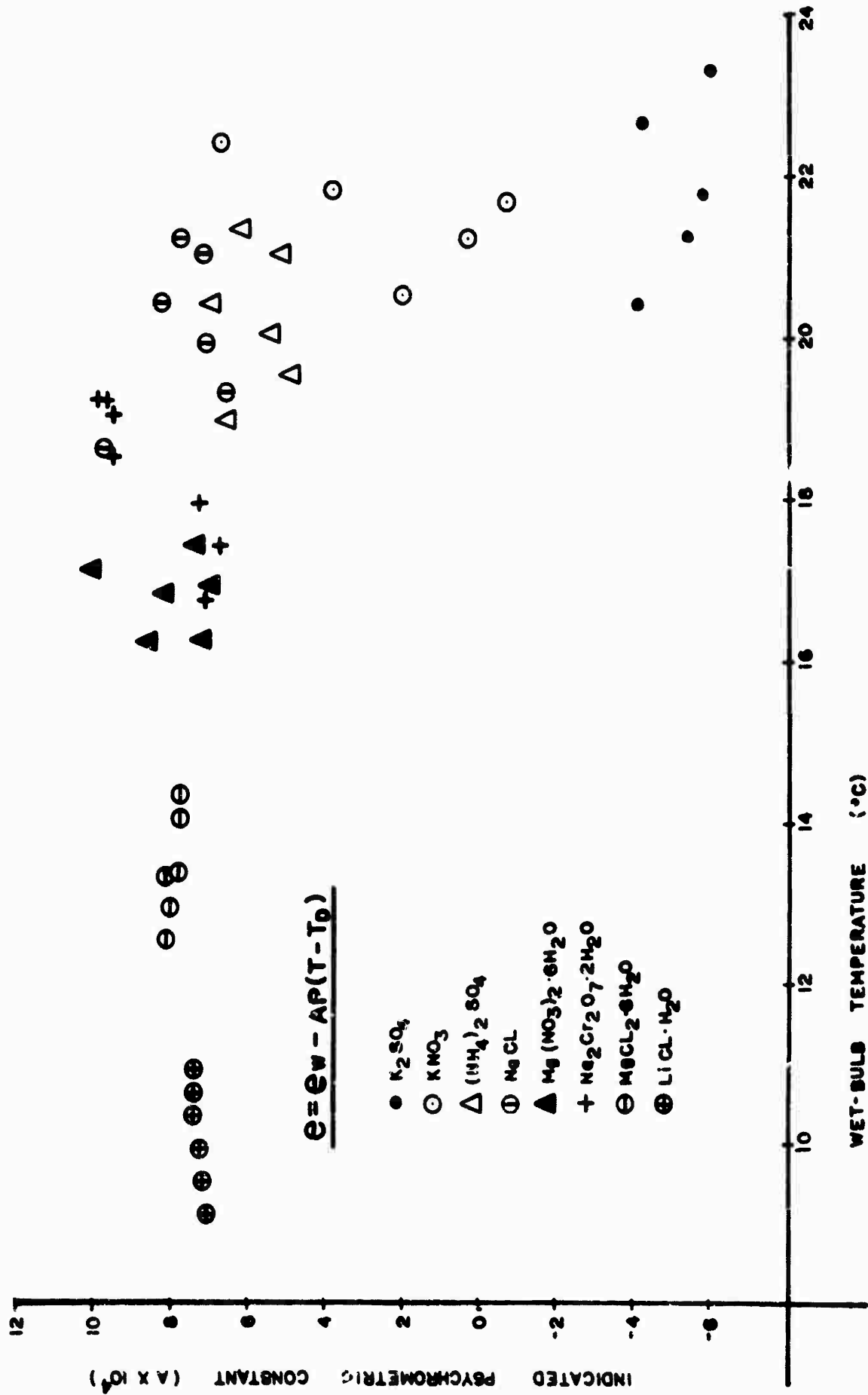


Figure 25: Relationship between psychrometric constant and wet-bulb temperature

The results in Figure 25 demonstrate an important feature of this secondary method of calibration. It will be noted that there apparently is no simple relationship between the psychrometric "constant" A and the wet-bulb temperature. The wide dispersion of points, as obtained through the use of different saturated salt solutions, was present also in the results reported by Wexler and Hasegawa (1954). Hygrometer calibration by means of the primary methods referred to above also shows a linear relationship between A and the wet-bulb temperature, a trend which is lacking in the present calibration. It is apparent that either some technique in the design of the present hygrometer has been overlooked, or that the secondary method of calibration suffers from gross inaccuracies in spite of all of the reasonable precautions observed.

It has been assumed in subsequent use of this hygrometer that the secondary method of calibration is faulty. Further, it has been assumed that the Wexler-Brombacher form of the psychrometric formula (Table 4) is the appropriate one for this hygrometer, since it has been derived from precise calibrations and is in widespread use. The validity of these assumptions is supported by the close agreement between measured air refractivity and the refractivity that is deduced from the hygrometer information through the use of the Wexler-Brombacher formula, as reported in Section 7.2.

5.5 Computation of Refractive Index

The refractive index of the air within the jet of the wind tunnel is finally deduced from the measurements upon the separate components that contribute to air refractivity. As has been indicated in Section 5.1, these contributing components are the air temperature, the total air pressure and the partial pressure of water vapour. The total atmospheric pressure is measured by a Casella Aneroid Barometer, Mark I, type 6143, mounted

in the wind tunnel jet. Since the partial pressure of water vapour is not measured directly, it is deduced from measurements upon the wet- and the dry-bulb temperature within the jet. The computation that is required to deduce the partial water vapour pressure from the temperature information is laborious, especially in an extensive program of refractivity studies. For this reason, a program of computation has been drawn up, which makes use of the IBM 650 Electronic Computer, on the campus of this university.

The computation procedure may be summarized briefly. After the information from the experiment has been recorded on paper charts, the latter are examined and the appropriate readings are transferred to a table. Figure 26 shows a sample of the analysis table. Here, the time reference τ lies to appropriate periods during each observation when prescribed conditions within the jet were obtained; R_{01} refers to the apparent resistance of the wet-bulb temperature probe as indicated by its precision bridge; $q_1 dx_1$ represents the change in the resistance of the temperature probe for the indicated deflection of the recorder pen; Z_1 refers to the correction factor which accounts for the resistance of the electrical leads to the temperature probe (Equation 58); finally, the corrected resistance of the wet-bulb temperature probe, R_{T1} , is calculated through Equations (53) and (54).

The wet-bulb temperature within the jet now is deduced from the information in this table. The relationship between R_{T1} and the wet-bulb temperature T_D is given in Equation (57). A table which gives this relationship for the range of temperatures between 0°C and 50°C has been computed by means of the IBM 650 computer. The program for this computation is given in Appendix V. These tables cover the range of variables:

$$100.000 \text{ ohms} \leq R_T \leq 119.999 \text{ ohms} \quad (59)$$

$$0.27^\circ\text{C} \leq T_D \leq 50.30^\circ\text{C}$$

The saturation vapour pressure at the wet-bulb temperature (e_w) is now deduced from the above information. Here, it is necessary to refer further to the tables in Appendix IV.

The final step in the calculations is made through a single computer program. This program combines the operations of Equations (51), (53), (54) and (55) to ascertain the dry-bulb temperature from the recorder chart information (Figure 26). It then inserts the information upon dry-bulb temperature, wet-bulb temperature, saturation vapour pressure at this wet-bulb temperature, and the observed air pressure into Equation (44). For this purpose, the psychrometric equation with the coefficients from Wexler and Brombacher (see Table 4) has been employed to ascertain the partial vapour pressure. Then, the computer program continues with Equation (40) to determine the refractive index of the air in the jet. Appendix IV gives the appropriate computer program, and a sample calculation is also included.

Date	PLATINUM PROBE-BRUSH RECORDER TEMPERATURE ANALYSIS								
April 20/63	Remarks: Microwave Refractometer Temperature Compensation Test, $T = 25^{\circ}\text{C}$ Invar-Brass Cavity $p = 982.3 \text{ mbs.}$								
Time Reference	Channel I (wet)						Channel II (dry)		
	R_{01}	q_1	αx_1	z_1	R_{T1}	T_D	R_{02}	dx_2	e_w
1	105.20	0.010256	7.50	1.01095	106.448	15.959	109.70	1.25	18.144
2			7.75		106.450	15.964		3.25	18.144
3			10.50		106.479	16.037		11.25	18.236
4			15.00		106.525	16.153	109.90	5.50	18.365
5	105.40		0.50		106.577	16.284		18.00	18.518
6			5.00		106.624	16.403	110.10	11.00	18.661
7			9.50		106.671	16.522	110.30	3.50	18.803
8			13.50		106.712	16.625		13.75	18.935
9			17.00		106.748	16.716	110.50	4.00	19.043
10	105.60		1.25		106.787	16.814		12.00	19.153
11			4.75		106.824	16.908	110.70	1.50	19.274
12			8.00		106.857	16.991		9.00	19.373
13			11.50		106.894	17.084		17.00	19.484
14			10.50		106.883	17.057		9.00	19.459
15			6.00		106.836	16.938	110.50	12.75	19.311
16	105.40		20.00		106.779	16.794	110.30	15.00	19.129
17			15.50		106.733	16.678		1.00	18.995
18			11.00		106.686	16.559	110.10	5.00	18.851
19			7.00		106.645	16.456	109.90	11.00	18.732
20			3.25		106.606	16.358	109.70	18.25	18.613
21	105.20		18.75		106.564	16.252		7.75	18.483
22			15.75		106.533	16.173	109.50	17.50	18.388
23			12.75		106.502	16.095		8.75	18.306
24			10.00		106.474	16.025		1.50	18.225
25			7.25		106.445	15.951	109.30	12.75	18.132
26			5.00		106.422	15.893		6.50	18.063
27			2.50		106.396	15.828	109.10	18.75	17.994
28	105.00		19.50		106.370	15.762		13.25	17.914
29			17.25		106.346	15.701		7.50	17.845
30			15.00		106.323	15.644		2.00	17.777
31			13.25		106.305	15.598	108.90	16.50	17.732

Figure 26: Sample temperature analysis table

6. The Optical Ellipsometer

An auxilliary study of surface adsorption has been undertaken to provide additional information on the refractometer sensors. The method used here employs optical techniques to observe the formation of an adsorbed layer upon the surfaces of quartz and invar. Plane-polarized light is reflected from the surface under study, and the change in the ellipticity of polarization upon reflection is used as an indication of the thickness of the adsorbed layer.

Various techniques of optical ellipsometry have been described in the literature. The simplest method, and that used in the present study, is attributed to Rothen (1945). More complex improvements in the technique have been described by others, including Rothen and Hanson (1948), Derjagvin and Zorin (1957), and Silverman (1930).

The experimental arrangement is illustrated in Figure 27. The monochromatic light is provided by a sodium source. The sodium light passes through a narrow slit, and is focussed through a polaroid upon the surface under study, at an angle of incidence of 60° . The reflected light is passed through a quarter-wave mica plate, where it is analyzed by a Nicol prism and observed visually.

Observations upon the reflected polarized light are carried out within a darkened room. Initially, the quarter-wave plate and the analyzer are adjusted successively for the deepest null in the reflected light intensity. Then, with the reflecting quartz or invar plate in the bell-jar, the relative humidity in the chamber is increased by adding water via the reservoir and bubbling air through it, or decreased by removing the water via the reservoir and blowing in dry air. The relative humidity of the air in the chamber is determined by the readings of the wet- and dry-bulb

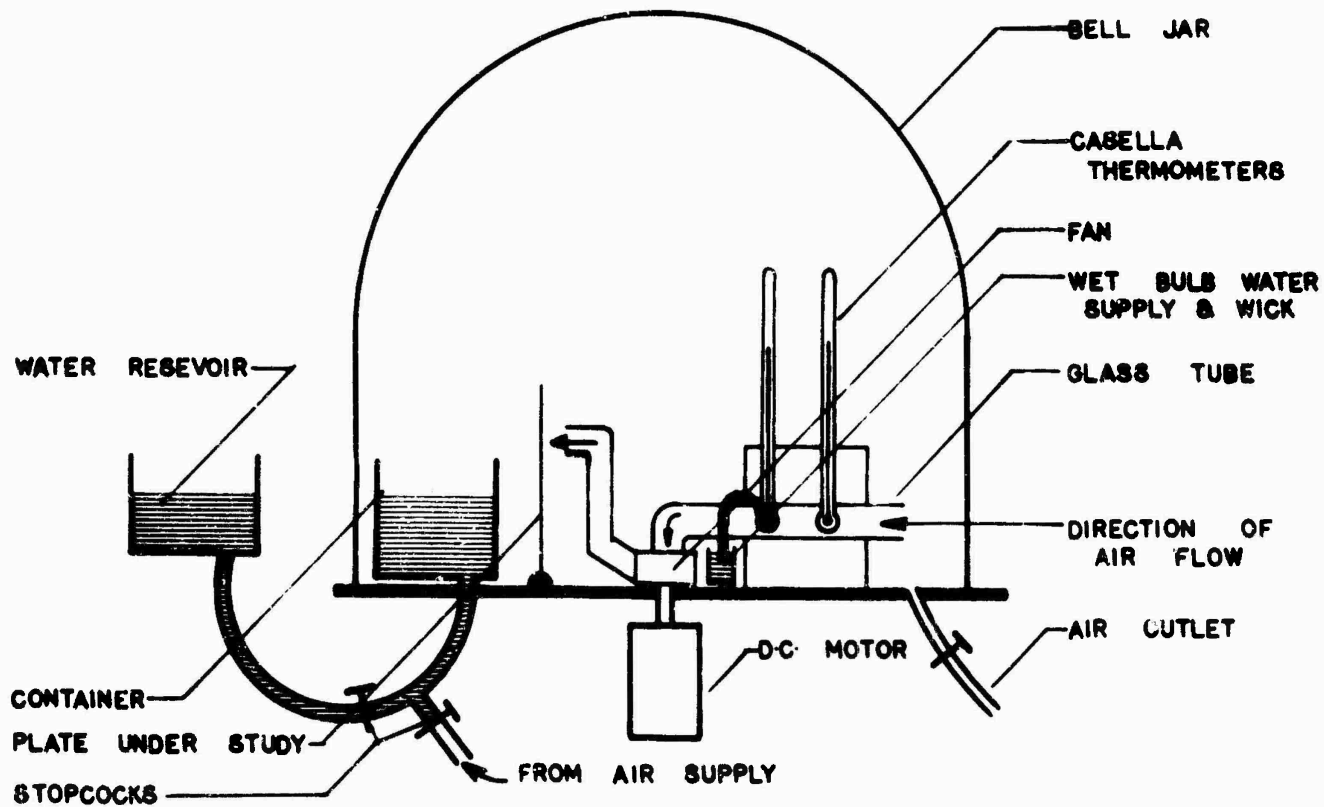
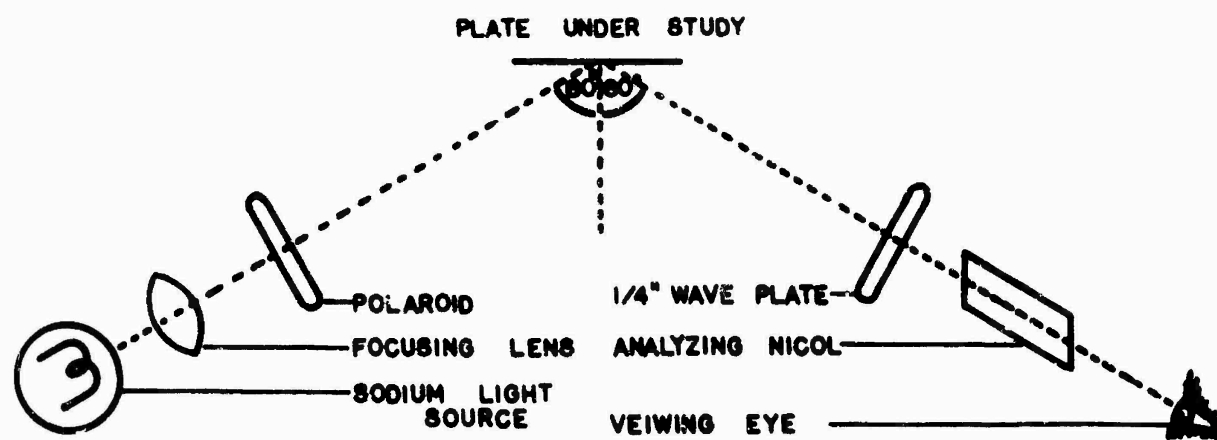


Figure 27: The optical ellipsometer

thermometers. After the moist air is introduced, the rotation of the analyzer alone is adjusted, again for the deepest null in reflected light.

The amount of rotation of the plane of polarization of the reflected light is taken as an indication of the thickness of the adsorbed layer upon the sample. Rothen (1945) has calibrated his system with films of barium stearate; this calibration has shown a linear relationship between the amount of rotation and the thickness of the layer. However, no calibration of this sort has been provided for the present experiment with water films. Only qualitative information on the layer thickness has been obtained in the experiment reported here.

Some ten groups of observations have been made upon quartz and invar plates. The results of these observations are summarized in Table 8.

Table 8

Ellipsometer Observations Upon Samples of Quartz Plate and Invar Plate

<u>Material</u>	<u>No. of Observations</u>	<u>Remarks</u>
Invar plate (flat), untreated	1 - unventilated	Not able to observe null setting
Invar plate (flat), cleaned with abrasive cleaner	3 - unventilated	No detectable rotation of polarization (within $\pm 2.5^\circ$) for R.H. up to saturation.
Invar plate (flat), cleaned with abrasive cleaner	3 - ventilated (800 ft. per minute)	(same as in previous observations)
Fused quartz plate (flat).	3 - ventilated (800 ft. per minute)	Rotation of polarization increased as R.H. increased above 20 percent, with rotation of 15 degrees as R.H. approached 50 percent. At R.H. = 50 percent, polarization rotation increased abruptly to approx. 30 degrees. For R.H. greater than 50 percent, polarization rotation varied erratically.

Further consideration will be given to these observations in Section 8.

7. Experimental Observations in the Wind Tunnel

This section will describe the experimental observations upon the microwave refractometer and upon the capacitor-type refractometer within the jet of the wind tunnel. Before these measurements were undertaken, the hygrometer probes were mounted in the mouth of the exit cone, at a position off the central axis of the jet. This position was ascertained through numerous measurements, such that the hygrometer did not interfere appreciably with the distribution of temperatures within the jet, and yet it gave an accurate indication of the temperature at the refractometer sensor. Care was taken to assure that the hygrometer wetting system was properly adjusted before each observation described in the following sections. The barograph was mounted at the edge of the jet, near the exit cone; this position was found to give a sensitive indication of pressure within the jet. The experimental arrangement has been indicated in Figure 9.

All experimental observations have been made with the refractometer sensors mounted in the most homogeneous part of the jet. In each case, the axis of the sensor was parallel to the direction of air flow. The microwave cavity was suspended within the jet by nylon cords; however, after numerous trials, it was found necessary to mount the capacitor-type refractometer upon a rigid glass stand within the jet. The trolley system had been removed previously from the region of the jet, to prevent its interference with these observations.

The appropriate conditions of temperature and relative humidity within the jet were maintained by adjustment of the manual controls of the refrigeration unit, electric heater, dehumidifier and water vapour injector, as indicated previously. All recordings of temperature, pressure and

refractivity were synchronized, and the series of desired events noted upon the recordings during each observation. Through these precautions, it was found that the indicated refractivities under stationary conditions were repeatable within two parts per million.

The refractometer sensors were prepared carefully before each set of observations. No modifications of the sensor in the microwave refractometer were made, but several changes were made in the sensor of the capacitor-type refractometer. These are described in Section 7.3. In the latter, the reference capacitor was isolated from changes in external humidity by surrounding it with a stiff waxed paper cover; further, all sharp edges of the refractometer surface were smoothed, and unnecessary protrusions removed to eliminate pockets that may trap water vapour.

7.1 Temperature Coefficient of the Refractometers

It is necessary to establish the effect of a temperature change upon the refractometer sensors, apart from the associated change in air refractivity. This temperature coefficient of the refractometers has been ascertained by operating each of the two refractometers within the jet as the air temperature is varied and the relative humidity of the air is maintained at a value below 20 percent. No attempt has been made to incorporate temperature compensation into the refractometer sensors, beyond that which existed prior to these experimental observations. The rate of change of temperature has been sufficiently slow that the refractometer sensors and the hygrometer probes were in equilibrium with the air in the jet.

The temperature coefficient of the refractometers has been ascertained for each of the types of sensor used in the following observations. This coefficient is deduced by noting the difference between the true air

refractivity as deduced from the temperature and pressure readings, and the refractivity as indicated by the refractometer, for a change of several degrees in the jet temperature. A sample indication of the temperature coefficient for the microwave refractometer is shown in Figure 28. The mean temperature for this measurement was 20°C . It will be seen that the microwave cavity is adequately temperature compensated for the precision of measurements in this experiment.

A sample indication of the temperature coefficient of the capacitor-type refractometer also is indicated in Figure 28. Here, the temperature coefficient is 20 parts per million per $^{\circ}\text{C}$. Similar measurements have been made at mean temperatures also of 10, 30 and 40°C . These have shown that the temperature coefficient is essentially constant over this range of temperatures.

This information on the temperature coefficient of the two refractometers has been applied in the following observations. In each case, the contribution to indicated refractivity that arises from changes in the sensor dimensions has been deducted. The remaining changes in indicated refractivity, then, are attributed to the air within the sensing element. In practice, the temperature of the air within the jet has been maintained constant within 0.1°C throughout each observation interval, and hence the necessary temperature correction is small.

7.2 Refractivity Change with Humidity - The Microwave Refractometer

Nine sets of observations have been made with the microwave refractometer. In these, the temperature has been maintained essentially constant at approximately 27°C , 32°C and 51°C while relative humidity is changed from approximately 20 percent upwards to saturation. Figure 29 illustrates the analysis of these observations. It will be seen that the refractivity

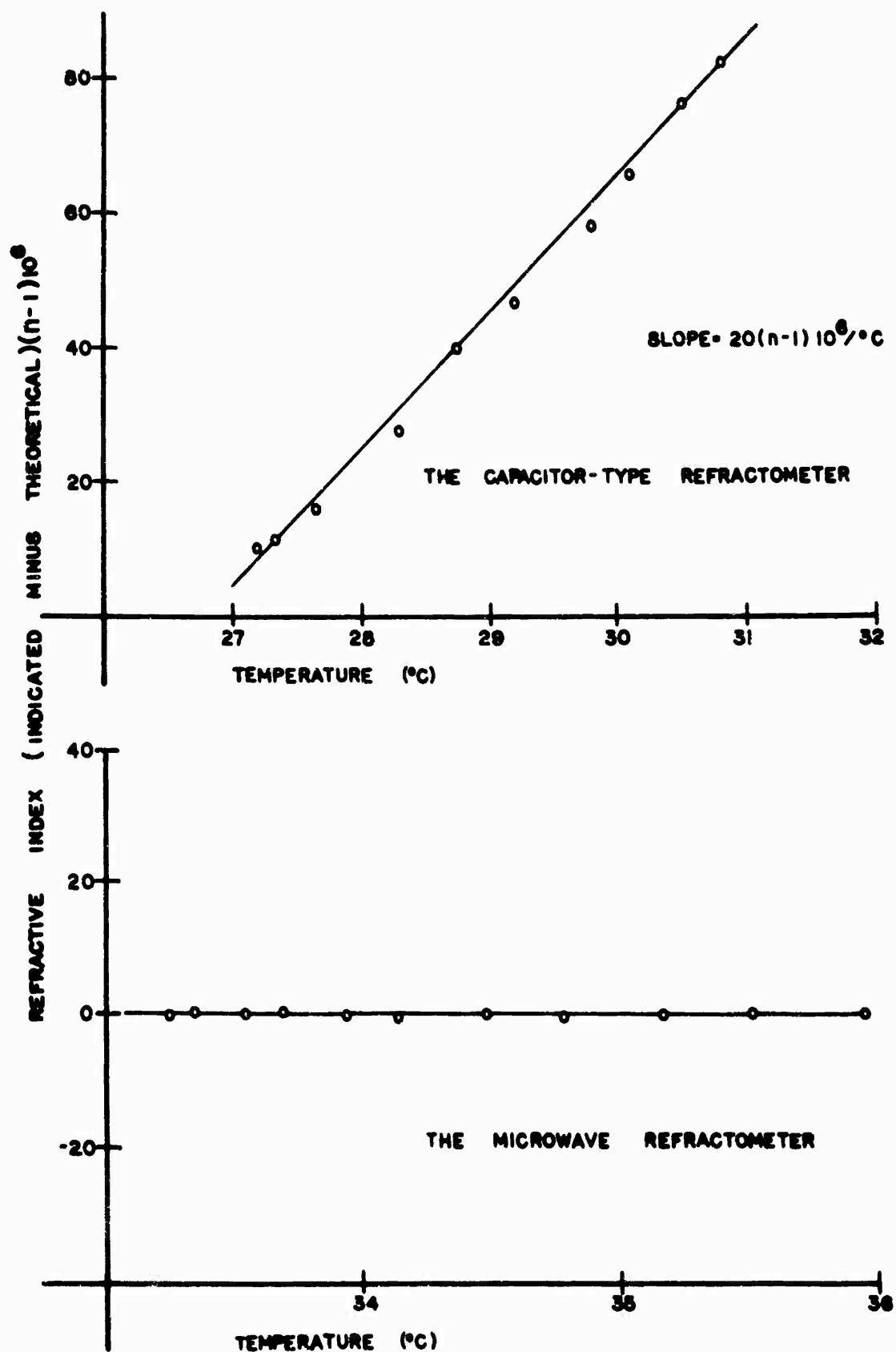


Figure 28: Temperature coefficients of the refractometer sensors

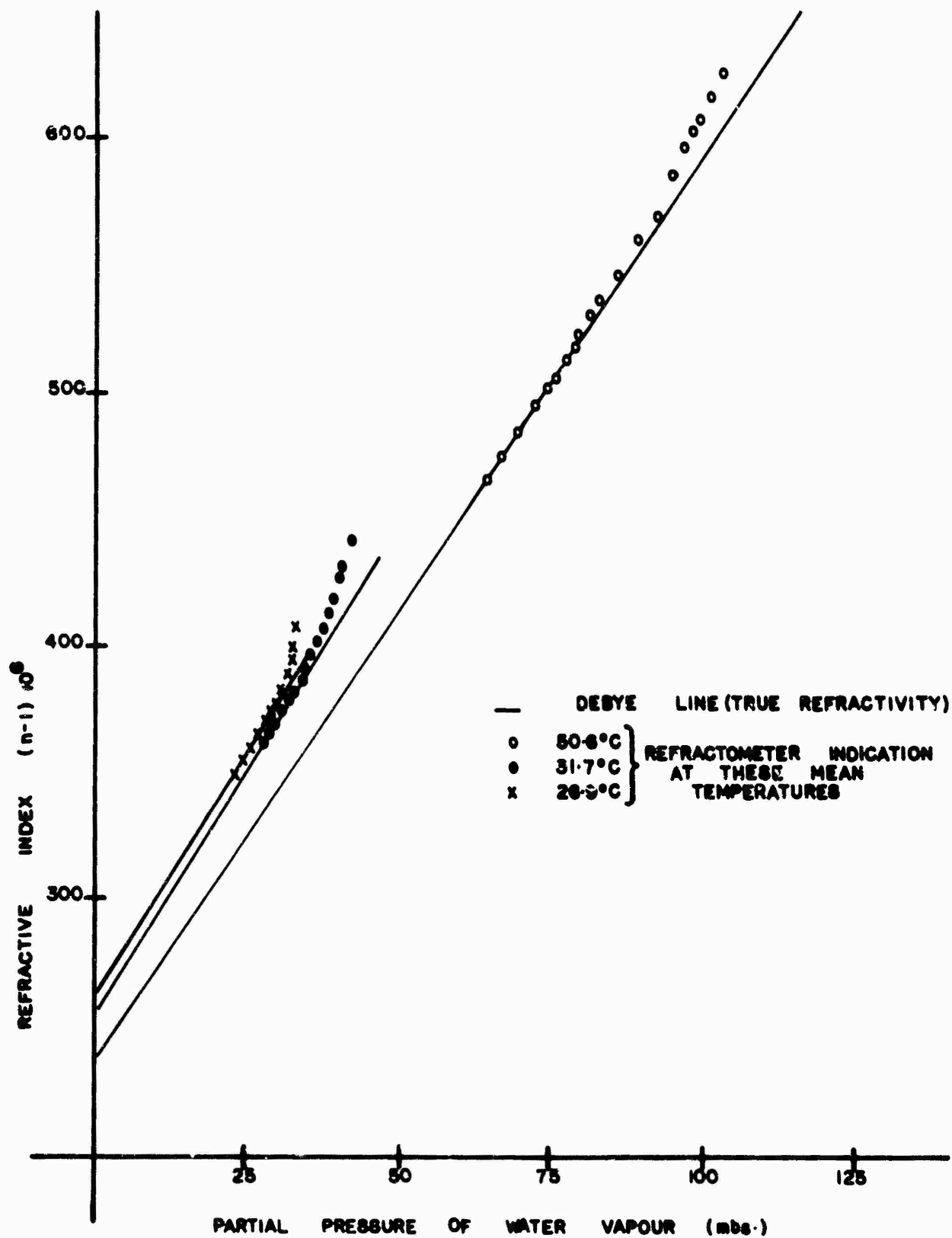


Figure 29: Comparison between indicated and true refractivity, -
The Microwave Refractometer

as indicated by the microwave refractometer follows the true refractivity of the air within the jet for relative humidities less than 85, 75 and 50 percent, respectively, at temperatures 27° , 32° and 51°C ; for greater relative humidities, the indicated refractivity departs from the true refractivity, and the amount of the departure increases by approximately 7 parts per million per millibar change in vapour pressure.

7.3 Refractivity Change with Humidity - The Capacitor-Type Refractometer

Several changes have been made in the physical construction of the sensing element of the capacitor-type refractometer. These changes have been designed to yield information on the process of vapour adsorption. The results of each modification upon the indicated refractivity are described in the separate sub-sections below.

(a) Quartz-Invar Sensor with Six Quartz Spacers - Uncoated

The combination of quartz and invar in the sensing capacitor has been used because of the low temperature coefficient of expansion. Figure 17 has illustrated the physical construction of this capacitor. It will be noted that the quartz spacers are cylindrical, with shallow slits cut along one side to seat the invar plates. These plates are fastened in place with water-resistant resin glue (Lepage's "Bondfast", baked in an oven for several hours to remove moisture.)

The refractivity of the air within the jet has been measured with this sensor containing six quartz spacers. These measurements were made with mean air temperatures of 9° , 24° , 33° and 47°C , as the humidity of the air was increased from about 20 percent to saturation. Figure 30 illustrates the results of these observations. It will be seen that in each case the indicated refractivity follows the true (Debye) refractivity for relative humidities up to 46 percent. At higher relative humidities,

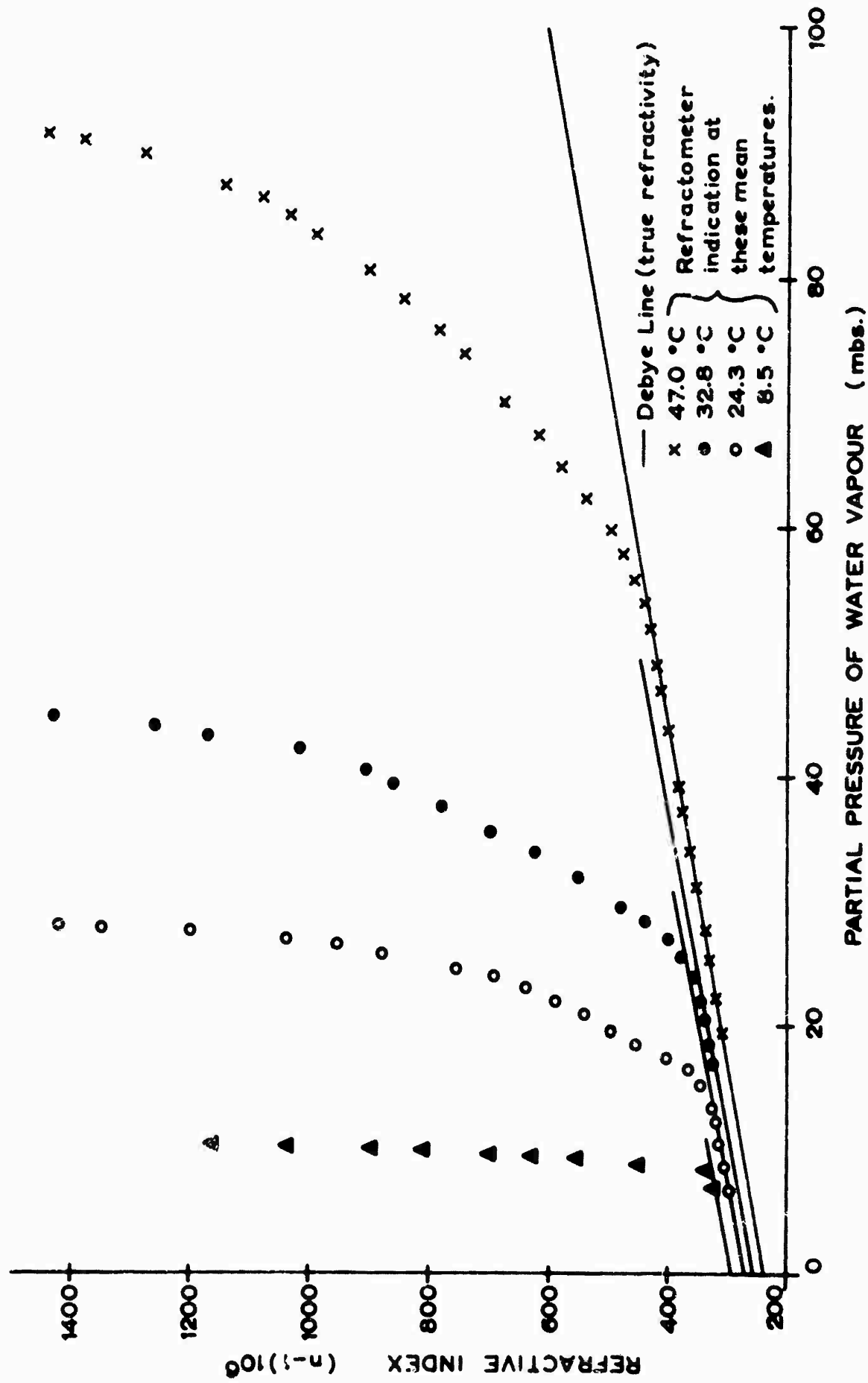


Figure 30: Comparison between indicated and true refractivity, - The Capacitor-Type Refractometer
(Invar capacitor with 6 quartz spacers - uncoated)

the indicated air refractivity departs rapidly from the true refractivity, with the non-linear increase becoming very large in the neighbourhood of saturation. (The Debye line terminates at saturation, in each case, except for that of 47°C).

(b) Quartz-Invar Sensor with Six Quartz Spacers - Coated with Siliclad

The effect of a hydrophobic coating upon the refractivity indication has been examined in this set of observations. The configuration of the refractometer sensor is the same as that in the previous study, and the hydrophobic material is water-soluble silicone concentrate (siliclad, manufactured by Clay-Adams Incorporated, New York 10, New York).

Two sets of measurements have been made upon this type of refractometer sensor. In one, only the quartz spacers have been coated with the hydrophobic material; it was found that the indicated refractivity departed from the true (Debye) refractivity at a relative humidity of 35 percent. For greater relative humidities, the trend of the departure is similar to that described under (a) above. When both the quartz spacers and the invar plates of the capacitor were coated with the hydrophobic compound, the departure from the true refractivity was somewhat similar, but to a lesser extent. The second set of points in Figure 31 indicates the observations for the latter case.

(c) Quartz-Invar Sensor with Six Quartz Spacers - Coated with Cup-Grease

The procedure of section (b) has been repeated, but with a different hydrophobic material. These results are illustrated also in Figure 31. The application of a thin layer of cup-grease to the quartz spacers alone results in a marked decrease in the departure of indicated refractivity from true refractivity; the departure begins at a relative humidity of 48 percent, and the trend in the departure is similar to that of the

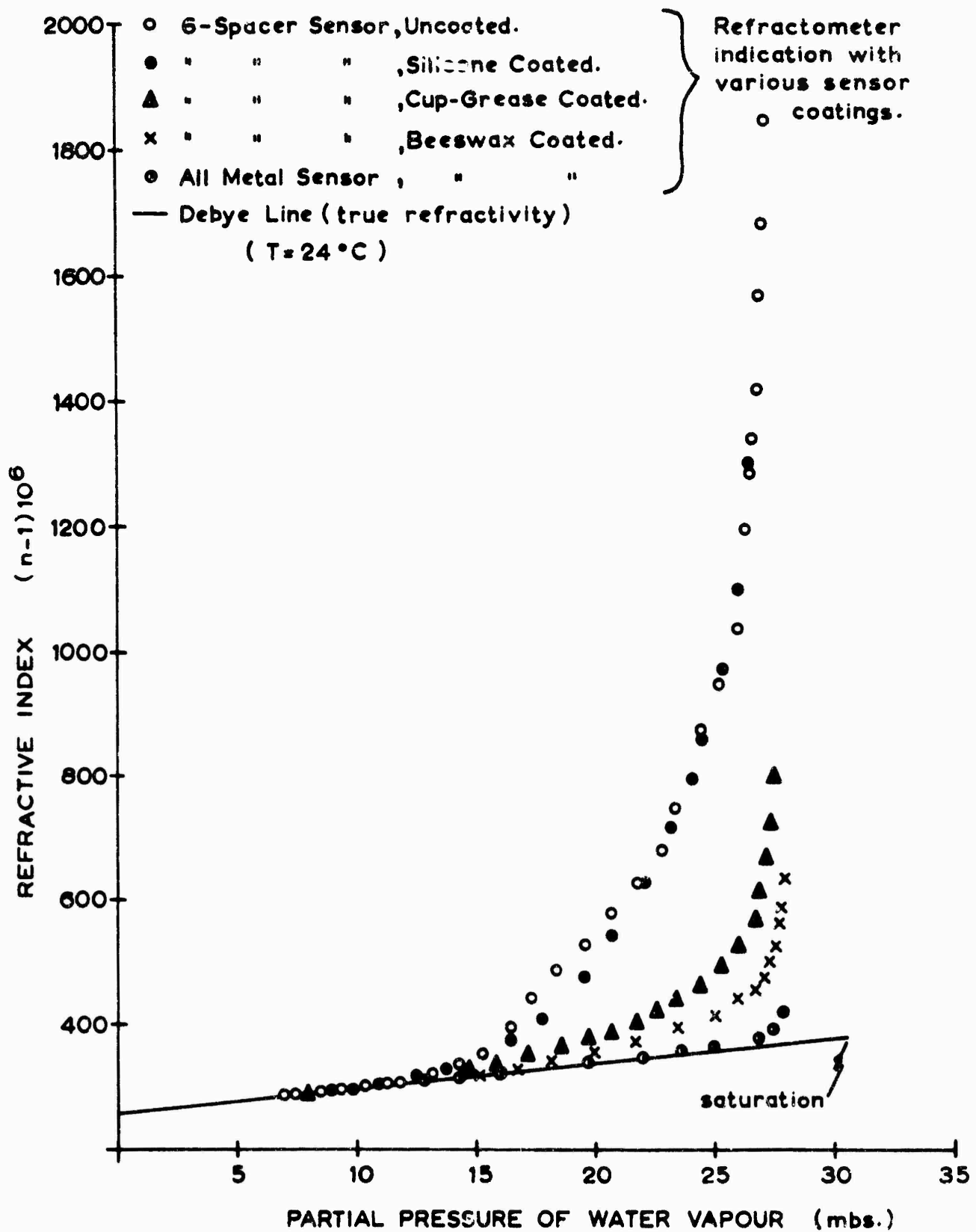


Figure 31: Comparison between indicated and true refractivity, -

The Capacitor-Type Refractometer:

Effects of hydrophobic coatings

previous observations. When the whole of the capacitor is covered with a thin layer of cup-grease, the departure between indicated and true refractivity is even less than above; in this case, the departure also begins at a relative humidity of 48 percent. The third set of points in Figure 31 applies to the latter case.

(d) Quartz-Invar Sensor with Varied Number of Quartz Spacers, - Uncoated

A study has been made upon the adsorption of water vapour upon the quartz spacers, by varying the number of spacers. The number of spacers was varied from six to zero; in the latter, the configuration is as shown in the photograph of Figure 17. Here, the only solid dielectric in the capacitor is at the mounting base where it contacts the box of the refractometer. The capacitor plates are held in position by rigid bolts that fasten to projections from each plate.

Figure 32 illustrates the results of these observations. In all cases, the indicated refractivity departs from the true refractivity at a relative humidity of about 50 percent, but the extent of the departure decreases with the decreasing number of quartz spacers in the capacitor.

(e) Quartz-Invar Sensor and Invar Sensor, - Coated with Beeswax

The final set of observations has been made upon the poorest and the best of the capacitor configurations that were used in the previous studies. In each case, the whole of the capacitor was coated with a thin layer of beeswax, dissolved in benzene. The results of these measurements are shown in the two right-hand curves of Figure 31. Again, it will be seen that the indicated refractivity departs from the true refractivity at a relative humidity in excess of 48 percent. For the capacitor containing six quartz spacers, the total departure from true refractivity is less than that observed when the capacitor was coated

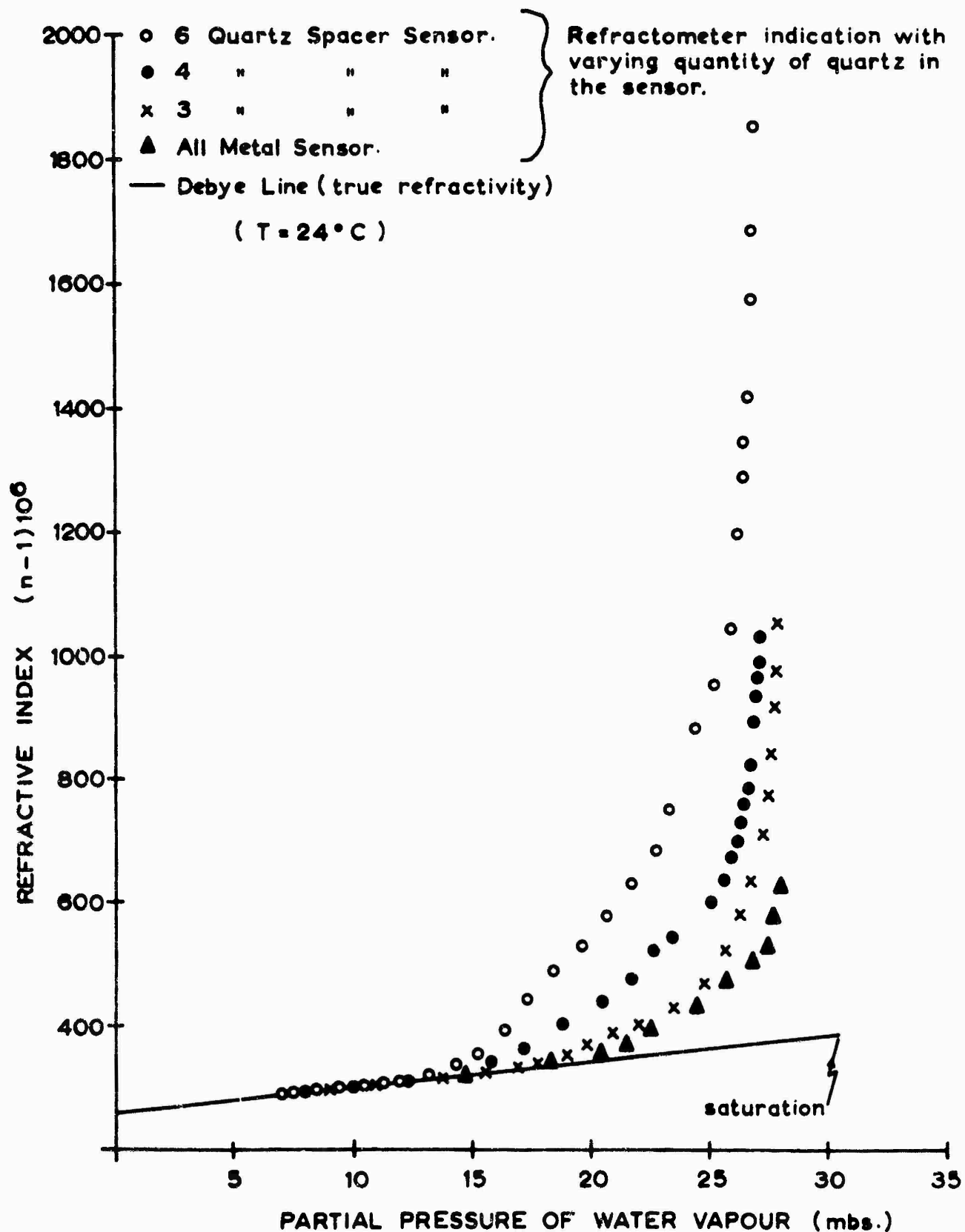


Figure 32: Comparison between indicated and true refractivity, -
The Capacitor-Type Refractometer: Invar capacitor
with variable number of quartz spacers, uncoated

with cup-grease. A further improvement is noted when all of the quartz spacers are removed from the capacitor; here, the performance approaches that of the microwave refractometer.

4. Interpretation and Remarks

The interpretation of the observations in the experiment reported here will be based upon a number of assumptions. First, it will be recognized that the process of water vapour adsorption probably is responsible for the anomalous behaviour of the refractometer sensors at high relative humidities. This assumption appears entirely reasonable, in view of the previous work reported in Section 2.2. Secondly, the extensive difficulties that are encountered in the precise calibration of a hygrometer have made it necessary to assume the Wexler-Brombacher form of the psychrometric equation. This form has been obtained through careful laboratory measurements, and it has been used widely. Thirdly, the form of the Debye equation that is attributed to Smith and Weintraub also has been used in the calculation of refractive index from the hygrometer measurements. Although this form of the equation has not been accepted universally, it has been found satisfactory for most refractivity observations as reported in the literature. The goodness of the second and third assumptions in the present experiment has been demonstrated at least for a wide range of variation in relative humidity by the close agreement between the refractive index of the air as measured by the microwave refractometer and the improved Hay refractometer, and the calculated refractivity as deduced from the hygrometer measurements through the application of the Wexler-Brombacher formula and the Smith-Weintraub equation.

A fourth assumption involves the lack of dispersion in air refractivity over the radio frequency spectrum. It has been demonstrated by Kerr (1951, Chapter VIII) that the refractive index (or dielectric constant) and the electromagnetic absorption of a non-conducting and non-ferromagnetic medium such as the air in the troposphere are closely related by the physical

properties of the medium. A change in the refractive index of the medium must be accompanied by a predictable change in the absorption or attenuation of the medium. In this way, it may be shown that the refractive index of the air varies by much less than one part per million over the whole of the radio frequency spectrum. Consequently, the same refractivity indication must be made by the capacitor-type refractometer at a frequency of approximately 6 Mc/s and the microwave refractometer at a frequency of 10,000 Mc/s.

8.1 Deductions from the Present Experiment

The observations with the optical ellipsometer have raised an important question. The processes of adsorption upon quartz and upon invar plates apparently are notably different. Although the observations were only qualitative, a comparison of the two materials under similar conditions showed that adsorption of vapour occurs readily upon the quartz surface, but not perceptibly upon the isolated invar surface. Further, it is reasonable to assume that the sensitivity of the ellipsometer is sufficient for the present experiment, since it indicated the onset of adsorption at a much lower relative humidity than the observations within the wind tunnel. Although adsorption upon the quartz surface was observed for relative humidities in excess of 20 percent, the amount of adsorption becomes sufficient to affect the capacitor-type sensor only at the large and erratic increase for relative humidities exceeding 50 percent.

A further question arises from a comparison of the ellipsometer observations with those obtained in the wind tunnel. Although the process of adsorption appears to take place upon the metal surfaces of the capacitor-type sensor and the microwave cavity, at least for relative humidities exceeding 85 percent, no adsorption was observed upon the isolated invar

plate within the optical ellipsometer at humidities up to saturation. If it is accepted that the optical ellipsometer is sufficiently sensitive to indicate the presence of an adsorbed layer upon the metal, then it may be suggested that the physical arrangement for the metal within the ellipsometer does not represent the conditions found in the refractometer sensors. One possible difference is the presence of an electric field within the refractometer sensors, which is absent in the isolated invar plate within the ellipsometer. It is suggested further, that the difference in the behaviour of the microwave refractometer sensor and the improved capacitor-type sensor at higher relative humidities is due to the difference in the electric field intensity at the metal surfaces in these two types of sensors, and the consequent effects upon the process of water vapour adsorption.

The results of the refractometer study using the experimental wind tunnel may be summarized as follows. The physical process of vapour adsorption occurs in both the microwave refractometer cavity and in the capacitor-type refractometer sensor, in an amount which is sufficient to affect the indication of refractive index at high relative humidities. However, the effect is notably different within the two sensors: the departure between the true refractivity (Debye) and the indicated refractivity exceeds one part per million for a minimum relative humidity which depends upon the air temperature in the microwave refractometer, and for a minimum relative humidity which is essentially independent of temperature in the untreated capacitor-type refractometer sensor. The departure increases almost linearly with increase in vapour pressure within the microwave cavity, but the departure is non-linear with increasing vapour pressure in the capacitor sensor.

Two factors are important to the physical process of adsorption within the capacitor sensor. The amount of adsorption upon the sensor surfaces depends upon the quantity of quartz present in the capacitor; here, the effects of adsorption decrease with decreasing quantity of quartz. Secondly, adsorption depends upon the type of surface coating on the capacitor. Various types of hydrophobic materials when applied in a thin layer to the surfaces of the capacitor, tend to discourage the adsorption process to different degrees. A thin layer of beeswax has been found to provide the greatest protection against adsorption when applied to all surfaces of the capacitor sensor. It should be noted further, that even when all of the quartz dielectric is removed from the region of strong electric field within the capacitor sensor, the onset of significant adsorption for an air temperature of about 26°C occurs at a lower relative humidity in the capacitor sensor than in the microwave cavity sensor.

8.2 Comments Upon Practical Applications

The results of the present experiment have indicated several points of practical importance. First, it has demonstrated the need for care in interpreting refractivity measurements upon air at high relative humidities; errors in apparent refractivity, well in excess of one part per million, will occur in measurements with the microwave refractometer and with the capacitor-type refractometer at high relative humidities. Secondly, it is possible to obtain a considerable improvement in the accuracy of refractivity indication (at least in the capacitor-type refractometer) through appropriate design of the sensing element. This includes construction of the capacitor with the quartz dielectric removed from the region of strong electric field, and the coating of the metal

plates with a suitable hydrophobic material. An incidental result is derived from the observations upon the temperature coefficient of expansion of the sensing element; the temperature coefficient in the capacitor-type refractometer is predictable with a high degree of precision over a wide range of temperatures.

The present experiment suggests the need for further study. It is desirable that an examination be made of the value of other types of hydrophobic coating upon the refractometer sensor; this investigation should be applied not only to the capacitor-type refractometer, but also to the microwave refractometer. This study may also be extended to include other types of metal in the sensing element. The possibility of reducing undesirable defects of adsorption through reducing the strength of the electric field intensity at the sensing element also deserves further consideration. In addition, the study of temperature compensation in the refractometer sensors may be carried out readily with the wind-tunnel facility.

8.3 Comments upon the Physical Process of Adsorption

An academic interest in the physical process of vapour adsorption upon solid surfaces raises several questions from the results of the present experiment. The apparent difference in the adsorption upon quartz and upon invar indicates a need for a further study on the basic physical processes. This would include a study of the roles played by an electric field at the surface of the material, by various types of materials and contaminations upon the surface, and by the motion of the humid air at the surface. At the present time, the processes of adsorption and condensation upon solid dielectric and metal surfaces at saturation vapour pressures are poorly understood; the techniques for this study

would also require careful consideration. An extensive bibliography on water vapour adsorption at solid surfaces has been compiled and included in Appendix VII.

A better understanding of the process of vapour adsorption at metal surfaces would permit a further investigation into some of the assumptions made in this last section. Of considerable interest is the accuracy of the coefficients in the Smith-Weintraub form of the Debye equation, especially at high relative humidities. Further, the construction of an improved refractometer sensor would permit a more careful comparison between the measured refractivity of a sample of air and that predicted from hygrometer and barometer measurements through the application of the Debye and the psychrometric equations.

Appendix I

Circuits of the Microwave Refractometer

Figure A-1: Block diagram of Microwave Refractometer.

Figure A-2: Circuits of cathode follower and integrator, and of blanking amplitude control.

Figure A-3: Pulse-sharpening circuits.

Figure A-4: Pulse and Sawtooth Waveform Generators.

Figure A-5: 1000 c/s crystal-controlled oscillator.

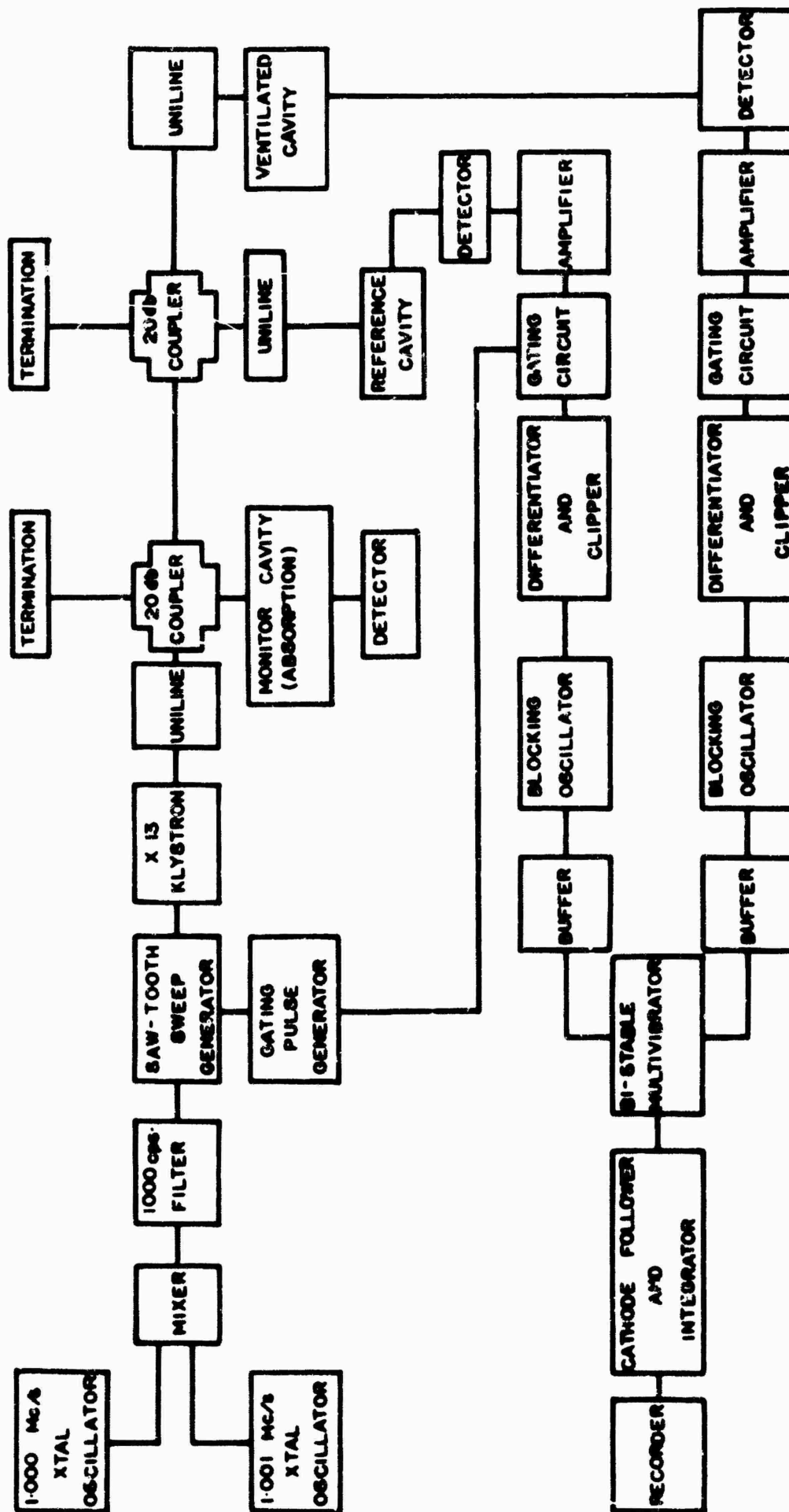


Figure A-1: Block diagram of the Microwave Refractometer

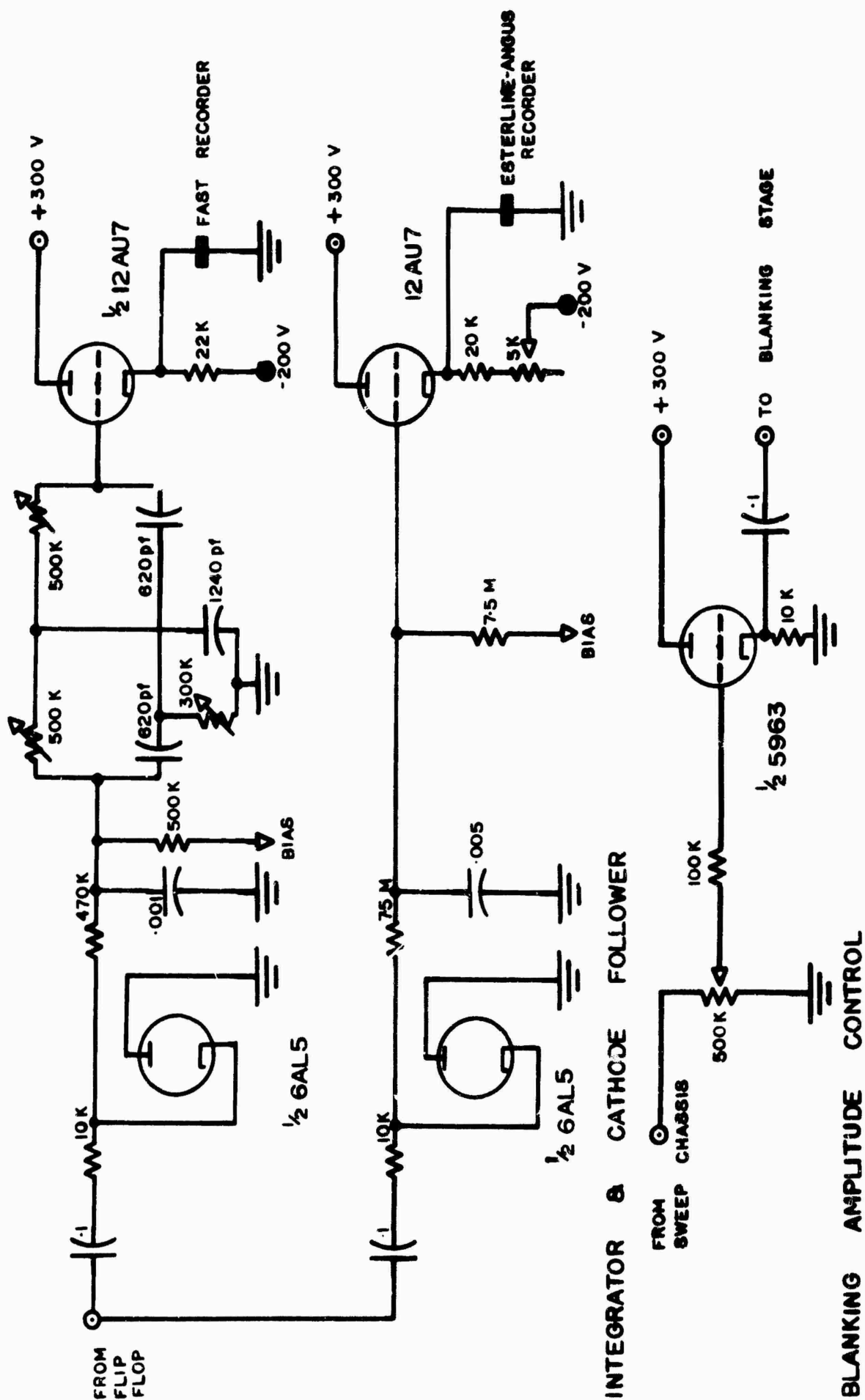


Figure A-2: Circuits of cathode follower and integrator, and of blanking amplitude control

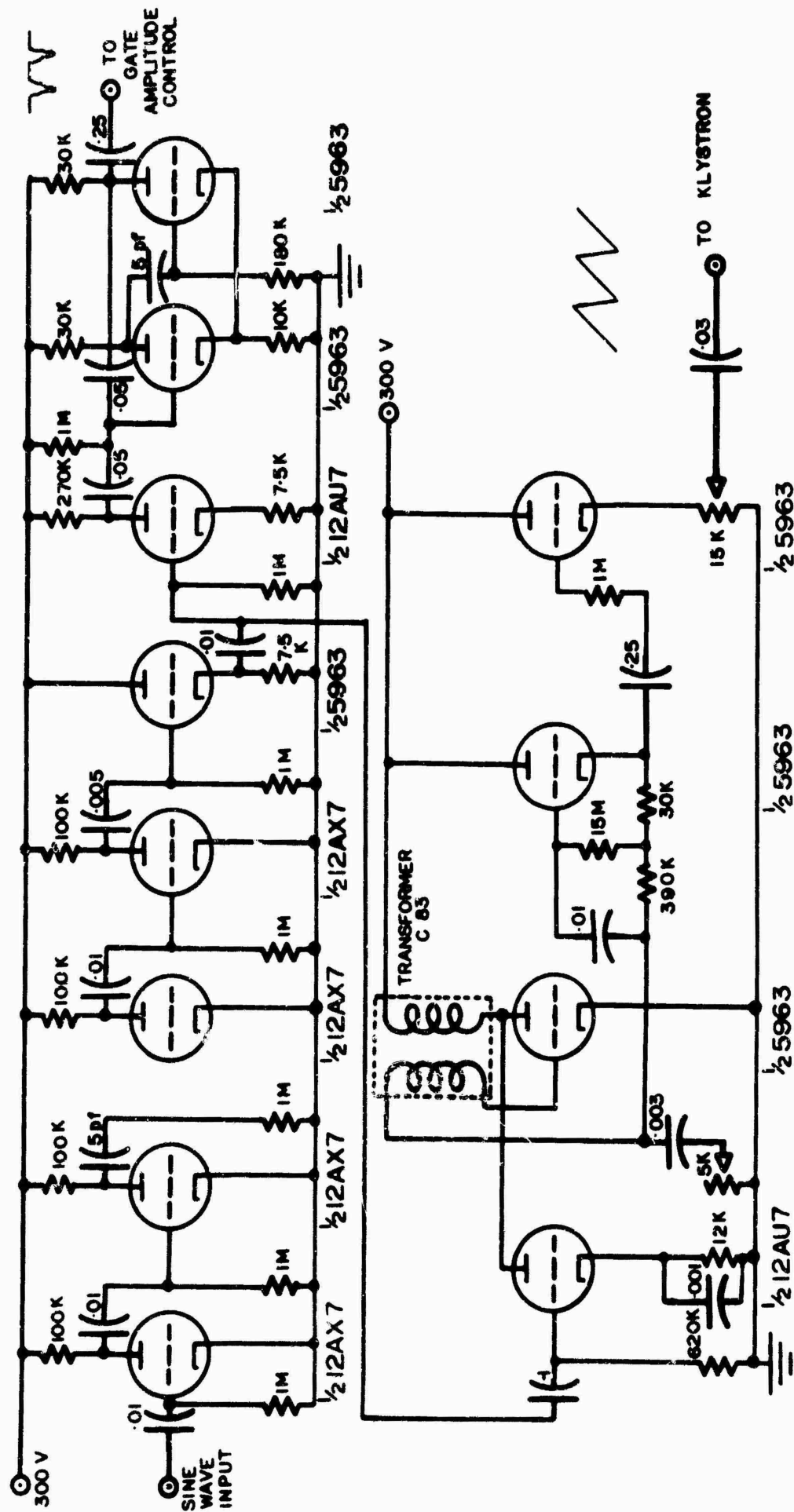


Figure A-4: The pulse and sawtooth waveform generators

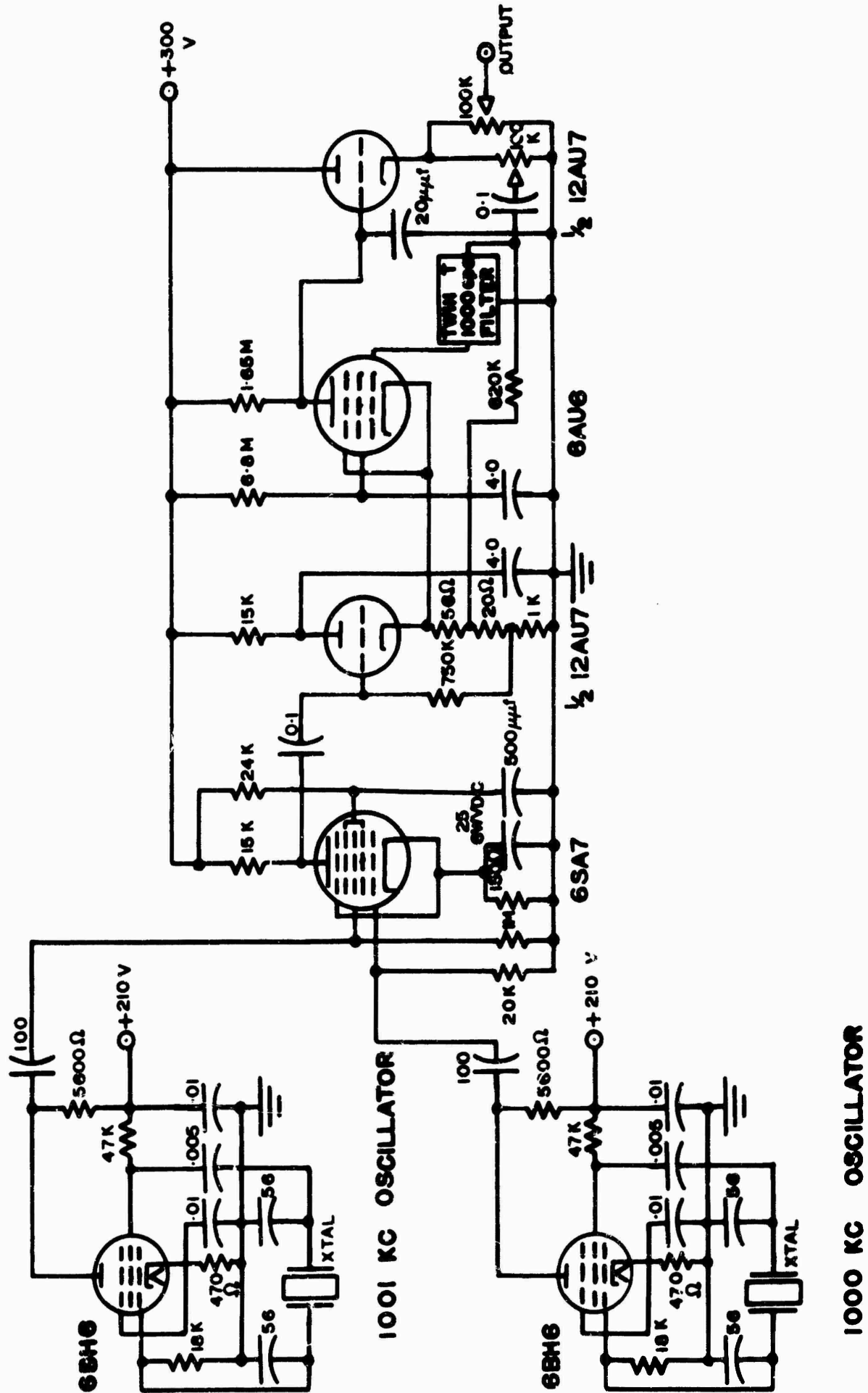


Figure A-5: The 1000 c/s crystal-controlled oscillator

Appendix II

Experimental Procedure for Calibration of the Platinum Wire Resistance Hygrometer

The following experimental procedure has been followed for each set of observations upon the hygrometer in the humidity calibration chamber:

1. All parts of the calibration chamber and its associated apparatus are cleaned with detergent and Bon Ami, and finally with distilled water.
2. The calibrating salt solutions are prepared several hours in advance of the calibration, in covered pyrex dishes, to allow the temperature of the solution to approach room temperature.
3. On the evening before the calibration, the following procedures are carried out:
 - (a) Turn on all electronic equipment.
 - (b) Place required solution in the pyrex plate within the bell-jar.
 - (c) Empty the water reservoir for the wet-bulb probe.
4. On the morning of the calibration the procedure is as follows:
 - (a) Apply bias potential to the platinum resistance probes.
 - (b) Fill the water reservoir for the wet-bulb probe.
 - (c) After waiting ten minutes, take the barometer and manometer readings and the temperature of the calibrating solution.
 - (d) Ventilate the chamber at the prescribed rate and record the probe temperatures for three minutes.
 - (e) Take the barometer and manometer readings and the temperature of the calibrating solution immediately after the completion of the previous step.
 - (f) Turn off chamber ventilation, and take the barometer and manometer readings, and the temperature of the calibrating solution. Then record the temperature probe readings for two minutes.

- (g) Take the readings of the barometer and manometer and the solution temperature immediately after the preceeding step.
- (h) Check the zero setting and the calibrations of the recorder amplifiers.
- (i) After waiting for 15 minutes, repeat the three previous steps.
- (j) Wait for one hour, and check the level of the water in the reservoir for the wet-bulb probe.
- (k) Repeat the above recording procedure.
- (l) Remove the water from the reservoir for the wet-bulb temperature probe.
- (m) After waiting for two hours, repeat all of the above steps.
- (n) Prepare for next day's calibration as in procedure 3 above.

Appendix III

Sample Analysis of Observations Taken in Hygrometer Calibration

Calibrating Solution: K_2SO_4 (R.H. approx. 97 percent)

Equation to be solved: $e = e_w - A p(T - T_D) \dots\dots\dots (a)$

where A is the unknown to be ascertained.

Information obtained from the observations:

Temperature of calibrating solution = T_S °C

Barometric pressure of air in the chamber = p (millibars)

Temperature of air in chamber, before ventilation = T_0 °C

At point "a" in recordings (when T_D first reaches minimum value):

Air temperature = $(T)_a$

Wet-bulb temperature = $(T_D)_a$

Similarly for other subsequent points "b", "c", etc. in recordings.

Then the above information for each of points "a", "b", etc. is applied as follows:

- (i) Average of T_S and T_0 taken to ascertain relative humidity of air in chamber before ventilation (RH_0), from graphs in paper by Wexler and Hasegawa (1954).
- (ii) Vapour pressure of air in chamber before ventilation (e_0) is found from tables of saturation vapour pressure (e_s), from appropriate e_s at temperature T_0 , and from RH_0 .
- (iii) For observations at point "a", temperatures are found to have increased and hence e_a is greater than e_0 .
Since $e_0 = x T_0$, (according to the gas law), x may be deduced, and then $e_a = x(T)_a$. (assuming negligible loss or gain of water vapour in the time between sets of observations).

This value is substituted in the hygrometric formula (a) above
to give:

$$e_a = e_s(T_D)_a - A p [(T)_a - (T_D)_a] \dots\dots\dots (b)$$

Example: (Feb. 25, 1963: 11:11 a.m.)

$$T_S = 21.0^{\circ}\text{C}, \text{ corrected to } 21.1^{\circ}\text{C}$$

$$p = 29.32 \text{ inches Hg.}, \text{ corrected to } 28.93 \text{ inches} = 979.7 \text{ millibars}$$

Manometer levels inside and outside of calibrating chamber equal.

$$T_O = 20.96^{\circ}\text{C}$$

$$\text{Mean of } T_S \text{ and } T_O = 21.03^{\circ}\text{C}$$

$$\text{R.H. at this mean temperature} = 97.2 - \frac{1.03}{5.00} \times 0.3 = 97.14 \text{ percent.}$$

$$\text{But } e_{ST_O} = 24.82 \text{ millibars}$$

$$\text{Then } e_o = \frac{97.14}{100} \times 24.82 = 24.11 \text{ millibars.}$$

$$\text{Also, since } e_o = x T_O, \text{ then } x = \frac{24.11}{20.96} = 1.150$$

Then, for readings at point "a":

$$(T)_a = 21.09^{\circ}\text{C}, \quad (T_D)_a = 20.40^{\circ}\text{C}$$

$$e_a = x (T)_a = 1.150 \times 21.09 = 24.26 \text{ millibars}$$

$$\text{and } e_s(T_D)_A = 23.98 \text{ millibars.}$$

Eqn. (b) becomes:

$$24.26 = 23.98 - A (979.7)(0.69)$$

$$\text{or } A = -0.415 \times 10^{-3}$$

Appendix IV

Table of Vapour Pressures of Liquid Water
(in millibars), for Temperatures from 0°C
to 50°C, corrected for Atmospheric Pressure.

Vapour Pressures of Liquid Water From 0°C to 50°C
(Pressures given in millibars)

t, °C	.00	.01	.02	.03	.04	.05	.06	.07	.08	.09
0.0	6.110	6.115	6.119	6.124	6.128	6.133	6.137	6.142	6.146	6.151
0.1	6.155	6.160	6.164	6.168	6.173	6.178	6.183	6.187	6.192	6.196
0.2	6.201	6.206	6.210	6.215	6.219	6.224	6.228	6.233	6.237	6.242
0.3	6.246	6.251	6.255	6.260	6.264	6.269	6.273	6.278	6.282	6.287
0.4	6.291	6.296	6.300	6.305	6.310	6.315	6.319	6.323	6.329	6.333
0.5	6.338	6.343	6.347	6.352	6.357	6.362	6.366	6.371	6.376	6.380
0.6	6.385	6.390	6.394	6.399	6.403	6.408	6.413	6.417	6.422	6.426
0.7	6.431	6.436	6.440	6.445	6.450	6.455	6.459	6.463	6.469	6.473
0.8	6.478	6.483	6.487	6.492	6.497	6.502	6.506	6.511	6.516	6.520
0.9	6.525	6.530	6.535	6.539	6.544	6.549	6.554	6.559	6.563	6.568
1.0	6.573	6.578	6.583	6.587	6.592	6.597	6.602	6.607	6.611	6.616
1.1	6.621	6.626	6.631	6.635	6.640	6.645	6.650	6.655	6.659	6.664
1.2	6.669	6.674	6.679	6.683	6.688	6.693	6.698	6.703	6.707	6.712
1.3	6.717	6.722	6.727	6.731	6.736	6.741	6.745	6.751	6.755	6.760
1.4	6.765	6.770	6.775	6.780	6.785	6.790	6.794	6.799	6.804	6.809
1.5	6.814	6.819	6.824	6.829	6.834	6.839	6.843	6.848	6.853	6.858
1.6	6.863	6.868	6.873	6.878	6.883	6.888	6.893	6.898	6.903	6.908
1.7	6.913	6.918	6.923	6.928	6.933	6.938	6.943	6.948	6.953	6.958
1.8	6.963	6.968	6.973	6.978	6.983	6.988	6.993	6.998	7.003	7.008
1.9	7.013	7.018	7.023	7.028	7.033	7.038	7.043	7.048	7.053	7.058
2.0	7.063	7.068	7.073	7.078	7.083	7.089	7.094	7.099	7.104	7.108
2.1	7.114	7.119	7.124	7.129	7.134	7.140	7.145	7.150	7.155	7.160
2.2	7.165	7.170	7.175	7.180	7.185	7.190	7.195	7.200	7.205	7.210
2.3	7.215	7.220	7.225	7.231	7.236	7.241	7.246	7.251	7.257	7.262
2.4	7.267	7.272	7.277	7.283	7.288	7.293	7.298	7.303	7.309	7.314
2.5	7.319	7.324	7.329	7.335	7.340	7.345	7.350	7.355	7.361	7.366
2.6	7.371	7.376	7.382	7.387	7.393	7.398	7.403	7.409	7.415	7.420
2.7	7.425	7.430	7.436	7.441	7.446	7.452	7.457	7.462	7.468	7.473
2.8	7.478	7.483	7.489	7.494	7.499	7.505	7.510	7.515	7.521	7.526
2.9	7.531	7.536	7.542	7.547	7.553	7.558	7.563	7.569	7.574	7.580
3.0	7.585	7.590	7.596	7.601	7.606	7.612	7.617	7.622	7.627	7.633
3.1	7.638	7.644	7.649	7.655	7.660	7.666	7.671	7.677	7.682	7.688
3.2	7.693	7.698	7.704	7.709	7.715	7.720	7.725	7.731	7.736	7.742
3.3	7.747	7.753	7.758	7.764	7.769	7.775	7.780	7.786	7.791	7.797
3.4	7.802	7.808	7.813	7.819	7.824	7.830	7.835	7.841	7.846	7.852
3.5	7.857	7.863	7.868	7.874	7.880	7.886	7.891	7.897	7.903	7.908

t, °C	.00	.01	.02	.03	.04	.05	.06	.07	.08	.09
3.6	7.914	7.920	7.925	7.931	7.936	7.942	7.948	7.953	7.959	7.964
3.7	7.970	7.976	7.981	7.987	7.992	7.998	8.004	8.009	8.015	8.020
3.8	8.026	8.032	8.037	8.043	8.049	8.055	8.060	8.066	8.072	8.077
3.9	8.083	8.089	8.095	8.100	8.106	8.112	8.118	8.124	8.129	8.135
4.0	8.141	8.147	8.152	8.158	8.164	8.170	8.175	8.181	8.187	8.192
4.1	8.198	8.204	8.209	8.215	8.221	8.227	8.232	8.238	8.244	8.249
4.2	8.255	8.261	8.267	8.272	8.278	8.284	8.290	8.296	8.301	8.307
4.3	8.313	8.319	8.325	8.330	8.336	8.342	8.348	8.354	8.359	8.365
4.4	8.371	8.377	8.383	8.389	8.395	8.401	8.406	8.412	8.418	8.424
4.5	8.430	8.436	8.442	8.448	8.454	8.460	8.466	8.472	8.478	8.484
4.6	8.490	8.496	8.502	8.508	8.514	8.520	8.526	8.532	8.538	8.544
4.7	8.550	8.556	8.562	8.568	8.574	8.580	8.586	8.592	8.598	8.604
4.8	8.610	8.616	8.622	8.628	8.634	8.640	8.646	8.652	8.658	8.664
4.9	8.670	8.676	8.682	8.688	8.694	8.700	8.706	8.712	8.718	8.724
5.0	8.730	8.736	8.742	8.748	8.755	8.761	8.767	8.773	8.779	8.785
5.1	8.791	8.797	8.803	8.809	8.815	8.822	8.828	8.834	8.840	8.846
5.2	8.852	8.858	8.864	8.871	8.877	8.883	8.889	8.895	8.902	8.908
5.3	8.914	8.920	8.926	8.933	8.939	8.945	8.951	8.957	8.964	8.970
5.4	8.976	8.982	8.989	8.995	9.001	9.008	9.014	9.120	9.026	9.033
5.5	9.039	9.045	9.052	9.058	9.064	9.071	9.077	9.083	9.089	9.096
5.6	9.102	9.108	9.114	9.121	9.127	9.133	9.139	9.145	9.152	9.158
5.7	9.164	9.170	9.177	9.183	9.190	9.196	9.202	9.209	9.215	9.222
5.8	9.228	9.234	9.241	9.247	9.254	9.260	9.266	9.273	9.279	9.286
5.9	9.292	9.298	9.305	9.311	9.318	9.324	9.330	9.337	9.343	9.350
6.0	9.356	9.363	9.369	9.376	9.382	9.389	9.396	9.402	9.409	9.415
6.1	9.422	9.429	9.435	9.442	9.448	9.455	9.461	9.468	9.474	9.481
6.2	9.487	9.494	9.500	9.507	9.513	9.520	9.526	9.533	9.539	9.546
6.3	9.552	9.559	9.565	9.572	9.578	9.585	9.592	9.598	9.605	9.611
6.4	9.618	9.625	9.631	9.638	9.644	9.651	9.658	9.664	9.671	9.677
6.5	9.684	9.691	9.698	9.704	9.711	9.718	9.725	9.732	9.738	9.745
6.6	9.752	9.759	9.766	9.772	9.779	9.786	9.793	9.800	9.806	9.813
6.7	9.820	9.827	9.834	9.840	9.847	9.854	9.861	9.868	9.874	9.881
6.8	9.888	9.895	9.902	9.908	9.915	9.922	9.929	9.936	9.942	9.949
6.9	9.956	9.963	9.970	9.976	9.983	9.990	9.997	10.004	10.010	10.017
7.0	10.024	10.031	10.038	10.045	10.052	10.059	10.065	10.073	10.080	10.087
7.1	10.094	10.101	10.108	10.115	10.122	10.129	10.135	10.142	10.149	10.156
7.2	10.163	10.170	10.177	10.184	10.191	10.198	10.204	10.211	10.218	10.225
7.3	10.232	10.239	10.246	10.253	10.260	10.267	10.274	10.281	10.288	10.295
7.4	10.302	10.309	10.316	10.324	10.331	10.338	10.345	10.352	10.360	10.367
7.5	10.374	10.381	10.388	10.395	10.402	10.409	10.416	10.423	10.430	10.437

t, °C	.00	.01	.02	.03	.04	.05	.06	.07	.08	.09
7.6	10.444	10.451	10.458	10.466	10.473	10.480	10.487	10.494	10.502	10.509
7.7	10.516	10.523	10.530	10.538	10.545	10.552	10.559	10.566	10.574	10.581
7.8	10.588	10.595	10.602	10.610	10.617	10.624	10.631	10.638	10.646	10.653
7.9	10.660	10.667	10.675	10.682	10.690	10.697	10.704	10.712	10.719	10.727
8.0	10.734	10.741	10.749	10.756	10.763	10.771	10.778	10.785	10.792	10.800
8.1	10.807	10.814	10.822	10.829	10.836	10.844	10.851	10.858	10.865	10.873
8.2	10.880	10.888	10.895	10.903	10.910	10.918	10.925	10.933	10.940	10.948
8.3	10.955	10.963	10.970	10.978	10.985	10.993	11.000	11.008	11.005	11.023
8.4	11.030	11.037	11.045	11.052	11.060	11.067	11.074	11.082	11.089	11.097
8.5	11.104	11.112	11.119	11.127	11.134	11.142	11.150	11.157	11.165	11.172
8.6	11.180	11.188	11.195	11.203	11.210	11.218	11.225	11.233	11.240	11.248
8.7	11.255	11.263	11.270	11.278	11.286	11.294	11.301	11.309	11.317	11.324
8.8	11.332	11.340	11.347	11.355	11.362	11.370	11.378	11.385	11.393	11.400
8.9	11.408	11.416	11.424	11.431	11.439	11.447	11.455	11.463	11.470	11.478
9.0	11.486	11.494	11.502	11.509	11.517	11.525	11.533	11.541	11.548	11.556
9.1	11.564	11.572	11.580	11.588	11.596	11.604	11.612	11.620	11.628	11.636
9.2	11.644	11.652	11.660	11.668	11.676	11.684	11.691	11.699	11.707	11.715
9.3	11.723	11.731	11.739	11.746	11.754	11.762	11.770	11.778	11.785	11.793
9.4	11.801	11.809	11.817	11.825	11.833	11.841	11.849	11.857	11.865	11.873
9.5	11.881	11.889	11.897	11.905	11.913	11.921	11.929	11.937	11.945	11.953
9.6	11.961	11.969	11.977	11.985	11.993	12.001	12.009	12.017	12.025	12.033
9.7	12.041	12.049	12.057	12.066	12.074	12.082	12.090	12.098	12.107	12.115
9.8	12.123	12.131	12.139	12.147	12.155	12.164	12.172	12.180	12.188	12.196
9.9	12.204	12.212	12.221	12.229	12.237	12.246	12.254	12.262	12.270	12.279
10.0	12.287	12.295	12.303	12.312	12.320	12.328	12.336	12.344	12.353	12.361
10.1	12.369	12.377	12.386	12.394	12.402	12.411	12.419	12.427	12.435	12.444
10.2	12.452	12.460	12.469	12.477	12.485	12.494	12.502	12.510	12.518	12.527
10.3	12.535	12.543	12.552	12.560	12.569	12.577	12.585	12.594	12.602	12.611
10.4	12.619	12.627	12.636	12.644	12.652	12.661	12.669	12.677	12.685	12.694
10.5	12.702	12.711	12.719	12.728	12.736	12.745	12.754	12.762	12.771	12.779
10.6	12.788	12.797	12.805	12.814	12.822	12.831	12.839	12.848	12.856	12.865
10.7	12.873	12.882	12.890	12.899	12.908	12.917	12.925	12.934	12.943	12.951
10.8	12.960	12.969	12.977	12.986	12.995	13.004	13.012	13.021	13.030	13.038
10.9	13.047	13.056	13.064	13.073	13.081	13.090	13.099	13.107	13.116	13.124
11.0	13.133	13.142	13.150	13.159	13.168	13.177	13.185	13.194	13.203	13.211
11.1	13.220	13.229	13.238	13.247	13.256	13.265	13.273	13.282	13.291	13.300
11.2	13.309	13.318	13.327	13.335	13.344	13.353	13.362	13.371	13.379	13.388
11.3	13.397	13.406	13.415	13.424	13.433	13.442	13.451	13.460	13.469	13.478
11.4	13.487	13.496	13.505	13.514	13.523	13.532	13.541	13.550	13.559	13.568
11.5	13.577	13.586	13.595	13.604	13.613	13.623	13.632	13.641	13.650	13.659

t, °C	.00	.01	.02	.03	.04	.05	.06	.07	.08	.09
11.6	13.668	13.677	13.686	13.695	13.704	13.714	13.723	13.732	13.741	13.750
11.7	13.759	13.768	13.777	13.786	13.795	13.804	13.813	13.822	13.831	13.840
11.8	13.849	13.858	13.867	13.877	13.886	13.895	13.904	13.913	13.923	13.932
11.9	13.941	13.950	13.959	13.969	13.978	13.987	13.996	14.005	14.015	14.024
12.0	14.033	14.042	14.052	14.061	14.071	14.080	14.089	14.099	14.108	14.118
12.1	14.127	14.136	14.146	14.155	14.164	14.174	14.183	14.192	14.201	14.211
12.2	14.220	14.229	14.239	14.248	14.257	14.267	14.276	14.285	14.294	14.304
12.3	14.313	14.322	14.332	14.341	14.351	14.360	14.369	14.379	14.388	14.398
12.4	14.407	14.417	14.426	14.436	14.445	14.455	14.464	14.474	14.483	14.493
12.5	14.502	14.512	14.521	14.531	14.540	14.550	14.559	14.569	14.578	14.588
12.6	14.597	14.607	14.616	14.626	14.635	14.645	14.655	14.664	14.674	14.683
12.7	14.693	14.703	14.712	14.722	14.731	14.741	14.751	14.760	14.770	14.779
12.8	14.789	14.799	14.809	14.818	14.828	14.838	14.848	14.858	14.867	14.877
12.9	14.887	14.897	14.906	14.916	14.925	14.935	14.945	14.954	14.964	14.973
13.0	14.983	14.993	15.003	15.013	15.023	15.033	15.042	15.052	15.062	15.072
13.1	15.082	15.092	15.102	15.112	15.122	15.132	15.141	15.151	15.161	15.171
13.2	15.181	15.191	15.201	15.211	15.221	15.231	15.240	15.250	15.260	15.270
13.3	15.280	15.290	15.300	15.310	15.320	15.330	15.340	15.350	15.360	15.370
13.4	15.380	15.390	15.400	15.411	15.421	15.431	15.441	15.451	15.462	15.472
13.5	15.482	15.492	15.502	15.513	15.523	15.533	15.543	15.553	15.564	15.574
13.6	15.584	15.594	15.604	15.614	15.624	15.635	15.645	15.655	15.665	15.675
13.7	15.685	15.695	15.706	15.716	15.726	15.737	15.747	15.757	15.767	15.778
13.8	15.788	15.798	15.808	15.819	15.829	15.839	15.849	15.859	15.870	15.880
13.9	15.890	15.900	15.911	15.921	15.931	15.942	15.952	15.962	15.972	15.983
14.0	15.993	16.003	16.014	16.024	16.035	16.045	16.055	16.066	16.076	16.087
14.1	16.097	16.108	16.118	16.129	16.139	16.150	16.160	16.171	16.181	16.192
14.2	16.202	16.213	16.223	16.234	16.245	16.256	16.266	16.277	16.288	16.298
14.3	16.309	16.319	16.330	16.340	16.351	16.361	16.371	16.382	16.392	16.403
14.4	16.413	16.424	16.434	16.445	16.456	16.467	16.477	16.488	16.499	16.509
14.5	16.520	16.531	16.541	16.552	16.562	16.573	16.584	16.594	16.605	16.615
14.6	16.626	16.637	16.648	16.658	16.669	16.680	16.691	16.702	16.712	16.723
14.7	16.734	16.745	16.756	16.766	16.777	16.788	16.799	16.810	16.820	16.831
14.8	16.842	16.853	16.864	16.875	16.886	16.897	16.908	16.919	16.930	16.941
14.9	16.952	16.963	16.974	16.985	16.996	17.007	17.017	17.028	17.039	17.050
15.0	17.061	17.072	17.083	17.094	17.105	17.116	17.126	17.137	17.148	17.159
15.1	17.170	17.181	17.192	17.204	17.215	17.226	17.237	17.248	17.260	17.271
15.2	17.282	17.293	17.304	17.316	17.327	17.338	17.349	17.360	17.372	17.383
15.3	17.394	17.405	17.416	17.428	17.439	17.450	17.461	17.472	17.484	17.495
15.4	17.506	17.517	17.528	17.540	17.551	17.562	17.573	17.584	17.596	17.607
15.5	17.618	17.629	17.641	17.652	17.664	17.675	17.686	17.698	17.709	17.721

t, °C	.00	.01	.02	.03	.04	.05	.06	.07	.08	.09
15.6	17.732	17.743	17.755	17.766	17.777	17.789	17.800	17.811	17.822	17.834
15.7	17.845	17.857	17.868	17.880	17.891	17.903	17.914	17.926	17.937	17.949
15.8	17.960	17.971	17.983	17.994	18.005	18.017	18.028	18.040	18.051	18.063
15.9	18.074	18.086	18.097	18.109	18.120	18.132	18.144	18.155	18.167	18.178
16.0	18.190	18.202	18.213	18.225	18.236	18.248	18.260	18.271	18.283	18.294
16.1	18.306	18.318	18.329	18.341	18.353	18.365	18.376	18.388	18.400	18.411
16.2	18.423	18.435	18.447	18.459	18.471	18.483	18.494	18.506	18.518	18.530
16.3	18.542	18.554	18.566	18.578	18.590	18.602	18.613	18.625	18.637	18.649
16.4	18.661	18.673	18.685	18.696	18.708	18.720	18.732	18.744	18.755	18.767
16.5	18.779	18.791	18.803	18.815	18.827	18.839	18.851	18.863	18.875	18.887
16.6	18.899	18.911	18.923	18.935	18.947	18.959	18.971	18.983	18.995	19.007
16.7	19.019	19.031	19.043	19.056	19.068	19.080	19.092	19.104	19.117	19.129
16.8	19.141	19.153	19.165	19.177	19.189	19.202	19.214	19.226	19.238	19.250
16.9	19.262	19.274	19.287	19.299	19.311	19.324	19.336	19.348	19.360	19.373
17.0	19.385	19.397	19.410	19.422	19.435	19.447	19.459	19.472	19.484	19.497
17.1	19.509	19.521	19.534	19.546	19.559	19.571	19.583	19.596	19.608	19.621
17.2	19.633	19.646	19.659	19.671	19.683	19.696	19.708	19.721	19.733	19.746
17.3	19.758	19.771	19.783	19.796	19.808	19.821	19.833	19.846	19.858	19.871
17.4	19.883	19.896	19.908	19.921	19.933	19.946	19.959	19.971	19.984	19.996
17.5	20.009	20.022	20.034	20.047	20.059	20.072	20.085	20.097	20.110	20.122
17.6	20.135	20.148	20.161	20.173	20.186	20.199	20.212	20.225	20.237	20.250
17.7	20.263	20.276	20.289	20.301	20.314	20.327	20.340	20.353	20.365	20.378
17.8	20.391	20.404	20.417	20.429	20.442	20.455	20.468	20.481	20.493	20.506
17.9	20.519	20.532	20.545	20.558	20.571	20.584	20.597	20.610	20.623	20.636
18.0	20.649	20.662	20.675	20.688	20.701	20.714	20.727	20.740	20.753	20.766
18.1	20.779	20.792	20.805	20.818	20.831	20.845	20.858	20.871	20.884	20.897
18.2	20.910	20.923	20.936	20.949	20.963	20.976	20.989	21.002	21.016	21.029
18.3	21.042	21.055	21.068	21.082	21.095	21.108	21.121	21.134	21.148	21.161
18.4	21.174	21.187	21.201	21.214	21.227	21.241	21.254	21.267	21.280	21.294
18.5	21.307	21.321	21.334	21.348	21.361	21.375	21.388	21.402	21.415	21.429
18.6	21.442	21.455	21.469	21.482	21.495	21.509	21.522	21.535	21.548	21.562
18.7	21.575	21.589	21.602	21.616	21.629	21.643	21.656	21.670	21.683	21.697
18.8	21.710	21.724	21.737	21.751	21.764	21.778	21.792	21.805	21.819	21.832
18.9	21.846	21.860	21.873	21.887	21.901	21.915	21.928	21.942	21.956	21.969
19.0	21.983	21.997	22.011	22.025	22.039	22.053	22.066	22.080	22.094	22.108
19.1	22.122	22.136	22.150	22.163	22.177	22.191	22.205	22.219	22.232	22.246
19.2	22.260	22.274	22.288	22.302	22.316	22.330	22.343	22.357	22.371	22.385
19.3	22.399	22.413	22.427	22.441	22.455	22.469	22.483	22.497	22.511	22.525
19.4	22.539	22.553	22.567	22.581	22.595	22.609	22.623	22.637	22.651	22.665
19.5	22.679	22.693	22.707	22.721	22.735	22.750	22.764	22.778	22.792	22.806

t, °C	.00	.01	.02	.03	.04	.05	.06	.07	.08	.09
19.6	22.820	22.834	22.849	22.863	22.877	22.892	22.906	22.920	22.934	22.949
19.7	22.963	22.977	22.992	23.006	23.020	23.035	23.049	23.063	23.077	23.092
19.8	23.106	23.120	23.135	23.149	23.164	23.178	23.192	23.207	23.221	23.236
19.9	23.250	23.264	23.279	23.293	23.308	23.322	23.336	23.351	23.365	23.380
20.0	23.394	23.409	23.423	23.438	23.452	23.467	23.482	23.496	23.511	23.525
20.1	23.540	23.555	23.569	23.584	23.598	23.613	23.628	23.642	23.657	23.671
20.2	23.686	23.701	23.715	23.730	23.744	23.759	23.774	23.788	23.803	23.817
20.3	23.832	23.847	23.862	23.876	23.891	23.906	23.921	23.936	23.950	23.965
20.4	23.980	23.995	24.010	24.024	24.039	24.054	24.069	24.084	24.098	24.113
20.5	24.128	24.143	24.158	24.173	24.188	24.203	24.218	24.233	24.248	24.263
20.6	24.278	24.293	24.308	24.323	24.338	24.353	24.367	24.382	24.397	24.412
20.7	24.427	24.442	24.457	24.472	24.487	24.503	24.518	24.533	24.548	24.563
20.8	24.578	24.593	24.608	24.624	24.639	24.654	24.669	24.684	24.700	24.715
20.9	24.730	24.745	24.760	24.776	24.791	24.806	24.821	24.836	24.852	24.867
21.0	24.882	24.897	24.912	24.928	24.943	24.958	24.973	24.988	25.004	25.019
21.1	25.034	25.049	25.065	25.080	25.096	25.111	25.126	25.142	25.157	25.173
21.2	25.188	25.204	25.219	25.235	25.250	25.266	25.281	25.297	25.312	25.328
21.3	25.343	25.359	25.374	25.390	25.406	25.422	25.437	25.453	25.469	25.484
21.4	25.500	25.516	25.531	25.547	25.563	25.579	25.594	25.610	25.626	25.641
21.5	25.657	25.673	25.689	25.704	25.720	25.736	25.752	25.768	25.783	25.799
21.6	25.815	25.831	25.847	25.862	25.878	25.894	25.910	25.926	25.941	25.957
21.7	25.973	25.989	26.005	26.021	26.037	26.053	26.068	26.084	26.100	26.116
21.8	26.132	26.148	26.164	26.180	26.196	26.212	26.228	26.244	26.260	26.276
21.9	26.292	26.308	26.324	26.340	26.356	26.372	26.388	26.404	26.420	26.436
22.0	26.452	26.468	26.484	26.500	26.516	26.533	26.549	26.565	26.581	26.597
22.1	26.613	26.629	26.646	26.662	26.678	26.695	26.711	26.727	26.743	26.760
22.2	26.776	26.792	26.809	26.825	26.842	26.858	26.874	26.891	26.908	26.924
22.3	26.940	26.956	26.973	26.989	27.006	27.022	27.038	27.055	27.071	27.088
22.4	27.104	27.121	27.137	27.154	27.170	27.187	27.203	27.220	27.236	27.253
22.5	27.269	27.286	27.302	27.319	27.336	27.353	27.369	27.386	27.403	27.419
22.6	27.436	27.453	27.470	27.486	27.503	27.520	27.537	27.554	27.570	27.587
22.7	27.604	27.621	27.637	27.654	27.671	27.688	27.704	27.721	27.738	27.754
22.8	27.771	27.788	27.805	27.821	27.838	27.855	27.872	27.889	27.905	27.922
22.9	27.939	27.956	27.973	27.990	28.007	28.024	28.040	28.057	28.074	28.091
23.0	28.108	28.125	28.142	28.159	28.176	28.194	28.211	28.228	28.245	28.262
23.1	28.279	28.296	28.313	28.330	28.347	28.364	28.381	28.398	28.415	28.432
23.2	28.449	28.466	28.483	28.501	28.518	28.535	28.552	28.569	28.587	28.604
23.3	28.621	28.638	28.656	28.673	28.690	28.708	28.725	28.742	28.759	28.777
23.4	28.794	28.812	28.829	28.847	28.864	28.882	28.899	28.917	28.934	28.952
23.5	28.969	28.987	29.004	29.022	29.039	29.057	29.074	29.092	29.109	29.127

t, °C	.00	.01	.02	.03	.04	.05	.06	.07	.08	.09
23.6	29.144	29.162	29.179	29.197	29.214	29.232	29.250	29.267	29.285	29.302
23.7	29.320	29.338	29.355	29.373	29.391	29.408	29.426	29.444	29.462	29.479
23.8	29.497	29.515	29.533	29.551	29.569	29.587	29.604	29.622	29.640	29.658
23.9	29.676	29.694	29.712	29.729	29.747	29.765	29.783	29.800	29.818	29.836
24.0	29.854	29.872	29.890	29.908	29.926	29.944	29.962	29.980	29.998	30.016
24.1	30.034	30.052	30.070	30.089	30.107	30.125	30.143	30.161	30.180	30.198
24.2	30.216	30.234	30.252	30.271	30.289	30.307	30.325	30.343	30.362	30.380
24.3	30.398	30.416	30.435	30.453	30.471	30.490	30.508	30.526	30.544	30.563
24.4	30.581	30.599	30.618	30.636	30.655	30.673	30.691	30.710	30.728	30.747
24.5	30.765	30.783	30.802	30.820	30.839	30.857	30.875	30.894	30.912	30.931
24.6	30.949	30.968	30.986	31.005	31.023	31.042	31.060	31.079	31.097	31.116
24.7	31.134	31.153	31.171	31.190	31.208	31.227	31.246	31.264	31.283	31.301
24.8	31.320	31.339	31.357	31.376	31.394	31.413	31.432	31.450	31.469	31.487
24.9	31.506	31.525	31.544	31.562	31.581	31.600	31.619	31.638	31.656	31.675
25.0	31.694	31.713	31.732	31.750	31.769	31.788	31.807	31.826	31.844	31.863
25.1	31.882	31.901	31.920	31.939	31.958	31.977	31.995	32.014	32.033	32.052
25.2	32.071	32.090	32.109	32.128	32.147	32.167	32.186	32.205	32.224	32.243
25.3	32.262	32.281	32.300	32.320	32.339	32.358	32.377	32.396	32.416	32.435
25.4	32.454	32.473	32.493	32.512	32.531	32.551	32.570	32.589	32.608	32.628
25.5	32.647	32.667	32.686	32.706	32.725	32.745	32.764	32.784	32.803	32.823
25.6	32.842	32.862	32.881	32.901	32.920	32.940	32.960	32.979	32.999	33.018
25.7	33.038	33.058	33.077	33.097	33.117	33.137	33.156	33.176	33.196	33.215
25.8	33.235	33.255	33.275	33.294	33.314	33.334	33.354	33.374	33.393	33.413
25.9	33.433	33.453	33.473	33.492	33.512	33.532	33.552	33.572	33.591	33.611
26.0	33.631	33.651	33.671	33.692	33.712	33.732	33.752	33.772	33.793	33.813
26.1	33.833	33.853	33.873	33.893	33.913	33.933	33.953	33.973	33.993	34.013
26.2	34.033	34.053	34.073	34.093	34.113	34.134	34.154	34.174	34.194	34.214
26.3	34.234	34.254	34.275	34.295	34.315	34.336	34.356	34.376	34.396	34.417
26.4	34.437	34.457	34.477	34.498	34.518	34.538	34.558	34.578	34.599	34.619
26.5	34.639	34.659	34.680	34.700	34.721	34.741	34.761	34.782	34.802	34.823
26.6	34.843	34.864	34.884	34.905	34.925	34.946	34.966	34.987	35.007	35.028
26.7	35.048	35.069	35.089	35.110	35.131	35.152	35.172	35.193	35.214	35.234
26.8	35.255	35.276	35.297	35.317	35.338	35.359	35.380	35.401	35.421	35.442
26.9	35.463	35.484	35.505	35.526	35.547	35.568	35.588	35.609	35.630	35.651
27.0	35.672	35.693	35.714	35.736	35.757	35.778	35.799	35.820	35.842	35.863
27.1	35.884	35.905	35.926	35.947	35.968	35.990	36.011	36.032	36.053	36.074
27.2	36.095	36.116	36.137	36.159	36.180	36.201	36.222	36.243	36.265	36.286
27.3	36.307	36.328	36.350	36.371	36.392	36.414	36.435	36.456	36.477	36.499
27.4	36.520	36.542	36.563	36.585	36.606	36.628	36.649	36.671	36.692	36.714
27.5	36.735	36.757	36.778	36.800	36.821	36.843	36.864	36.886	36.907	36.929

t, °C	.00	.01	.02	.03	.04	.05	.06	.07	.08	.09
27.6	36.950	36.972	36.993	37.015	37.036	37.058	37.080	37.101	37.123	37.144
27.7	37.166	37.188	37.209	37.231	37.253	37.275	37.296	37.318	37.340	37.361
27.8	37.383	37.405	37.427	37.449	37.471	37.493	37.514	37.536	37.558	37.580
27.9	37.602	37.624	37.646	37.667	37.689	37.711	37.733	37.755	37.776	37.798
28.0	37.820	37.842	37.864	37.887	37.909	37.931	37.953	37.975	37.997	38.020
28.1	38.042	38.064	38.086	38.108	38.130	38.153	38.175	38.197	38.219	38.241
28.2	38.263	38.285	38.307	38.330	38.352	38.374	38.396	38.418	38.441	38.463
28.3	38.485	38.507	38.530	38.552	38.575	38.597	38.619	38.642	38.664	38.687
28.4	38.709	38.732	38.754	38.777	38.799	38.822	38.845	38.867	38.890	38.912
28.5	38.935	38.958	38.980	39.003	39.025	39.048	39.071	39.093	39.116	39.138
28.6	39.161	39.184	39.207	39.229	39.252	39.275	39.298	39.321	39.343	39.366
28.7	39.389	39.412	39.435	39.458	39.481	39.504	39.527	39.550	39.573	39.596
28.8	39.619	39.642	39.665	39.688	38.711	39.734	39.757	39.780	39.803	39.826
28.9	39.849	39.872	39.895	38.919	39.942	39.965	39.988	40.011	40.035	40.058
29.0	40.081	40.104	40.127	40.151	40.174	40.197	40.220	40.243	40.267	40.290
29.1	40.313	40.336	40.360	40.383	40.407	40.430	40.453	40.477	40.500	40.524
29.2	40.547	40.570	40.594	40.617	40.641	40.664	40.687	40.711	40.734	40.758
29.3	40.781	40.805	40.828	40.852	40.875	40.899	40.923	40.946	40.970	40.993
29.4	41.017	41.041	41.065	41.088	41.112	41.136	41.160	41.184	41.207	41.231
29.5	41.255	41.279	41.303	41.326	41.350	41.374	41.398	41.422	41.445	41.469
29.6	41.493	41.517	41.541	41.565	41.589	41.613	41.636	41.660	41.684	41.708
29.7	41.732	41.756	41.780	41.804	41.828	41.852	41.876	41.900	41.924	41.948
29.8	41.972	41.996	42.020	42.045	42.069	42.093	42.117	42.141	42.166	42.190
29.9	42.214	42.238	42.263	42.287	42.311	42.336	42.360	42.384	42.408	42.433
30.0	42.457	42.481	42.506	42.530	42.555	42.579	42.603	42.628	42.652	42.677
30.1	42.701	42.726	42.750	42.775	42.799	42.824	42.848	42.873	42.897	42.922
30.2	42.946	42.971	42.995	43.020	43.045	43.070	43.094	43.119	43.144	43.168
30.3	43.193	43.218	43.242	43.267	43.292	43.317	43.341	43.366	43.391	43.415
30.4	43.440	43.465	43.490	43.514	43.539	43.564	43.589	43.614	43.638	43.663
30.5	43.688	43.712	43.738	43.763	43.788	43.813	43.837	43.862	43.887	43.912
30.6	43.937	43.962	43.987	44.012	44.037	44.063	44.088	44.113	44.138	44.163
30.7	44.188	44.213	44.239	44.264	44.290	44.315	44.340	44.366	44.391	44.417
30.8	44.442	44.468	44.493	44.519	44.544	44.570	44.595	44.621	44.646	44.672
30.9	44.697	44.723	44.748	44.774	44.799	44.825	44.851	44.876	44.902	44.927
31.0	44.953	44.979	45.004	45.030	45.056	45.082	45.107	45.133	45.159	45.184
31.1	45.210	45.236	45.262	45.288	45.314	45.340	45.365	45.391	45.417	45.443
31.2	45.469	45.495	45.521	45.546	45.572	45.598	45.624	45.650	45.675	45.701
31.3	45.727	45.753	45.779	45.805	45.831	45.857	45.883	45.909	45.935	45.961
31.4	45.987	46.013	46.039	46.066	46.092	46.118	46.144	46.170	46.197	46.223
31.5	46.249	46.275	46.302	46.328	46.355	46.381	46.407	46.434	46.460	46.487

$t, ^\circ\text{C}$.00	.01	.02	.03	.04	.05	.06	.07	.08	.09
31.6	46.513	46.539	46.566	46.592	46.619	46.645	46.671	46.698	46.724	46.751
31.7	46.777	46.804	46.830	46.857	46.883	46.910	46.936	46.963	46.989	47.016
31.8	47.042	47.069	47.096	47.122	47.149	47.176	47.203	47.230	47.256	47.283
31.9	47.310	47.337	47.364	47.390	47.417	47.444	47.471	47.498	47.524	47.551
32.0	47.578	47.605	47.632	47.659	47.686	47.713	47.739	47.766	47.793	47.820
32.1	47.847	47.874	47.901	47.928	47.955	47.983	48.010	48.037	48.064	48.091
32.2	48.118	48.145	48.172	48.200	48.227	48.254	48.281	48.308	48.336	48.363
32.3	48.390	48.417	48.445	48.472	48.500	48.527	48.554	48.582	48.609	48.637
32.4	48.664	48.692	48.719	48.747	48.774	48.802	48.829	48.857	48.884	48.912
32.5	48.939	48.967	48.994	49.022	49.050	49.078	49.105	49.133	49.161	49.188
32.6	49.216	49.244	49.272	49.299	49.327	49.355	49.383	49.411	49.438	49.466
32.7	49.494	49.522	49.550	49.577	49.605	49.633	49.661	49.689	49.716	49.744
32.8	49.772	49.800	49.828	49.856	49.884	49.912	49.940	49.968	49.996	50.024
32.9	50.052	50.080	50.108	50.137	50.165	50.193	50.221	50.249	50.278	50.306
33.0	50.334	50.362	50.391	50.419	50.448	50.476	50.504	50.533	50.561	50.590
33.1	50.618	50.647	50.675	50.704	50.732	50.761	50.789	50.818	50.846	50.875
33.2	50.903	50.932	50.960	50.989	51.017	51.046	51.074	51.103	51.131	51.160
33.3	51.188	51.217	51.245	51.274	51.303	51.332	51.360	51.389	51.418	51.446
33.4	51.475	51.504	51.533	51.562	51.591	51.620	51.548	51.677	51.706	51.735
33.5	51.764	51.793	51.822	51.851	51.880	51.909	51.937	51.966	51.995	52.024
33.6	52.053	52.082	52.111	52.141	52.170	52.199	52.228	52.257	52.287	52.316
33.7	52.345	52.374	52.404	52.433	52.463	52.492	52.521	52.551	52.580	52.610
33.8	52.639	52.668	52.698	52.727	52.757	52.786	52.815	52.845	52.874	52.904
33.9	52.933	52.963	52.992	53.022	53.051	53.081	53.110	53.140	53.169	53.199
34.0	53.228	53.258	53.287	53.317	53.347	53.377	53.406	53.436	53.466	53.495
34.1	53.525	53.555	53.585	53.614	53.644	53.674	53.704	53.734	53.763	53.793
34.2	53.823	53.853	53.883	53.913	53.943	53.973	54.003	54.033	54.063	54.093
34.3	54.123	54.153	54.183	54.214	54.244	54.274	54.304	54.334	54.365	54.395
34.4	54.425	54.455	54.486	54.516	54.546	54.577	54.607	54.637	54.667	54.698
34.5	54.728	54.759	54.789	54.820	54.850	54.881	54.911	54.942	54.972	55.003
34.6	55.033	55.064	55.094	55.125	55.155	55.186	55.216	55.247	55.277	55.308
34.7	55.338	55.369	55.399	55.430	55.461	55.492	55.522	55.553	55.584	55.614
34.8	55.645	55.676	55.706	55.737	55.767	55.798	55.828	55.859	55.889	55.920
34.9	55.95	55.98	56.01	56.04	56.08	56.11	56.14	56.17	56.20	56.23
35.0	56.265	56.296	56.327	56.359	56.390	56.421	56.452	56.483	56.515	56.546
35.1	56.577	56.608	56.640	56.671	56.702	56.734	56.765	56.796	56.827	56.859
35.2	56.890	56.922	56.953	56.985	57.016	57.048	57.079	57.111	57.142	57.174
35.3	57.205	57.237	57.268	57.300	57.332	57.364	57.395	57.427	57.459	57.490
35.4	57.522	57.554	57.586	57.617	57.649	57.681	57.713	57.745	57.776	57.808
35.5	57.840	57.872	57.904	57.936	57.968	58.000	58.032	58.064	58.096	58.128

t, °C	.00	.01	.02	.03	.04	.05	.06	.07	.08	.09
35.6	58.160	58.192	58.224	58.256	58.288	58.321	58.353	58.385	58.417	58.449
35.7	58.481	58.513	58.545	58.578	58.610	58.642	58.674	58.706	58.739	58.771
35.8	58.803	58.835	58.868	58.900	58.932	58.965	58.997	59.029	59.061	59.094
35.9	59.126	59.159	59.191	59.224	59.256	59.289	59.321	59.354	59.386	59.419
36.0	59.451	59.484	59.516	59.549	59.582	59.615	59.647	59.680	59.713	59.745
36.1	59.778	59.811	59.844	59.876	59.909	59.942	59.975	60.008	60.040	60.073
36.2	60.106	60.139	60.172	60.205	60.238	60.271	60.303	60.336	60.369	60.402
36.3	60.435	60.468	60.501	60.534	60.567	60.601	60.634	60.667	60.700	60.733
36.4	60.766	60.799	60.833	60.866	60.899	60.933	60.966	60.999	61.032	61.066
36.5	61.099	61.133	61.166	61.200	61.233	61.267	61.300	61.334	61.367	61.401
36.6	61.434	61.468	61.501	61.535	61.569	61.603	61.636	61.670	61.704	61.737
36.7	61.771	61.805	61.839	61.873	61.907	61.941	61.974	62.008	62.042	62.076
36.8	62.110	62.144	62.178	62.212	62.246	62.280	62.314	62.348	62.382	62.416
36.9	62.450	62.484	62.518	62.552	62.586	62.621	62.655	62.689	62.723	62.757
37.0	62.791	62.825	62.860	62.894	62.928	62.963	62.997	63.031	63.065	63.100
37.1	63.134	63.168	63.203	63.237	63.272	63.306	63.340	63.375	63.409	63.444
37.2	63.478	63.513	63.547	63.582	63.616	63.651	63.685	63.720	63.754	63.789
37.3	63.823	63.858	63.893	63.928	63.963	63.998	64.032	64.067	64.102	64.137
37.4	64.172	64.207	64.242	64.277	64.312	64.347	64.382	64.417	64.452	64.487
37.5	64.522	64.557	64.592	64.627	64.662	64.697	64.732	64.767	64.802	64.837
37.6	64.872	64.907	64.942	64.978	65.013	65.048	65.083	65.118	65.154	65.189
37.7	65.224	65.260	65.295	65.331	65.366	65.402	65.437	65.473	65.508	65.544
37.8	65.579	65.615	65.650	65.686	65.721	65.757	65.793	65.828	65.864	65.899
37.9	65.935	65.971	66.007	66.042	66.078	66.114	66.150	66.186	66.221	66.257
38.0	66.293	66.329	66.365	66.401	66.437	66.473	66.508	66.544	66.580	66.616
38.1	66.652	66.688	66.724	66.760	66.796	66.832	66.868	66.904	66.940	66.976
38.2	67.012	67.048	67.084	67.120	67.156	67.193	67.229	67.265	67.301	67.337
38.3	67.373	67.409	67.446	67.482	67.518	67.555	67.591	67.627	67.663	67.700
38.4	67.736	67.773	67.809	67.846	67.882	67.919	67.955	67.992	68.028	68.065
38.5	68.101	68.138	68.175	68.211	68.248	68.285	68.322	68.359	68.395	68.432
38.6	68.469	68.506	68.543	68.580	68.617	68.654	68.690	68.727	68.764	68.801
38.7	68.838	68.875	68.912	68.950	68.987	69.024	69.061	69.098	69.136	69.173
38.8	69.210	69.248	69.285	69.323	69.360	69.398	69.435	69.473	69.510	69.548
38.9	69.585	69.623	69.660	69.698	69.735	69.773	69.811	69.848	69.886	69.923
39.0	69.961	69.999	70.036	70.074	70.112	70.150	70.187	70.225	70.263	70.300
39.1	70.338	70.376	70.414	70.452	70.490	70.528	70.566	70.604	70.642	70.680
39.2	70.718	70.756	70.794	70.832	70.870	70.908	70.946	70.984	71.022	71.060
39.3	71.098	71.136	71.174	71.213	71.251	71.289	71.327	71.365	71.404	71.442
39.4	71.480	71.518	71.556	71.595	71.633	71.671	71.709	71.747	71.786	71.824
39.5	71.862	71.901	71.939	71.978	72.016	72.055	72.093	72.132	72.170	72.209

t, °C	.00	.01	.02	.03	.04	.05	.06	.07	.08	.09
39.6	72.247	72.286	72.324	72.363	72.402	72.441	72.479	72.518	72.557	72.595
39.7	72.634	72.673	72.712	72.751	72.790	72.829	72.867	72.906	72.945	72.984
39.8	73.023	73.062	73.101	73.140	73.179	73.219	73.258	73.297	73.336	73.375
39.9	73.414	73.453	73.492	73.532	73.571	73.610	73.649	73.688	73.728	73.767
40.0	73.806	73.844	73.883	73.921	73.960	73.998	74.036	74.075	74.113	74.152
40.1	74.19	74.23	74.27	74.31	74.35	74.39	74.43	74.47	74.51	74.55
40.2	74.59	74.63	74.67	74.71	74.75	74.79	74.83	74.87	74.91	74.95
40.3	74.99	75.03	75.07	75.11	75.15	75.19	75.23	75.27	75.31	75.35
40.4	75.39	75.43	75.47	75.51	75.55	75.59	75.63	75.67	75.71	75.75
40.5	75.79	75.83	75.87	75.91	75.95	75.99	76.03	76.07	76.11	76.15
40.6	76.19	76.23	76.27	76.31	76.35	76.39	76.43	76.47	76.51	76.55
40.7	76.59	76.63	76.67	76.72	76.76	76.80	76.84	76.88	76.93	76.97
40.8	77.01	77.05	77.09	77.13	77.17	77.22	77.26	77.30	77.34	77.38
40.9	77.42	77.46	77.50	77.54	77.58	77.63	77.67	77.71	77.75	77.79
41.0	77.83	77.87	77.91	77.96	78.00	78.04	78.08	78.12	78.17	78.21
41.1	78.25	78.29	78.33	78.37	78.41	78.46	78.50	78.54	78.58	78.62
41.2	78.66	78.70	78.74	78.78	78.82	78.87	78.91	78.95	78.99	79.03
41.3	79.07	79.11	79.15	79.20	79.24	79.28	79.32	79.36	79.41	79.45
41.4	79.49	79.53	79.57	79.62	79.66	79.70	79.74	79.78	79.83	79.87
41.5	79.91	79.95	80.00	80.04	80.08	80.13	80.17	80.21	80.25	80.30
41.6	80.34	80.38	80.43	80.47	80.51	80.56	80.60	80.64	80.68	80.73
41.7	80.77	80.81	80.85	80.90	80.94	80.98	81.02	81.06	81.11	81.15
41.8	81.19	81.23	81.28	81.32	81.36	81.41	81.45	81.49	81.53	81.58
41.9	81.62	81.66	81.71	81.75	81.79	81.84	81.88	81.92	81.96	82.01
42.0	82.05	82.09	82.13	82.18	82.22	82.26	82.30	82.34	82.39	82.43
42.1	82.47	82.51	82.56	82.60	82.64	82.69	82.73	82.77	82.81	82.86
42.2	82.90	82.94	82.99	83.03	83.08	83.12	83.16	83.21	83.25	83.30
42.3	83.34	83.38	83.43	83.47	83.52	83.56	83.60	83.65	83.69	83.74
42.4	83.78	83.82	83.87	83.91	83.96	84.00	84.04	84.09	84.13	84.18
42.5	84.22	84.26	84.31	84.35	84.40	84.44	84.48	84.53	84.57	84.62
42.6	84.66	84.70	84.75	84.79	84.84	84.88	84.92	84.97	85.01	85.06
42.7	85.10	85.14	85.19	85.23	85.28	85.32	85.36	85.41	85.45	85.50
42.8	85.54	85.59	85.63	85.68	85.72	85.77	85.81	85.86	85.90	85.95
42.9	85.99	86.04	86.08	86.13	86.17	86.22	86.26	86.31	86.35	86.40
43.0	86.44	86.49	86.53	86.58	86.62	86.67	86.72	86.76	86.81	86.85
43.1	86.90	86.95	86.99	87.04	87.08	87.13	87.17	87.22	87.26	87.31
43.2	87.35	87.40	87.44	87.49	87.53	87.58	87.62	87.67	87.71	87.76
43.3	87.80	87.85	87.89	87.94	87.98	88.03	88.08	88.12	88.17	88.21
43.4	88.26	88.31	88.35	88.40	88.44	88.49	88.54	88.58	88.63	88.67
43.5	88.72	88.77	88.81	88.86	88.91	88.96	89.00	89.05	89.10	89.14

t, °C	.00	.01	.02	.03	.04	.05	.06	.07	.08	.09
43.6	89.19	89.24	89.28	89.33	89.38	89.43	89.47	89.52	89.57	89.61
43.7	89.66	89.71	89.75	89.80	89.84	89.89	89.94	89.98	90.03	90.07
43.8	90.12	90.17	90.21	90.26	90.31	90.36	90.40	90.45	90.50	90.54
43.9	90.59	90.64	90.68	90.73	90.78	90.83	90.87	90.92	90.97	91.01
44.0	91.06	91.11	91.15	91.20	91.24	91.29	91.34	91.38	91.43	91.47
44.1	91.52	91.57	91.62	91.66	91.71	91.76	91.81	91.86	91.90	91.95
44.2	92.00	92.05	92.10	92.14	92.19	92.24	92.29	92.34	92.38	92.43
44.3	92.48	92.53	92.58	92.62	92.67	92.72	92.77	92.82	92.86	92.91
44.4	92.96	93.01	93.06	93.10	93.15	93.20	93.25	93.30	93.34	93.39
44.5	93.44	93.49	93.54	93.58	93.63	93.68	93.73	93.78	93.82	93.87
44.6	93.92	93.97	94.02	94.06	94.11	94.16	94.21	94.26	94.30	94.35
44.7	94.40	94.45	94.50	94.55	94.60	94.66	94.71	94.76	94.81	94.86
44.8	94.91	94.96	95.01	95.06	95.11	95.16	95.20	95.25	95.30	95.35
44.9	95.40	95.45	95.50	95.55	95.60	95.65	95.69	95.74	95.79	95.84
45.0	95.89	95.94	95.99	96.04	96.09	96.14	96.19	96.24	96.29	96.34
45.1	96.39	96.44	96.49	96.54	96.59	96.63	96.68	96.73	96.78	96.83
45.2	96.88	96.93	96.98	97.03	97.08	97.13	97.18	97.23	97.28	97.33
45.3	97.38	97.43	97.48	97.53	97.58	97.63	97.67	97.72	97.77	97.82
45.4	97.87	97.92	97.97	98.02	98.07	98.13	98.18	98.23	98.28	98.33
45.5	98.38	98.43	98.48	98.53	98.58	98.63	98.68	98.73	98.78	98.83
45.6	98.88	98.93	98.98	99.03	99.08	99.14	99.19	99.24	99.29	99.34
45.7	99.39	99.44	99.49	99.54	99.59	99.65	99.70	99.75	99.80	99.85
45.8	99.90	99.95	100.00	100.05	100.10	100.15	100.20	100.25	100.30	100.35
45.9	100.40	100.45	100.50	100.56	100.61	100.66	100.71	100.76	100.82	100.87
46.0	100.92	100.97	101.02	101.08	101.13	101.18	101.23	101.28	101.34	101.39
46.1	101.44	101.49	101.54	101.60	101.65	101.70	101.75	101.80	101.86	101.91
46.2	101.96	102.01	102.06	102.12	102.17	102.22	102.27	102.32	102.38	102.43
46.3	102.48	102.53	102.58	102.64	102.69	102.74	102.79	102.84	102.90	102.95
46.4	103.00	103.05	103.10	103.16	103.21	103.26	103.31	103.36	103.42	103.47
46.5	103.52	103.57	103.63	103.68	103.74	103.79	103.84	103.90	103.95	104.01
46.6	104.06	104.11	104.16	104.22	104.27	104.32	104.37	104.42	104.48	104.53
46.7	104.58	104.63	104.69	104.74	104.80	104.85	104.90	104.96	105.01	105.07
46.8	105.12	105.17	105.23	105.28	105.34	105.39	105.44	105.50	105.55	105.61
46.9	105.66	105.71	105.77	105.82	105.87	105.93	105.98	106.03	106.08	106.14
47.0	106.19	106.24	106.30	106.35	106.40	106.46	106.51	106.56	106.61	106.67
47.1	106.72	106.78	106.83	106.89	106.94	107.00	107.05	107.11	107.16	107.22
47.2	107.27	107.33	107.38	107.44	107.49	107.55	107.60	107.66	107.71	107.77
47.3	107.82	107.87	107.93	107.98	108.04	108.09	108.14	108.20	108.25	108.31
47.4	108.36	108.42	108.47	108.53	108.58	108.64	108.69	108.75	108.80	108.86
47.5	108.91	108.97	109.02	109.08	109.13	109.19	109.24	109.30	109.35	109.41

t, °C	.00	.01	.02	.03	.04	.05	.06	.07	.08	.09
47.6	109.46	109.51	109.57	109.62	109.68	109.73	109.78	109.84	109.89	109.95
47.7	110.00	110.06	110.11	110.17	110.22	110.28	110.33	110.39	110.44	110.50
47.8	110.55	110.61	110.66	110.72	110.77	110.83	110.89	110.94	111.00	111.05
47.9	111.11	111.17	111.22	111.28	111.33	111.39	111.45	111.50	111.56	111.61
48.0	111.67	111.73	111.78	111.84	111.89	111.95	112.01	112.06	112.12	112.17
48.1	112.23	112.29	112.34	112.40	112.46	112.52	112.57	112.63	112.69	112.74
48.2	112.80	112.86	112.92	112.97	113.03	113.09	113.15	113.21	113.26	113.32
48.3	113.38	113.44	113.49	113.55	113.61	113.67	113.72	113.78	113.84	113.89
48.4	113.95	114.01	114.06	114.12	114.18	114.24	114.29	114.35	114.41	114.46
48.5	114.52	114.58	114.64	114.69	114.75	114.81	114.87	114.93	114.98	115.04
48.6	115.10	115.16	115.21	115.27	115.33	115.39	115.44	115.50	115.56	115.61
48.7	115.67	115.73	115.78	115.84	115.90	115.96	116.01	116.07	116.13	116.18
48.8	116.24	116.30	116.36	116.42	116.48	116.54	116.59	116.65	116.71	116.77
48.9	116.83	116.89	116.95	117.00	117.06	117.12	117.18	117.24	117.29	117.35
49.0	117.41	117.47	117.53	117.59	117.65	117.71	117.76	117.82	117.88	117.94
49.1	118.00	118.06	118.12	118.18	118.24	118.30	118.36	118.42	118.48	118.54
49.2	118.60	118.66	118.72	118.78	118.84	118.90	118.95	119.01	119.07	119.13
49.3	119.19	119.25	119.31	119.37	119.43	119.49	119.55	119.61	119.67	119.73
49.4	119.79	119.85	119.91	119.97	120.03	120.09	120.15	120.21	120.27	120.33
49.5	120.39	120.45	120.51	120.57	120.63	120.69	120.75	120.81	120.87	120.93
49.6	120.99	121.05	121.11	121.17	121.23	121.29	121.35	121.41	121.47	121.53
49.7	121.59	121.65	121.71	121.77	121.83	121.89	121.95	122.01	122.07	122.13
49.8	122.19	122.25	122.31	122.37	122.43	122.50	122.56	122.62	122.68	122.74
49.9	122.80	122.86	122.92	122.98	123.04	123.11	123.17	123.23	123.29	123.35
50.0	123.41	124.04	124.66	125.29	125.91	126.54	127.17	127.79	128.42	129.04
50.1	129.67	130.32	130.97	131.63	132.28	132.93	133.58	134.23	134.89	135.54
50.2	136.19	136.87	137.55	138.24	138.92	139.60	140.28	140.96	141.65	142.33
50.3	143.01	143.72	144.43	145.13	145.84	146.55	147.26	147.97	148.67	149.38
50.4	150.09	150.83	151.56	152.30	153.04	153.78	154.51	155.25	155.99	156.72
50.5	157.46	158.23	159.00	159.77	160.54	161.31	162.08	162.85	163.62	164.39
50.6	165.16	165.96	166.76	167.57	168.37	169.17	169.97	170.77	171.58	172.38
50.7	173.18	174.02	174.85	175.69	176.52	177.36	178.19	179.03	179.86	180.70
50.8	181.53	182.40	183.27	184.14	185.01	185.88	186.75	187.62	188.49	189.36
50.9	190.23									

Appendix V

Solution of equation (57):

$$T_D = \frac{6.80079 \times 10^3 - [46.2507 \times 10^6 - 0.683183 \times 10^5 (R_{TD}) - 100.109]^{1/2}}{2}$$

using

IBM 650 computer program

SOAP - II

[illegible]

0000
0050
0034
0006
0010/
0014
0021/
0029/
0035
0001/
0002/
0008/
0025
0033
0039
0026
0009
0011
0019
0022
0030
0023
0007
0013
0024
0027
0036
0040
0020
0028
0037
0012
0015

WET 1960
0052
00
0050
0034
0006
0010
0051
0021
0029
0035
0001
0002
0008
0025
0033
0039
0026
0009
0011
0019
0023
0030
0023
0007
0013
0024
0027
0036
0040
0020
0028
0037
0012
0015
0032

U

R	WET	TO	TEMP
		BLR	1951
		REL	0000
		RER	0000
		REU	SRT
		STR	0003
50		LDR	0007
34		STR	0038
6		MI	0041
10		NE	0014
14		STU	0018
21		RAJ	0001
29		SLT	0001
35		RAC	0003
1		LDR	0040
2		STR	0005
8		SLT	0007
25		SUP	0003
33		SLT	0002
39		MY	0004
26		ALO	0001
9		AUP	0005
11		SUP	0003
19		NE	0022
22		RAJ	0001
30		FAB	0001
33		FAC	0001
37		RAC	0003
13		RAJ	0003
24		AUP	0018
27		SLD	0002
36		FAD	0001
40		FAD	0001
20		RAJ	0003
28		AUP	0031
37		SLD	0002
12		FAC	0001
15		EX	0001

Appendix VI

Computation of the refractive index of air in the
jet using IBM 650 Computer.

(a) SOAP - II

(b) Sample calculation

[illegible]

0000
0050
0034
0006
0010
0014
0021
0039
0035
0001
0002
0008
0025
0033
0039
0026
0009
0011
0019
0022
0030
0023
0007
0013
0024
0027
0036
0040
0020
0028
0037
0012
0015

[illegible]

SAMPLE	E	S	OLUT	I	O	NS
1	158	66	00	00	52	22
2	159	18	00	00	52	22
3	163	50	00	00	52	22
4	170	57	00	00	52	22
5	177	51	00	00	52	22
6	184	18	00	00	52	22
7	190	08	00	00	52	22
8	195	44	00	00	52	22
9	200	62	00	00	52	22
10	205	01	00	00	52	22
11	208	35	00	00	52	22
12	211	83	00	00	52	22
13	213	07	00	00	52	22
14	215	30	00	00	52	22
15	216	41	00	00	52	22
16	217	20	00	00	52	22
17	217	52	00	00	52	22
18	217	93	00	00	52	22
19	218	10	00	00	52	22
20	218	51	00	00	52	22
21	218	58	00	00	52	22
22	218	71	00	00	52	22
23	218	76	00	00	52	22
24	218	76	00	00	52	22
25	218	84	00	00	52	22
26	218	84	00	00	52	22

[illegible]

Appendix VII

Bibliography on Adsorption of Water Vapour

- Low, M.J.D. and Taylor, H.A. 1959. "The rates of adsorption of water and carbon monoxide by zinc oxide", J. Phys. Chem., 63, 1317.
- Ehrlich, G. 1959. "Molecular dissociation and reconstitution on solids", J. Chem. Phys., 31, 1111.
- Eberhagen, A., Jaeckel, R. and Strier, F. 1959. "Measurement of contact potential variations during gas adsorption at metal surfaces with constant capacity of the measuring condenser", Z. Angew. Phys., 11, 131. (In German).
- Tuzi, Y. 1962. "Sorption of water vapour on glass surface in vacuum apparatus", J. Phys. Soc. Japan, 17, 218.
- Farnsworth, H.E., Schlier, R.E., George, T.H. and Burger, R.M. 1958. "Application of the ion-bombardment cleaning method to titanium, germanium, silicon and nickel as determined by low energy electron diffraction", J. Appl. Phys., 29, 1150.
- Kawasaki, K., Kanou, K. and Sekita, Y. 1958. "Liquid-like layers in the adsorbed film of H₂O on glass", J. Phys. Soc. Japan, 13, 222.
- Thorp, J.M. 1959. "The dielectric behaviour of vapours adsorbed on porous solids", Trans. Faraday Soc., 55, 442.
- Vaughan, F. and Dinsdale, A. 1959. "Adsorption and desorption of moisture in fired ceramic materials", Nature (London), 183, 600.
- LaMer, V.K. and Robbins, M.L. 1956. "The effect of the spreading solvent on the properties of monolayers", J. Phys. Chem., 62, 1291.
- Okamoto, H. and Tuzi, Y. 1958. "Adsorption of water vapour on glass and other materials in vacuum", J. Phys. Soc. Japan, 13, 649.
- Tuzi, Y. and Okamoto, H. 1958. "Adsorption of water vapour on lead borosilicate glass in vacuum", J. Phys. Soc. Japan, 13, 960.

- Kasteleijn, P.W. 1956. "The statistics of an adsorbed monolayer with repulsive interaction between the adsorbed particles", *Physica*, 22, 397.
- LeBot, J. and LeMontagner, S. 1955. "Dielectric properties at centimetre wavelengths of water adsorbed on silica gel.", *J. Phys. Radium*, 16, 79. (In French).
- Garbatski, U. and Folman, M. 1954. "Multilayer adsorption of water near saturation pressure on plane glass surfaces", *J. Chem. Phys.*, 22, 2086.
- Waldman, M.H. and McIntosh, R. 1955. "An apparatus for the measurement of dielectric constants of adsorbed gases at frequencies up to 100 Mc/s", *Canad. J. Chem.*, 33, 268.
- Carman, P.C. and Haul, R.A.W. 1954. "Measurement of diffusion coefficients", *Proc. Roy. Soc. A*, 222, 109.
- Rice, S.A. 1953. "A note on the kinetics of unitary processes", *J. Chem. Phys.*, 21, 2227.
- Seidl, R. 1953. "Adsorption of a gas phase on a solid surface", *Czech. J. Phys.*, 3, 258. (In German).
- Koga, S. 1953. "Experimental study of surface potential analysis. III. Physical adsorption of water vapour", *J. Sci. Res. Inst. (Tokyo)*, 47, 189.
- Breyer, B. and Macobian, S. 1952. "Tensametry: a method of investigating surface phenomena by A.C. measurements", *Austral. J. Sci. Res. A*, 5, 500.
- Czyzak, S.J. 1952. "On the theory of dipole interactions with metals", *Amer. J. Phys.*, 20, 440.

- Abdrakhmanova, I.F. and Deryagin, B.V. 1958. "Surface conductivity of quartz in the presence of adsorbed layers", Dokl. Akad. Nauk SSSR, 120, 94. (In Russian).
- Kafalas, J.A. and Gatos, H.C. 1956. "Apparatus for the direct measurement of adsorption on solid surfaces from liquids", Rev. Sci. Instrum., 29, 47.
- Bartell, L.S. 1956. "Observation of anomalous dispersion of adsorbed films by ellipsometry", J. Chem. Phys., 24, 1108.
- Tunakan, S. 1956. "Resistance variation of thin metallic films brought about by absorption of gases", Rev. Fac. Sci. Univ. Istanbul, 21, 16. (In German).
- Tunakan, S. 1957. "Variation of resistance of thin, freely supported copper and gold films due to surrounding gas", Naturwissenschaften, 44, 6. (In German).
- Kurusaki, S., Saito, S. and Sato, G. 1955. "Transformation of adsorbed water on solid surfaces and its dielectric losses and conductivities", J. Chem. Phys., 23, 1816.
- Seehof, J.M. and Trurnit, H.J. 1955. "Effect of sorbed water vapour upon the electrical conductivity of conditioned chromium films", J. Chem. Phys., 23, 2459.
- Jason, A.C. and Wood, J.L. 1955. "Some electrical effects of the adsorption of water vapour by anodized aluminium", Proc. Phys. Soc. B, 68, 1105.
- Frisch, H.L. and Sinha, R. 1956. "Monolayers of linear macromolecules", J. Chem. Phys., 24, 652.
- Freymann, R. 1956. "Debye's dipolar absorption", Cahiers de Phys., 67 19. (In French).

- Amberg, C.H. and McIntosh, R. 1952. "A study of adsorption hysteresis by means of length changes of a rod of porous glass", *Canad. J. Chem.*, 30, 1012.
- Sebba, F. and Sutin, N. (July) "A new apparatus for studying the evaporation of water through monolayers", *J. Chem. Soc.*, 1952, 2513.
- Smith, R.N. 1952. "Phase transitions in surface films on solids", *J. Amer. Chem Soc.*, 74, 3477.
- Snedgrove, J.A., Greenspon, H. and McIntosh, R. 1953. "The dielectric behaviour of vapours adsorbed on silica gel.", *Canad. J. Chem.*, 31, 72.
- Cremer, E. 1950. "Basic laws of adsorption (Historical Survey)", *Z. Phys. Chem.*, 196, 196. (In German).
- bowden, F.B. and Throssell, W.R. 1951. "Adsorption of water vapour on solid surfaces", *Proc. Roy. Soc. A*, 209, 297.
- Theimer, O. 1951. "Hüttigs adsorption isotherm", *Letter in Nature (London)*, 168, 873.
- Papée, D. 1952. "Relationship between the adsorption rate and the isotherm", *C.R. Acad. Sci. (Paris)*, 234, 437. (In French).
- Hansen, R.S. 1951. "On basic concepts in surface thermodynamics", *J. Phys. Coll. Chem.*, 55, 1195.
- Ward, A.F.H. and Tordai, L. 1952. "Time dependence of boundary tensions of solutions. IV. Kinetics of adsorption at liquid-liquid interfaces", *Rec. Trav. Chim. Pays-Bas*, 71, 572.
- Wylie, R.G. 1952. "On the hysteresis of adsorption on solid surfaces", *Aust. J. Sci. Res. A*, 5, 288.
- Vreedenburg, H.A. 1950. "The adsorption of carbon disulphide vapour flowing through a tube filled with activated charcoal", *Rec. Trav. Chim. Pays-Bas*, 69, 1233.

- Huang, K. and Wyllie, G. 1950. "Behaviour of a molecule near a metal surface",
Disc. Faraday Soc., #8, 18.
- Allen, J.A. and Mitchell, J.W. 1950. "The adsorption of gases on copper films",
Disc. Faraday Soc., #8, 309.
- McClellan, A.L. and Hackernion, N. 1951. "The sorption of gases on metals
at room temperature", J. Phys. Coll. Chem., 55, 374.
- Bowden, F.P. and Throssell, W.R. 1951. "Adsorption of water vapour on solid
surfaces", Letter in Nature, Lond., 167, 601.
- Stahl, P. 1951. "Effect of the adsorption of gases on the polymorphic
transformation $\alpha \rightleftharpoons \beta$ of quartz", C.R. Acad. Sci., Paris, 232,
1669. (In French).
- Vernon, W.H.J., Macauley, J.M. and Bowden, F.P. 1951. "Adsorption of water
vapour on solid surfaces", Letter in Nature, Lond. 167, 1037.
- McIntosh, R., Rideal, E.K. and Snelgrove, J.A. 1951. "The dielectric
behaviour of vapours adsorbed on activated silica gel.", Proc.
Roy. Soc. A, 208, 292.
- Bayley, S.T. 1951. "The dielectric properties of adsorbed water layers
on inorganic crystals", Trans. Faraday Soc., 47, 518.
- Conway, B.E., Bockris, J.O. and Ammar, I.A. 1951. "The dielectric constant
of the solution in the diffuse and helmholtz double layers at a
charge interface in aqueous sol'n", Trans. Faraday Soc., 47, 750.
- Foster, A.G. 1951. "Sorption hysteresis. I. Some factors determining the
size of the hysteresis loop", J. Phys. Coll. Chem., 55, 638.
- Perrot, M and Arcaix, S. 1949. "Effect of adsorption of gases on the
development (of the conductivity) of thin films", C.R. Acad. Sci.,
Paris, 229, 1139. (In French).

- Ahdanov, S.P. 1949. "The phenomenon of the irreversible hysteresis of the sorption isothermals of water on porous glass and silica gel.", Dokl. Akad. Nauk, SSSR, 68, 99. (In Russian).
- Smith, R.N. and Pierce, C. 1948. "Heats of adsorption II", J. Phys. Coll. Chem., 52, 1115.
- Crank, J. and Henry, M.E. 1949. "A comparison of the rates of conditioning by different methods", Proc. Phys. Soc., London B, 62, 257.
- Razouk, R.I. and Salem, A.S. 1948. "The adsorption of water vapour on glass surfaces", J. Phys. Coll. Chem., 52, 1208.
- Emmett, P.H. 1948. "Studies of metal surfaces by low-temperature gas adsorption", Proc. Pittsburgh Internat. Conf. Surface Reactions, 82.
- Harriss, B.L. and Emmett, P.H. 1949. "Adsorption studies - physical adsorption of nitrogen, toluene, benzene, ethyl iodide, hydrogen sulfide, water vapour, carbon disulphide and pentane on various porous and non-porous solids", J. Phys. Coll. Chem., 53, 811.
- Cockbain, E.G. 1947. "Recent advances in surface chemistry", Research, Lond., 1, 115.
- Josefowitz, S. and Othmer, D.F. 1948. "Adsorption of vapours", Industr. Engng. Chem., 40, 739.
- Norrish, R.G.W. and Russell, K.E. 1947. "Adsorption of water vapour in high vacuum apparatus", Nature, Lond., 160, 57.
- Went, J.J. 1941. "Adsorption phenomena on massive metal surfaces measured by means of electrical contact resistances", Physica, 's Grav., 8, 233.
- Broad, D.W. and Foster, A.G. 1945. "Comparative isothermals of water and deuterium oxide on porous solids", J. Chem. Soc., 372.

Gulbransen, E.A. and Copan, T.P. 1959. "Microtopology of the surface reactions of oxygen and water vapour with metals", Disc. Faraday Soc. (GB), #28, 229.

REFERENCES

- Adey, A.W. 1957. "Microwave refractometer cavity design", Can. J. Tech. 34, 519.
- Anderson, L.J. 1959. "Hot-wire anemometer for laboratory and field use", Bull. Amer. Meteorol. Soc., 40, 49.
- Anderson, W.L., Beyers, N.J. and Rainey, R.J. 1960. "Comparison of experimental with computed tropospheric refraction", Trans. IRE, AP-8, 456.
- Bean, B.R. 1962. "The radio refractive index of air", Proc. IRE, 50, 260.
- Bean, B.R. and Dutton, E.J. 1961. "Concerning radiosondes, lag constants and radio refractive index profiles", J. Geophys. Res., 66, 3717.
- Berry, F.A., Bollay, E., and Beers, N.R. 1945. "Handbook of meteorology", McGraw-Hill Book Co., Inc., New York.
- Bird, R.B., Stewart, W.E. and Lightfoot, E.N. 1960. "Transport phenomena", J. Wiley and Sons, Inc., New York.
- Birnbaum, G. 1950. "A recording microwave refractometer", Rev. Sci. Instrum. 21, 169.
- Birnbaum, G. and Bussey, H.E. 1955. "Amplitude, scale and spectrum of refractive index inhomogeneities in the first 125 meters of the atmosphere" Proc. IRE, 43, 1412.
- Birnbaum, G. and Chatterjee, S.K. 1952. "The dielectric constant of water vapour in the microwave region" J. Appl. Phys. 23, 220.
- Booker, H.G. and de Bettencourt, J.T. 1955. "Theory of radio transmission by tropospheric scattering using very narrow beams" Proc. IRE, 43, 281.
- Bugnolo, D.S. 1959. "Correlation function and power spectra of radio links affected by random dielectric noise" Trans. IRE, AP-7, 137.

- Carrier, W.H., Newark, N.J., and Mackey, C.O. 1937. "A review of existing psychrometric data in relation to practical engineering problems" Trans. Amer. Soc. Mech. Engrs., 59, 33.
- Chapman, J.H., Heikkila, W.J. and Hogarth, J.E. 1957. "A new technique for the study of scatter propagation in the troposphere" Can. J. Phys., 35, 823.
- Crain, C.M. 1950. "Apparatus for recording fluctuations in refractive index of the atmosphere at 3.2 cms. wavelength", Rev. Sci. Instrum. 21, 456.
- Crain, C.M. 1955. "Survey of airborne microwave refractometer measurements" Proc. IRE, 43, 1405.
- Crain, C.M. and Williams, C.E. 1957. "Method of obtaining pressure and temperature insensitive microwave cavity resonators" Rev. Sci. Instrum., 28, 620.
- Crozier, A.L. 1958. "Captive balloon refractovariometer", Rev. Sci. Instrum. 29, 276.
- Cunningham, R.M., Planck, V.G. and Campen, C.F. 1956. "Cloud refractive index studies" Geophysical Research Papers No. 51, GRD/AFCRC.
- Deam, A.P. 1962. "Radiosonde for atmospheric refractive index measurements" Rev. Sci. Instrum., 33, 438.
- Derjaguin, V. and Zorin, Z.M. 1957. "Second International Congress on Surface Activity. II. Solid-Gas Interface." - Butterworth Scientific Publications, London, pg. 145.
- Eshbach, O.W. 1961. "Handbook of engineering fundamentals", J. Wiley and Sons, New York (Second edition, eighth printing).
- Essen, L. and Froome, K.D. 1951. "The refractive indices and dielectric constants of air and its principal constituents at 24,000 Mc/s" Proc. Phys. Soc. (London) B, 64, 862.

- Ewell, A.W. 1941. "Thermometry in hygrometric measurements"; in Vol. 1 - Temperature; its measurement and control in science and industry. Reinhold Publishing Corp., New York, pg. 650.
- Ford, L.H. 1948. "The effect of humidity on the calibration of precision air capacitors" J. Inst. Elect. Engrs. (London) 95, Pt. II, 709.
- Guide 1959. "Heating, Ventilating, Air Conditioning Guide 1959", Vol. 37, American Society of Heating and Air-Conditioning Engineers, Inc., N.Y. (Waverly Press).
- Hartman, W.J. 1960. "Limit of spatial resolution of refractometer cavities" J. Res. N.B.S., 64D, 65.
- Hay, D.R., Bell, M.B. and Johnston, R.W. 1962. "The environment of persistent and transitory angels". Paper presented at Joint Meeting of USA-Canadian U.R.S.I., Ottawa (15-17 October); also, in preparation for publication.
- Hay, D.R., Martin, H.C. and Turner, H.E. 1961. "Light-weight refractometer" Rev. Sci. Instrum., 32, 693.
- Hay, D.R. and Pemberton, E.V. 1962. "On the eddy diffusion of water vapor above an outdoor surface" Can. J. Phys., 40, 1182.
- Hay, D.R. and Reid, W.M. 1962. "Radar angels in the lower troposphere" Can. J. Phys., 40, 128.
- Hay, D.R., Storey, L.R.O. et. al. 1958. "Propagation factors affecting long-range UHF radars at high latitudes", Report 41-1-3, Defence Research Telecommunications Establishment, Ottawa, Canada
- Hirao, K. and Akita, K.I. 1957. "A new type refractive index variometer" J. Radio Res. Labs (Japan) 4, 423.
- Jordan, R.C. and Priester, G.B. 1956. "Refrigeration and air conditioning" Prentice Hall. (Second edition).

- Kerr, D.E. 1951. "Propagation of short radio waves", McGraw-Hill Book Company Inc., New York.
- Long, I.F. 1957. "Instruments for micro-meteorology" Quart. J. Roy. Meteorol. Soc., 83, 202.
- Lyons, H., Birnbaum, G. and Kryder, S.J., 1948. "Measurements of the complex dielectric constant of gases at microwaves" Phys. Rev. 74, 1210 (Abstract).
- Martin, H.C. 1961. "A study of air flow and temperature coefficient in a refractometer sensor", Thesis, Dept. of Physics, University of Western Ontario, London, Canada.
- Martin, S. 1962. "The control of conditioning atmospheres by saturated salt solutions". J. Sci. Instrum., 39, 370.
- McGavin, R.E. 1962. "A survey of the techniques for measuring the radio refractive index" Technical Note 99, National Bureau of Standards, Washington D.C.
- Middleton, W.E.K. and Spilhaus, A.F. 1953. "Meteorological instruments" University of Toronto Press, Toronto (3rd edition, revised).
- Monteith, J.L. 1954. "Error and accuracy in thermocouple psychrometry" Proc. Phys. Soc., B, 67, 217.
- Monteith, J.L. and Owen, P.C. 1958. "A thermocouple method for measuring relative humidity in the range 95-100 per cent", J. Sci. Instrum., 35, 444.
- Muchmore, R.B. and Wheelon, A.D. 1955. "Line-of-sight propagation phenomena - I. Ray treatment", Proc. I.R.E., 43, 1437.
- Noakes, G.R. 1953. "A Textbook of heat" MacMillan and Company, Ltd., London.
- O'Brien, F.E.M. 1948. "The control of humidity by saturated salt solutions" J. Sci. Instrum., 28, 73.

- Plank, V.G. 1956. "A meteorological study of radar angels" Geophys. Res. Papers No. 52, GRD/AFCRC.
- Plank, V.G. 1959. "Spurious echoes on radar, a survey" Geophys. Res. Papers No. 62, GRD/AFCRC.
- Pope, A. 1958. "Wind-tunnel testing", J. Wiley and Sons Inc., New York, (2nd edition).
- Prandtl, L. 1952. "Essentials of fluid dynamics". (authorized translation) Blackie and Son Ltd., London.
- Rothen, A. 1945. "The ellipsometer, an apparatus to measure thickness of thin surface films", Rev. Sci. Instrum., 16, 26.
- Rothen, A. and Hanson, M. 1948. "Optical measurements of surface films. I." Rev. Sci. Instrum., 19, 839.
- Sargent, J.A. 1959. "Recording microwave hygrometer" Rev. Sci. Instrum., 30, 348.
- Silverman, S. 1930. "Adsorption of methyl alcohol films on rock-salt", Phys. Rev., 36, 311.
- Slater, J.C. 1946. "Microwave electronics", Rev. Mod. Phys., 18, 480.
- Smith, R.D. 1960. "The 'Tellurometer' system-new applications to geodesy and hydrography", J. Geophys. Res., 65, 418.
- Spencer, H.M. 1926. "Laboratory Methods for maintaining constant humidity", International Critical Tables, Vol. 1, McGraw-Hill Book Co. Inc., New York. (1st edition). pg. 67.
- Stranathan, J.D. 1935. "Dielectric constant of water vapor", Phys. Rev. 48, 538.
- Stratton, J.A. 1941. "Electromagnetic theory", McGraw-Hill Book Co. Inc., New York (1st edition), Section 5.2.
- Theisen, J.F. and Gossard, E.E. 1961. "Free-balloon borne meteorological refractometer", J. Res. N.B.S., 65D, 149.

- Thompson, M.C., Freethey, F.E. and Waters, D.M. 1958. "Fabrication techniques for ceramic X-band cavity resonators", Rev. Sci. Instrum., 19, 865.
- Thompson, M.C., Freethey, F.E. and Waters, D.M. 1959. "End plate modification of X-band TE₀₁₁ cavity resonators", Trans. I.R.E., MTT-7, 388.
- Thompson, M.C. and Vetter, M.J. 1958. "Compact microwave refractometer for use in small aircraft", Rev. Sci. Instrum., 29, 1093.
- Thompson, M.C., Janes, H.B. and Kirkpatrick, A.W. 1960. "An analysis of time variations in tropospheric refractive index and apparent radio path length", J. Geophys. Res., 65, 193.
- Thorn, D.C. and Straiton, A.W. 1959. "Design of open-ended microwave resonant cavities", Trans. I.R.E., MTT-7, 389.
- Veith, H. 1960. "The influence of moisture on the characteristic electrical value of capacitors", Nachrichtentech. Z. (Germany) 13, 519.
- Vetter, M.J. and Thompson, M.C. 1962. "Absolute microwave refractometer" Rev. Sci. Instrum., 33, 656.
- Wagner, N.K. 1961. "The effect of the time constant of radiosonde sensors on the measurement of temperature and humidity discontinuities in the atmosphere", Bull. Amer. Meteorol. Soc., 42, 317.
- Washburn, E.W. 1928. "The vapor pressures of ice and water up to 100°C", International Critical Tables, III, (1st ed.), McGraw-Hill Book Co. Inc., New York. pg. 210.
- Waterman, A.T. 1958. "A rapid beam-swinging experiment in transhorizon propagation" Trans. I.R.E., AP-6, 338.
- Wexler, A. and Brombacher, W.G. 1951. "Methods of measuring humidity and testing hygrometers", Circular 512, National Bureau of Standards, Washington D.C.

- Wexler, A. and Hasegawa, S. 1954. "Relative humidity-temperature relationships of some saturated salt solutions in the temperature range 0° to 50°C ", J. Res. N.B.S., 53, 19.
- Wong, M.S. 1958. "Refraction anomalies in airborne propagation", Proc. I.R.E., 46, 1628.
- Zahn, C.T. 1926. "Association, adsorption and dielectric constant". Phys. Rev., 27, 329.

(Two sheets of ASTIA catalog Cards.)

(as per AFSCM 5-1)